From the

Institute of Veterinary Pathology

General Pathology and Pathological Anatomy

Chair: Prof. Dr. W. Hermanns

Ludwig-Maximilians-University Munich

and the

Laboratory for Functional Genome Analysis, Gene Center

Chair: Prof. Dr. E. Wolf

Ludwig-Maximilians-University Munich

Under the supervision of Prof. Dr. R. Wanke and Dr. G.J. Arnold

Differential proteomic analysis of isolated glomeruli from two murine nephropathy models at early stages of glomerulosclerosis

Inaugural - Dissertation

to achieve the doctor title of veterinary medicine

at the Faculty of Veterinary Medicine of the

Ludwig-Maximilians-University, Munich

by

Carolin Block

from Münster

Munich 2007

Gedruckt mit Genehmigung der Tierärztlichen Fakultät der
Ludwig-Maximilians-Universität München

Dekan:	Univ.-Prof. Dr. Braun
Berichterstatter:	Univ.-Prof. Dr. Wanke
1. Korreferent:	Univ.-Prof. Dr. Aigner
2. Korreferent:	Dr. André
3. Korreferent:	Priv.-Doz. Dr. Zakhartchenko
4. Korreferent:	Univ.Prof. Dr. Hirschberger

Tag der Promotion: 8. Februar 2008

This study was performed within the framework of the graduate college “Functional genomics in veterinary medicine” (grk 1029), supported by the Deutsche Forschungsgemeinschaft (DFG) in the period of January 2005 until May 2007.

Meinen Eltern

1. Introduction 1
2. Literature review 2
2.1 Chronic renal failure 2
2.2 Progressive glomerulosclerosis 3
2.3 Pathogenesis of glomerulosclerosis 4
2.3.1 Glomerular hypertrophy 4
2.3.2 Podocyte damage 5
2.3.3 Proteinuria 6
2.4 Animal models of glomerulosclerosis 7
2.4.1 GH transgenic mice 7
2.4.2 GIPR^{dn} transgenic mice 9
2.5 Proteomics 10
2.5.1 2D-gel electrophoresis 11
2.5.2 Mass spectrometry (MS) 13
2.5.3 Proteomics in nephrology 14
3. Animals, material and methods 22
3.1 Experimental design 22
3.2 Animals 24
3.2.1 Breeding, animal husbundary and numbers of mice used for analyses 24
3.2.2 PCR-Analysis 25
3.2.3 Detection of glucosuria 29
3.3 Urine protein analysis 30
3.3.1 Sodium dodecyl sulphate polyacrylamide gel electrophoresis (SDS-PAGE) 30
3.3.2 Western blot analysis 33
3.3.3 Determination of urinary albumin concentration by ELISA 34
3.4 Determination of body weight and nose-rump-length 36
3.5 Glomerulus isolation 36
3.6 Histological technique 38
3.6.1 Plastic histology 38
3.7 Determination of the mean glomerular volume 39
3.8 Lysis of glomerulus samples for proteomic analysis 40
3.9 Minimal labeling of proteins with fluorescent dyes 41

3.10 2D Difference gel electrophoresis (2D-DIGE) ... 41
3.10.1 Isoelectric focussing (IEF) ... 41
3.10.2 SDS-PAGE ... 42
3.10.3 Scanning and analyzing the gels ... 43
3.10.4 Staining of gels ... 43
3.11 Identification of proteins of interest ... 44
3.11.1 Spot excision and tryptic hydrolysis ... 44
3.11.2 Desalting of peptides ... 44
3.11.3 Mass spectrometry and database search ... 44
3.11.4 LC-ESI-MS/MS analysis ... 45
3.12 Statistical evaluation and data presentation ... 46
4. Results ... 47
4.1 Urine protein analysis ... 47
4.1.1 SDS-PAGE ... 47
4.1.2 Quantification of albuminuria ... 49
4.2 Body weight, kidney weight and nose-rump-length ... 50
4.3 Mean glomerular volume ... 51
4.4 Glomerulus isolation ... 54
4.5 2D-DIGE analysis of glomerulus preparations ... 55
4.5.1 GH transgenic (tg) mice vs. wild-type controls (co) ... 57
4.5.2 GIPR^{dn} transgenic (tg) mice vs. wild-type controls (co) ... 64
4.6 Identification of proteins of differentially abundant proteins ... 72
4.6.1 GH transgenic mice vs. their controls ... 80
4.6.2 GIPR^{dn} transgenic mice in stage 2 vs. their controls ... 81
4.6.3 Proteins with differential abundance in GH transgenic as well as GIPR^{dn} transgenic mice in stage 2 vs. their corresponding controls ... 83
5. Discussion ... 85
5.1 General aspects ... 85
5.2 Mouse models and analysed disease stages ... 85
5.3 Glomerulus isolation ... 88
5.4 Proteomic approach ... 89
5.5 Identification of proteins ... 91
6. Perspective ... 103

7. Summary 104
8. Zusammenfassung 106
9. References 108
10. Attachment 132
10.1 Silver stain for SDS-PAGE mini gels 132
10.2 Staining procedures for plastic embedded sections 133
10.2.1 Hemalaun & Eosin (H&E) 133
10.2.2 Periodic acid-Schiff stain (PAS) 133
10.3 PMF spectra of unambiguously identified differentially abundant spots .. 134
10.3.1 GH transgenic mice in stage 2 vs. their controls 134
10.3.2 $GIPR^{dn}$ transgenic mice in stage 2 vs. their controls 137
Acknowledgement 142

1. Introduction

Chronic kidney disease (CKD) in human beings is a major cause of morbidity and mortality worldwide. It is characterized by relentless progressive scarring of renal parenchyma that results in end-stage renal disease (ESRD) with the need for dialysis or transplantation (Fogo, 2006). The understanding of the underlying mechanisms of injury has been a major challenge for decades and is now urgently needed in the view of dramatically increasing incidence of CKD (Zoja et al., 2006). The variety of renal diseases implies various mechanisms leading to altered expression of proteins in the different renal microstructures. Therefore, analysis of the renal proteome during relevant disease states is crucial for a better understanding of the complexity of the pathogenesis and pathophysiology of the different renal diseases. The development of progressive glomerulosclerosis is a hallmark of CKD and represents a highly relevant problem in nephrology. Independent of disease specific initial pathogenic insults, the earliest stages of glomerulosclerosis are characterised by common morphological and functional alterations of the glomeruli. Glomerular hypertrophy and the subsequent development of albuminuria were both identified as key determinants of the progression of disease (Fogo and Ichikawa, 1991; Remuzzi, 1995). In the present study the glomerular proteome of two different mouse models of nephropathy was analysed at defined early stages of glomerulosclerosis in order to identify proteins with potential pathogenetic or diagnostic significance: Growth hormone (GH) transgenic mice are a well characterised model for progressive glomerulosclerosis. Transgenic mice expressing a dominant negative glucose-dependent insulinotropic polypeptide receptor ($GIPR^{dn}$) represent a model for diabetes-associated glomerular lesions. Because glomeruli represent only about 2 - 4 % of the whole kidney volume (Artacho-Perula et al., 1993; Nyengaard and Bendtsen, 1992; Wanke, 1996), a subproteome approach targeting isolated renal glomeruli was the method of choice. The first objective of the study was to identify differentially abundant proteins in transgenic mice as compared to wild-type controls within each analysed group and analysed disease stage. The overall aim was to reveal, whether molecular signatures detected by the quantitative profiling in both analysed mouse models would show similarities and if they would point to shared molecular mechanisms of disease.

2. Literature review

2.1 Chronic renal failure

Chronic kidney disease (CKD) in human beings is a major cause of morbidity and mortality worldwide (Fogo, 2006). Increasing numbers of patients are affected by CKD. This rise is reflected in the increasing number of people with end-stage renal disease (ESRD) treated by renal replacement therapy (RRT) – dialysis or transplantation, and is threatening to reach epidemic proportions over the next decade (El Nahas and Bello, 2005). Independent of various initial insults, the progression to ESRD is a common outcome in chronic nephropathies (Remuzzi et al., 2006). Worldwide, the number of patients undergoing treatment for ESRD was estimated to have reached 1.9 million by the end of 2005 with yearly growth rates about 6 – 7 % (Grassmann et al., 2006). In the United States prevalence counts of ESRD are expected to increase by 85 % from 382,000 in 2000 to over 700,000 in the year 2015 and the number of incident ESRD patients is expected to increase by about 44 % to 136,000 in 2015, respectively (Gilbertson et al., 2005). In the European Union there are currently approximately 436,000 RRT patients as compared to ~382,000 patients in 2002, with Germany counting for ~87,000 patients as compared to 75,000 in 2002 (ERA-EDTA-Registry, 2007; Frei and Schober-Halstenberg, 2006). This dramatic increase represents not only a major public health problem, but also an economic challenge due to very costly renal replacement therapies. In Europe, dialysis alone takes up about 2 % of health care budgets, with only a small proportion (< 0.01 %) of the population needing treatment (De Vecchi et al., 1999). Counting for about half of the cases diabetic nephropathy is the major cause of chronic renal failure (Mitka, 2005). Taking into account that worldwide more than 180 million people suffer from diabetes and the number is likely to be more than double in 2030, it will be of even more importance (www.who.int/diabetes). CKD is characterised by relentless progressive scarring of renal parenchyma that ultimately results in ESRD with the need for dialysis or transplantation (Fogo, 2006). The hallmarks of progressive nephropathies are glomerulosclerosis, tubular atrophy, and interstitial fibrosis (Fogo, 1999; Zoja et al., 2006). The majority of diseases which progress to chronic renal failure in humans as well as in laboratory animals begin at

the glomerulus (Klahr et al., 1988; Kriz and LeHir, 2005). Therefore, the focus in the following section will be laid on glomerulosclerosis.

2.2 Progressive glomerulosclerosis

The term “glomerulosclerosis” is commonly used to designate glomerular scarring. It describes a pathologic diagnosis based exclusively on morphologic criteria and contains no statement about etiology or pathogenesis of the lesion. Glomerulosclerosis refers to a variety of glomerular lesions including increases in mesangial matrix, collapse and obliteration of capillary lumina, accumulation of hyaline, and synechial attachments to Bowman’s capsule (Floege et al., 1992; Romen, 1976; Schwartz and Lewis, 1985; Striker, 1993). Glomerulosclerosis may be “diffuse“, if more than 80 % of investigated glomeruli are altered, whereas it is called “focal”, if only some glomeruli are involved. The terms “global” or “segmental” glomerulosclerosis stand for either the complete or partial sclerosis of a single glomerulus (Churg and Sobin, 1982).

Glomerulosclerotic changes have been documented extensively in literature of human nephrology as well as pathology. In humans, the so-called primary or idiopathic focal segmental glomerulosclerosis (FSGS) is an important cause of the idiopathic nephrotic syndrome (Goldszer et al., 1984) and takes up a special position in the group of sclerosing glomerulopathies. Alongside this clinical entity (Waldherr and Derks, 1989) exists the frequently occurring group of secondary glomeruloscleroses. In this form glomerulosclerosis develops in association with a variety of systemic or renal diseases (Goldszer et al., 1984). Systemic diseases in the context of which glomerulosclerosis can occur can be grouped into broad categories, such as vascular diseases (e.g. essential hypertension), metabolic disorders (e.g. diabetes mellitus), hereditary diseases (e.g. Fabry’s disease), and systemic immunological diseases (e.g. systemic lupus erythematosus). Among them diabetes mellitus is the most common cause of glomerulosclerosis in humans (Striker et al., 1995). Different forms of diffuse glomerulonephritis can also result in diffuse glomerulosclerosis (Klahr et al., 1988; Rennke and Klein, 1989; Schreiner, 1990). A once established chronic renal insufficiency tends to progress to end-stage renal failure which is characterised by progressive glomerulosclerosis independent of the nature of the initiating nephropathy (el Nahas, 1989). Progressive glomerulosclerosis

therefore represents a highly relevant problem in nephrology and the study of its pathogenesis is a key issue in nephrologic research.

2.3 Pathogenesis of glomerulosclerosis

2.3.1 Glomerular hypertrophy

Concerning the pathogenesis of progressive glomerulosclerosis several pathogenetic concepts with a uniform pathomechanism which determines the development of glomerulosclerosis exist. But they differ in the nature of the initiating event. In the early nineteen eighties it was postulated that adaptive glomerular hyperperfusion and hyperfiltration would initiate glomerulosclerosis in remnant glomeruli after glomerular ablation (Brenner et al., 1982). Later the initial hypothesis was revised and increased glomerular capillary pressure was found to be a key mediator of progressive renal sclerosis (Anderson et al., 1985). However, there was some doubt on the universal validity of this hypothesis. Yoshida and colleagues did not find a positive correlation between the magnitude of the early glomerular capillary pressure and the subsequent development of glomerulosclerosis in rats with remnant kidneys (Yoshida et al., 1988). They came to the conclusion that glomerular hypertension alone does little to promote glomerulosclerosis. It was postulated that not hemodynamics but glomerular hypertrophy has a direct causal impact on the development of glomerulosclerosis, because a strong positive correlation could be shown between the glomerular size and the degree of sclerosis (Yoshida et al., 1989). This was also supported by a number of other studies (Daniels and Hostetter, 1990; Fries et al., 1989). The importance of glomerular hypertrophy in the pathogenesis of glomerulosclerosis has been documented by several authors (Fogo and Ichikawa, 1991; Klahr et al., 1988; Olson and Heptinstall, 1988). The linkage between glomerular hypertrophy and sclerosis has been demonstrated in numerous diseases in humans as well as in experimental animal models (Fogo, 2000). Initial disease-specific pathogenic insults lead to a loss of functioning nephrons resulting in glomerular hypertrophy which initiates glomerulosclerosis. This represents the entry in a vicious cycle, because progressive glomerulosclerosis results in a further loss of nephrons. Finally, end stage renal disease develops (Ichikawa et al., 1991). In FSGS and diabetes glomerular hypertrophy occurs without prior nephron loss. In these

diseases the initial pathogenic mechanisms itself are linked to glomerular hypertrophy (Fogo and Ichikawa, 1989). The first obvious and earliest changes in the course of diabetes associated kidney lesions after manifestation of diabetes are renal and glomerular hypertrophy (Lehmann and Schleicher, 2000). Glomerular hypertrophy can be detected in experimentally induced diabetes within four days (Osterby and Gundersen, 1980). It is essential, that glomerular hypertrophy not only is a symptom of diabetes associated renal changes, but plays a vital role in the pathogenesis of diabetic glomerulosclerosis (Fogo and Ichikawa, 1989; Wolf, 2000). It is seen as a prerequisite rather than a consequence of hyperfunction (Cortes et al., 1987). The concept of glomerular hypertrophy is supported by studies on renal changes in growth hormone transgenic mice, a well-characterised model of progressive glomerulosclerosis (Doi et al., 1990; Wanke et al., 1991) (see 2.4.1).
Glomerular hypertrophy is characterised by hypertrophy and hyperplasia of mesangial and endothelial cells whereas podocytes only show hypertrophy and no change in cell number (Fogo, 1999; Wiggins et al., 2005). Due to glomerular hypertrophy a damage of podocytes occurs, causing disturbances in the glomerular filtration barrier (Kriz et al., 1994; Wanke et al., 2001).

2.3.2 Podocyte damage

Kidney function depends on an intact glomerular filtration barrier and podocytes are crucially involved in establishing the specific properties of the glomerular filter (Pavenstadt et al., 2003). The latter consists of the fenestrated endothelium, the glomerular basement membrane, and the slit diaphragm that connects interdigitating podocyte foot processes. Under physiological conditions it is freely permeable by water and small solutes, but not for proteins of the size of albumin and larger. Podocytes are highly differentiated neuron-like epithelial cells which have a limited capacity for cell replication (Wiggins et al., 2005). Their ability to adapt to an increase in glomerular size is also limited. It has been shown that podocytes react with a detailed sequence of structural alterations to the hypertrophy of the glomerulus (Wiggins et al., 2005). Early changes include podocyte hypertrophy and foot process effacement which represents the most characteristic change in podocyte phenotype under a great variety of experimental as well as human glomerulopathies (Shirato et al., 1996; Wanke et al., 2001). Recent studies have shown that podocyte injury is a trigger for glomerulosclerosis and plays a key role in the progression of

glomerulosclerosis as well as tubulointerstitial lesions (Ichikawa et al., 2005; Kriz, 2002). The filtration of serum proteins into the Bowman's space is not only a result but may also be a cause of podocyte damage (Ichikawa et al., 2005).

2.3.3 Proteinuria

Under physiological conditions proteins with a molecular size like albumin (67 kDa) and larger are not able to pass the glomerular filtration barrier, whereas smaller proteins are filtrated and then reabsorbed by the tubular system (Bergstein, 1999). Looking on the protein pattern in the urine one can determine the localisation of kidney damage. Large proteins indicate a glomerular damage. Podocyte damage causes a selective glomerular proteinuria (68 – 150 kDa), damage of glomerular basement membranes and mesangium cause an unselective glomerular proteinuria (68 – 350 kDa) (Bergstein, 1999; Stierle et al., 1990). A reduction in reabsorptive capacity due to tubular or interstitial alterations results in a loss of low molecular weight proteins (Marshall and Williams, 1996). Albuminuria is not only the earliest clinical evidence of nephropathy, but has been identified as a renal risk factor in both diabetic and non-diabetic subjects (Ruggenenti and Remuzzi, 2006; Shumway and Gambert, 2002). Microalbuminuria is seen as a more sensitive marker for glomerular disease than proteinuria. Proteinuria is a sign of established kidney damage with a direct pathogenetic role in the progression of renal disease and direct nephrotoxicity (Remuzzi, 1995; Ruggenenti and Remuzzi, 2006). It has been shown that the degree of proteinuria strongly correlates with the rate of progression of renal failure in diabetic and non-diabetic renal disease (Newman et al., 2000; Wang et al., 2000). Exposure of tubular cells to protein is a crucial step of perpetuating progression through activation of tubular epithelial cells and the start of interstitial fibrosis (Klahr, 1999; Odoni and Ritz, 1999; Wang et al., 2000). Therapeutic interventions that aim to decrease proteinuria effectively limit the progression to end-stage renal disease (Perico et al., 2005). Insights from studies in animal models will hopefully generate novel therapeutic modalities for the limitation of progression (Zoja et al., 2006).

2.4 Animal models of glomerulosclerosis

Diverse animal experimental approaches have been applied for studying the pathogenesis of glomerulosclerosis and progression of chronic kidney disease. Numerous models have been established in the rat with the aim to mirror the various elements of human glomerulosclerosis. But since transgenic technologies have become established many of these models have been translated to and new models have been developed in the mouse species (Fogo, 2003). The ease of physiologic manipulations, including direct micropuncture of the glomerulus or repeated renal biopsies from the same animal, had been advantages of rats. Due to their small size this is very challenging in mice. But having transgenic technologies at hand, the possibility of direct investigation of the impact of overexpressing or deletion of specific genes makes the mouse a very attractive model (Anders and Schlondorff, 2000; Fogo, 2003).

Generally, glomerulosclerosis models can be separated into three groups, the conventional experimental models, spontaneously occurring glomerulosclerosis as models, and via gene transfer established models. Overviews are given by Wanke (1996) and Anders and Schlöndorff (2000). In the group of conventional experimental models the so-called remnant kidney model in which more than 50 % of renal tissue is removed is the most commonly used model (Heptinstall, 1992; Lafferty and Brenner, 1990). Among the models that spontaneously develop glomerulosclerosis obesity and hypertension models must be mentioned. Several strategies of transgenic technologies have been used for the establishment of nephrologically relevant mouse models, including the overexpression of a transgene or the knock out of a specific gene (Anders and Schlondorff, 2000; Fogo, 2003; Zoja et al., 2006). A well-characterised murine model of progressive glomerulosclerosis is the growth hormone (GH) overexpressing transgenic mouse. An example for a model of diabetes-associated kidney changes are transgenic mice expressing a dominant negative glucose dependent insulinotropic polypeptide receptor ($GIPR^{dn}$).

2.4.1 GH transgenic mice

Mice transgenic for growth hormone were generated for the first time in 1982 (Palmiter et al., 1982). Since then, several strains of transgenic mice overexpressing heterologous GH genes under the transcriptional control of various regulatory

elements have been developed (Brem et al., 1989). The systemic overproduction of GH in transgenic mice – either due to ectopic expression of heterologous GH genes or to stimulation of endogeneous GH release by expression of a GH-releasing hormone transgene – regularly leads to a typical spectrum of renal alterations (Wolf and Wanke, 1997). These lesions were first reported in 1988 in MT-hGH (Brem and Wanke, 1988) and MT-bGH transgenic mice (Doi et al., 1988) and subsequently found in many different lines of GH transgenic mice (Wanke et al., 1991; Wanke et al., 1992).

Transgenic mice overexpressing the bovine growth hormone (bGH) under the transcriptional control of the rat phosphoenolpyruvate-carboxykinase-promoter (PEPCKbGH), which were used in this study, were first described by McGrane (1988). These GH transgenic mice display high serum levels of heterologous GH (Wolf et al., 1993). A markedly stimulated overall body growth is the most obvious phenotypical effect of high serum levels of GH. From three weeks of age onwards, GH transgenic mice display an increased body weight as well as visceromegaly and disproportionate skeletal gigantism (Wanke et al., 1992). They also demonstrate a typical spectrum of pathomorphological alterations of inner organs, with the kidney and liver being predominantly affected (Wanke et al., 1991; 1996). In the mouse systemic overexpression of GH leads to a typical spectrum of kidney alterations and results in chronic renal failure progressing to end-stage renal disease (Wolf and Wanke, 1997). Both, morphological and clinical-chemical findings indicate renal failure as the primary cause of shortened lifespan of GH transgenic mice (Wolf et al., 1993). Initial changes include renal and glomerular hypertrophy. Glomerular enlargement, which is overproportional in relation to both kidney and body weight, is progressive with age and associated with the development of glomerulosclerotic lesions (Wanke et al., 1991; 1992). Hypertrophic changes of glomeruli include mesangial extracellular matrix expansion, growth of glomerular capillaries and proliferation of endothelial as well as mesangial cells. These findings are associated with increased proteinuria as well as a variety of tubulo-interstitial changes (Wanke et al., 1993). End-stage renal lesions are characterised by a marked atrophy of nephrons, tubulocystic alterations, interstitial fibrosis and diffuse segmental or global sclerosis and/or hyalinosis of remnant glomeruli (Wanke et al., 1996; Wanke et al., 1992).

Glomerular lesions, especially mesangial lesions, in GH transgenic mice were found to bare strong resemblance to those observed in human diabetic glomerulosclerosis (Doi et al., 1988).
Thus, GH transgenic mice represent a valuable and well characterised model to study the pathogenesis of glomerulosclerosis and the mechanisms involved in the progression of chronic renal failure.

2.4.2 GIPR^{dn} transgenic mice

Transgenic mice expressing a dominant negative glucose dependent insulinotropic polypeptide receptor (GIPR^{dn}) were created by Volz (1997). The cDNA of the human GIP receptor was mutated in the region, coding for the third intracellular loop, by introducing a point mutation at amino acid position 340 (Ala → Glu) and a deletion of 8 amino acids (position 319 – 326). This sequence of G-protein coupled seven-transmembrane receptors is essential for signal transduction (Lefkowitz and Caron, 1988). Studies in stably transfected CHL-cells could show unchanged binding affinity of the mutated GIP receptor, but no increase in cAMP levels and thus no induction of signal transduction. Therefore, this receptor fulfilled all demands of a dominant negative receptor and was then chosen for generating transgenic mice. GIPR^{dn} transgenic mice were recently characterised clinically and pathomorphologically (Herbach, 2002; Herbach et al., 2005). They were found to develop severe early onset diabetes mellitus, characterised by hyperglycemia, hypoinsulinemia, polydipsia, polyuria and hyperphagia. The onset of diabetes mellitus in these mice was found to occur between 14 and 21 days of age. Fasting and postprandial blood glucose levels were significantly elevated in transgenic mice in comparison to healthy control mice, while serum insulin concentrations were significantly lower (18.8-fold in male transgenic mice and 6.1-fold in female transgenic mice), demonstrating an absolute insulin deficiency. Total volumes of pancreatic islets and beta-cells were dramatically reduced due to a disturbed development of the islets. In addition, GIPR^{dn} transgenic mice showed a drastically reduced life-span (Herbach, 2002). Studies of the kidneys indicate that GIPR^{dn} transgenic mice develop kidney lesions which resemble early diabetes-associated kidney alterations of diabetic humans. GIPR^{dn} transgenic mice show renal and glomerular hypertrophy. Additionally, glomerular lesions include mesangial expansion with accumulation of extracellular matrix, focal segmental glomerular hyalinosis as well as focal adhesions between the glomerular

tuft and the capsule of Bowman. Tubulo-interstial lesions include tubular atrophy, interstitial fibrosis and signs of proteinuria (Herbach, 2002; Herbach et al., 2003; Schairer, 2006).
In conclusion, GIPR^{dn} transgenic mice are a valuable model for studying diabetes-associated kidney lesions.

2.5 Proteomics

The proteome is defined as the set of all expressed proteins in a cell, tissue or organism (Pennington et al., 1997) and proteomics can be defined as the systematic analysis of this set of proteins for their identity, quantity and function (Peng and Gygi, 2001). Quantitative alterations are addressed in differential proteomic analyses. Characteristics and behavior of a biological system are to a high extent modulated by biochemical processes on the protein level. The concentration of individual proteins in cells or biological fluids is mainly the result of four very complex processes: (i) protein synthesis, (ii) protein processing, (iii) protein secretion, and (iv) protein degradation (Frohlich et al., 2006). As a consequence, systematic quantitative predictions of protein populations are impossible from genomic or transcriptional data. Therefore, studies on the proteome level have become an indespensible approach in the field of medicine, biochemistry, animal health and agricultural sciences (Frohlich et al., 2006; Gygi et al., 2000).
One of the most important technologies used for proteomics is the two-dimensional gel electrophoresis (2DE), which was introduced by O'Farrell and Klose in 1975 (Klose, 1975; O'Farrell, 1975). Proteins are separated in the first dimension by their isoelectric point and by their molecular weight in the second dimension.
Concerning protein identification great advances could be achieved by two ionisation techniques in mass spectrometry, the matrix assisted laser desorption ionisation (MALDI) developed by Koichi Tanaka in 1985 (Tanaka et al., 1988) and the electrospray ionisation (ESI) developed by John B. Fenn in 1988 (Mora et al., 2000). Both researchers were awarded the 2002 Nobel Prize in chemistry and their techniques are routinely used since the end of the 1990s. The overall growth of proteomics has increased dramatically over the last few years and the use of proteomic tools in renal research has been roughly proportional to it (Janech et al., 2007).

2.5.1 2D-gel electrophoresis

The two-dimensional polyacrylamide gel electophoresis (2DE) is a powerful and commonly used strategy in proteomic analyses. It enables the separation of complex protein mixtures according to their isoelectric point in the first and according to their molecular weight in the second dimension. Routinely, about 2000 different proteins can be separated in a single gel experiment. Its resolution and separation power is unreached even today, and therefore 2DE still represents a state-of-the-art technique (Gorg et al., 2004). In a 2D-gel specific information about a protein spot is available (isoelectric point and molecular weight), which can later be used to validate mass spectrometry identifications (Peng and Gygi, 2001). However, there are also some limitations of 2DE. Specific groups of proteins are known to be excluded or under-representated in 2DE. Very large and very small proteins as well as highly acidic or basic proteins are difficult to separate. The isoelectric focussing (IEF) step is incompatible with ionic detergents, such as sodium dodecyl sulphate (SDS), which are required for a full solubilisation of proteins. Very hydrophobic proteins can not sufficiently be solubilised and therefore not be detected in a gel. But also some solubilised proteins may precipitate due to increasing concentrations during the IEF step. This hinders a separation in the second dimension (Lilley and Friedman, 2004). One of the challenges in identifiying proteins in a complex proteome, such as human or animal proteome, is the presence of proteins in wide dynamic concentration ranges. Differences in the concentration of proteins in a cell may be over thousands to a million times. Hence, a large percentage of the expressed proteins are low abundant, for example about 80 % of the whole proteome in yeast, and might not be detected without pre fractionation or enrichment (Ahmed and Rice, 2005; Pedersen et al., 2003).

Following electrophoretic separation, staining of proteins is necessary for detection and quantification. Three principal staining techniques are commonly used, which differ in their sensitivity and linear dynamic range: Coomassie staining, silver staining, and fluorescent SYPRO stains (Gade et al., 2003). Coomassie is regarded as a less sensitive stain. Silver staining is a very sensitive stain, but it does not allow reliable quantification (Gorg et al., 2004). Both staining methods have a limited dynamic range of only one to two orders of magnitude. Fluorescent SYPRO stains, in particular SYPRO Ruby, are popular, because of the easy staining procedure, high

sensitivity and a theoretical linear dynamic range of about four orders of magnitude (Nishihara and Champion, 2002). All of these non-covalent staining techniques have in common that protein staining is performed after electrophoretic separation. In contrast, the 2D difference gel electrophoresis (2D-DIGE) is carried out by a covalent labelling of protein samples with different fluorescent dyes prior to the electrophoresis, enabling different samples to be co-separated on one gel. 2D-DIGE is improving the reproducibility and reliability of differential protein expression analysis between samples, while sensitivity and dynamic range are comparable to SYPRO stains (Alban et al., 2003; Gade et al., 2003).

2.5.1.1 Two-dimensional difference gel electrophoresis

The two-dimensional difference gel electrophoresis (2D-DIGE) was developed by Ünlü and colleagues and is an advancement of the classic 2DE (Unlu et al., 1997). It allows an improved quantitative analysis of a complex protein mixture. Up to three samples are labelled prior to IEF with different fluorescent CyDyes and afterwards run on the same 2D-gel under identical conditions. Due to individual excitation and emission wavelengths of the CyDyes three different images representing three different samples can be obtained from a single 2D-gel. There are two labelling techniques available, minimal and saturation labelling. Using minimal labelling the CyDyes are covalently bound to the ε-amino groups of lysine of the proteins. The amount of the added dye ensures that only 1 – 2 % of the available lysines are labelled, i.e. only a fraction of the molecules of an individual protein species is labelled at all. A so-called internal pooled standard (IPS) consists of aliquots of all samples analysed within a study. The IPS is used to normalize protein abundance measurements of each spot across multiple gels in an experiment (Alban et al., 2003). It is run on each gel and represents the average of all the samples being analyzed and ensures all proteins present in the samples are represented. For example, in one gel a transgenic and a wild-type sample (labelled with Cy3 and Cy5) plus the IPS (labelled with Cy2) are run together. Therefore, qualitative and quantitative comparison between the gels is improved and gel to gel variations are compensated (Gade et al., 2003). The number of gels in an experiment can be reduced by at least a factor of two because two different samples can be run in one gel. Moreover, covalent labelling allows a better quantification of spot abundancies. A further technique, referred to as “saturation labelling” targets all of the present

cysteine residues, thereby allowing the detection of very low protein amounts, i.e. approximately 2 µg/image. This technique is especially suitable for the analysis of scarce samples (Greengauz-Roberts et al., 2005; Shaw et al., 2003). The general workflow of a 2D-DIGE experiment used in this study mainly consists of four steps: Labelling and mixing of the protein samples, 2D-gelelectrophoresis and subsequent acquisition of the scanned images, software-assisted differential image analysis including quantitation and finally identification of the proteins of interest by mass spectrometry.

2.5.2 Mass spectrometry (MS)

From the two soft ionisation techniques mentioned in chapter 2.5 (MALDI and ESI) MALDI analysis is commonly performed to identify proteins in 2D-gel spots. MS-analysis of proteins is typically performed on the level of peptides, because the m/z-resolution reached with a mass spectrometer (about 4000 Da), is insufficient for an exact discrimination of whole proteins (Lottspeich, 2006). After a tryptic digest of the proteins, the analyte is spotted onto a MALDI plate together with a so-called matrix. The matrix used in the present study was α-cyano-4-hydroxycinnamic acid, enabling the ionization of a peptide by a number of laser impulses. Pulsed laser radiation is primarily absorbed by the matrix and then causes desorption and ionisation of the analyte.

In cases where the sample consists of a single protein, a very simple and fast strategy called peptide mass fingerprinting (PMF) (Henzel et al., 1993; 2003) is frequently applied. The technique is based on exact measurement of the peptide masses, followed by a comparison of these values with theoretical peptide masses in protein databases. The mass to charge ratio (m/z value) is in many cases not unique for a peptide, and therefore per se usually not sufficient for an unambiguous peptide or protein identification. The PMF method therefore depends on the assumption that all or at least the majority of peptide fragments are derived from a single protein species, thereby identifying the protein on the basis of several peptide masses. Tandem mass spectrometry or MS/MS is performed to generate additional information on the peptide ions and thereby complement the yield of protein identifications achieved by PMF analysis alone. In the first MS step the mass of the intact peptide, the so called precursor ion, is determined from the PMF spectrum. For the second MS step these precursor ions are isolated from all other peptide ions in

the instrument and dissociated into fragments. Peptide ions disintegrate under suitable energetic conditions at the peptide bonds in a rather controlled manner, leading to a set of C-terminally (y-ions) and N-terminally (b-ions) shortened peptide ions which give rise to sequence specific MS/MS spectra (Frohlich and Arnold, 2006). The most common fragmentation technique for peptide ions is the collision induced dissociation (CID) (Hayes and Gross, 1990; McLuckey, 1992) where peptide ions collide with inert gas atoms or molecules (He, Ar, N2, etc.). The MS/MS spectra obtained are then correlated with theoretical MS/MS spectra calculated from sequence databases. The sequence of the database peptide with the best correlation to the experimental spectrum serves as ‘‘sequence tag’’ for the identification of the corresponding protein.

As an alternative method to 2D gel separation LC-MS/MS analysis can be performed. Here liquid chromatography is directly coupled to a mass spectrometer, frequently using ESI as ionisation method. Peptide mixtures are first concentrated and separated by a reversed phase chromatography and the eluate is directly administered to the mass spectrometer (Frohlich and Arnold, 2006). During ESI ionisation, the liquid sample flows through a thin needle, and by application of high voltage the small droplets are charged and a very fine spray is generated. During the passage from the needle to the MS instrument the solvent is evaporated and the density of the charges within the droplets rises, causing a so called ‘‘Coulomb explosion’’, which results in charged analyte molecules. In cases of peptides these ions are commonly multiply charged. Peptide ions of interest are analysed by MS/MS analysis. In contrast to 2DE, with this method hydrophobic proteins and proteins with isoelectric point (pI) <3 or >10 can also be identified.

2.5.3 Proteomics in nephrology

Currently renal and urinary proteomics are performed to better understand renal physiology as well as to explore the complexity of disease mechanisms and renal pathophysiology (Thongboonkerd and Malasit, 2005). Renal proteomics is a rapidly growing field. Proteomic techniques have been used to examine the protein expression in the entire kidney or of isolated renal structures as well as to compare protein expression between different regions of the kidney (Janech et al., 2007).

One approach has been to create 2D proteome maps, that could be used as a reference for the same type of cell, tissue or sample for further studies, in which

additional mass spectrometry analysis would not be required, because protein spots on the gel had already been identified (Thongboonkerd, 2004). This must be seen from a critical point of view. Regarding the difficulties existing in every laboratory to generate positionally identical 2D gels, it is very unlikely that this method can be successful (Tonge et al., 2001). Even if one could refer to a spot with a presumably identical position, there wouldn't be a proof whether the formerly identified protein in the spot were identical as well. Due to comigration of proteins with the same pI and molecular mass in a 2D gel, the presence of several proteins in one spot is not unusual. Therefore, it can't be known just from the position in the gel which protein is present in the spot and eventually responsible for differential abundancies (Peng and Gygi, 2001). Nevertheless, these qualitative proteome maps can be used to get an overview which proteins may be present in a certain tissue or cell.

A number of qualitative maps of renal protein expression have already been created. A first 2D-gel based proteome map of human kidney cortex was established in 1997 in the SWISS-2DPAGE database (Sarto et al., 1997). With the accessibility of mass spectrometric protein identification this list has recently been expanded (Magni et al., 2005). Proteins from rat kidney cortex and medulla have been compared in two studies. Differences between the cytosolic fractions of cortex and medulla could be shown and in addition maps of cortical and medullary proteomes were established (Witzmann et al., 1998). A map of cortical and medullary proteins using whole cell lysates instead of cytosolic fractions has been published in 2002 (Arthur et al., 2002). These authors could also identify proteins with differential abundance between cortex and medulla. In another study proteome maps of several bovine tissues including the kidney could be created (D'Ambrosio et al., 2005). Concerning murine tissue, a 2D-gel based proteome map of kidneys from FVB mice has been established (Thongboonkerd et al., 2004). In this context it must be mentioned, that identical lysis and experimental conditions are crucial for the creation of identical 2D-gels. Kidneys of different mouse strains can look completely different as noticed by the same group in a later study (Thongboonkerd et al., 2006).

Comparison of protein abundances between different renal compartments or isolated structures as well as diseased versus healthy or transgenic animal models versus their wild-type controls is a powerful tool of proteomic analysis. Based on the results of these holistic approaches the formulation of new hypotheses may become possible which could be subject to further studies. An example is a comparative

proteomic analysis of kidneys from rats that had been exposed to episodic hypoxia (EH) (Thongboonkerd et al., 2002a). After 30 days of EH seven proteins were found to be differentially expressed in the kidney, revealing alterations in the renal kallikrein pathway. This led to the hypothesis that EH-induced hypertension would be at least in part a result from altered regulation of the renal kallikrein system. Most recently, changes in the expression of renal proteins associated with hypokalemic nephropathy induced by a K^+-depleted diet have been demonstrated in mice (Thongboonkerd et al., 2006). The identified differentially abundant proteins were mainly metabolic enzymes, signalling proteins and cytoskeletal proteins. In another study the renal proteome of a transgenic mouse model, which displays characteristics of type 1 diabetic nephropathy, with that of non-diabetic FVB mice was compared (Thongboonkerd et al., 2004; 2005). Initially, the focus was laid on coordinated changes of the monocyte/neutrophil elastase inhibitor (MNEI, increased) and elastase IIIB (decreased). An increased tubulointerstitial deposition of elastin as a hypothesized result of these changes could be confirmed by immunhistochemistry (Thongboonkerd et al., 2004). A second focus was laid on the protein with the greatest difference in abundance, the calcium-binding protein calbindin-D28k (Thongboonkerd et al., 2005). Increased expression in the kidneys of diabetic mice could be confirmed by Western blot analysis. Localization of increased expression of calbindin-D28k in tubular epithelial cells could be demonstrated by applying immunhistochemistry. The authors suggest that these results may indicate a compensatory mechanism for normalisation in tubular calcium reabsorption in diabetes.

In a very recent study 2DE combined with mass spectrometry was used to identify changes in protein expression patterns in the renal cortex of the *db/db* mouse, an animal model of type 2 diabetes (Tilton et al., 2007). Numerous diabetes-dysregulated proteins which modulate metabolism, catabolism, and biosynthesis were identified, including a high percentage of mitochondrial proteins. Another example for studying changes in proteomes in genetic models of diseases has been published recently (Valkova et al., 2005). The renal proteomes of jck mice, a model for autosomal recessive polycystic kidney disease, were compared to those of their wild-type littermates. An increase in abundance of three proteins, namely galectin-1, sorcin, and vimentin, could be shown in the polycystic kidneys. A relation of these

differences to the signalling and structural processes in the primary cilium of renal epithelial cells was proposed (Valkova et al., 2005).

Proteomic analyses of protein changes in the entire kidney give a good overview, but may not reveal specific processes in certain intrarenal structures. Subproteome analyses of these structures (e.g. glomeruli, tubular system, collecting duct) may be the method of choice to get a deeper insight in physiological as well as pathophysiological processes.

Proximal tubules play a major role in phosphorus homeostasis. Therefore, one approach examined the effect of dietary phosphorus restriction on protein expression in rat renal proximal tubules by 2DE (Cheung et al., 2002). Six differentially abundant proteins could be found and a general decrease in the number of protein species expressed in samples with phosphate restricted diet was observed. In a very recent study the adaptive responses of rat renal proximal tubules to metabolic acidosis were analysed by applying the 2D-DIGE technique (Curthoys et al., 2007). Well-characterised adaptive responses in glutaminase, glutamate dehydrogenase, and phosphoenolpyruvate carboxykinase could be confirmed. Additionally, previously unrecognised adaptive response proteins that differed in their abundance were found.

Some studies focused on the inner medullary collecting duct (IMCD), in which the final urine concentration takes place. It is involved as major site in vasopressin-mediated water and urea reabsorption (Janech et al., 2007). A standardised approach for isolation of native renal IMCD cells from rat kidneys was developed and its applicability for proteomic analysis was demonstrated in 2004 (Hoffert et al., 2004). A differential analysis using 2D-DIGE without internal standardization revealed 50 proteins that showed an increased abundance in the IMCD cells compared to non-IMCD cells, including enzymes, structural proteins, and signalling intermediates, as well as 35 proteins, being decreased in their abundance in IMCD cells compared to non-IMCD cells. The actions of vasopressin in the IMCD of the Brattleboro rat, which lacks endogeneous vasopressin, were also investigated by 2D-DIGE analysis without internal standardization (van Balkom et al., 2004). The authors could show differences in protein expression in vasopressin treated rats compared to non-treated animals. Some of the changes were confirmed by immunoblot analysis. In their results the authors see a role for vasopressin in the coordinate regulation of several determinants of nitric oxide levels and of proteins potentially involved in escape of the

antidiuretic action of vasopressin ("vasopressin escape"). Another study could reveal a protein regulatory network activated in vasopressin escape by applying both proteomics and pathways analysis (Hoorn et al., 2005). This approach enabled the identification of differentially expressed, mostly high-abundant proteins by DIGE. These proteins were taken for pathway analysis and additionally, the identification of relatively low-abundant proteins not detected in the 2D-DIGE analysis could be achieved. The investigators could reveal a "dominant regulatory protein network" in IMCD cells altered in association with vasopressin escape.

2.5.3.2 Urinary proteomics

Urinary proteomics is becoming an important field in nephrology. Urine samples, especially from humans, are easy to obtain and no invasive methods like a biopsy is needed. A better understanding of tubular and glomerular responses to physiological as well as to pathophysiological stimuli can be achieved by examining changes in urinary protein excretion (Thongboonkerd and Malasit, 2005). Like in the other applications of renal proteomics, several proteome maps of normal human urine have been created with gel-based (Bueler et al., 1995; Marshall and Williams, 1996; Oh et al., 2004; Thongboonkerd et al., 2002b) or gel-free (Adachi et al., 2006; Heine et al., 1997; Spahr et al., 2001; Wittke et al., 2003) approaches. In a recent gel-free approach it could be shown that the urinary proteome is unexpectedly complex, containing more than 1500 proteins (Adachi et al., 2006). Many studies on different physiological as well as pathophysiological situations have been published (Gonzalez-Buitrago et al., 2007; Thongboonkerd and Malasit, 2005). Some studies focused on changes in urinary proteins during diabetic nephropathy. One approach has been to identify specific urinary polypeptide patterns for healthy and diseased subjects (Mischak et al., 2004). Using a gel-free method the authors were able to differentiate "normal" (urine from healthy subjects), "diabetic" (diabetic and normoalbuminuric) and "diabetic renal damage" (diabetic with higher grade albuminuria) polypeptide patterns. Another study compared urine from diabetic patients with overt proteinuria with control urine by 2D-DIGE analysis (Sharma et al., 2005). Among the differentially abundant proteins, an increase in alpha 1 antitrypsin which was shown to be up-regulated in areas of renal fibrosis by immunostaining could be identified. In urine samples of microalbuminuric diabetic patients Jain and

colleagues (2005) could show the presence of additional proteins which could be used as markers for specific and accurate clinical analysis of diabetic nephropathy.

2.5.3.3 Glomerular proteomics

Analyses of renal subproteomes are crucial for a better understanding of kidney physiology and pathophysiology, because the kidney consists of many functional compartments, and specific protein patterns or changes in abundance can't be distinguished in whole kidney lysates. Especially for glomeruli, which only comprise about 2 – 4 % of the whole kidney volume in different species (Artacho-Perula et al., 1993; Nyengaard and Bendtsen, 1992; Wanke, 1996), such an approach is very useful. Despite this fact only a very limited number of studies on glomerular proteomics have been performed so far. Like on the whole kidney level the establishment of qualitative proteome maps to contribute to further proteomic studies has been one aspect of glomerular proteomics. An extensible markup language (XML)-based database of human glomeruli, which had been profiled by 2DE, has been constructed recently (Yoshida et al., 2005). Glomeruli were purified by a sieving method from morphologically unchanged kidney cortices of patients that had to undergo nephrectomy due to renal tumors. Cultured podocytes (Ransom et al., 2005) and cultured rat mesangial cells (Jiang et al., 2005) also served for the creation of 2DE based proteome maps. The podocyte proteome has been shown to be rich in cytoskeletal proteins and proteins involved in responses to cellular stress (Ransom et al., 2005).

Apart from the database construction only very few 2D-based proteomic studies have been performed on isolated glomeruli. Sitek and colleagues (2006) obtained murine glomeruli by magnetic isolation and compared the glomerular with the cortical proteome using 2D-DIGE saturation labelling. They could show significant differences between the expressed proteins in glomeruli and kidney cortex. In addition they could demonstrate that only ten human glomeruli (0.5 µg protein) picked by laser capture microdissection (LCM) were sufficient to visualize an appropriate number of spots on a 2D-gel. Very recently, the glomerular proteome of *db/db* diabetic and *db/m* non-diabetic mice was compared by 2DE (Barati et al., 2007). 40 protein spots showed an increased abundance in glomeruli of diabetic mice and 32 of them could be identified, suggesting the definition of altered cellular redox pathways and advanced glycation end product (AGE) metabolism.

As the mesangium plays an important role in glomerulosclerosis, some studies focused on 2D-gel based proteomic analyses of cultured mesangial cells. Stress-induced chaperone proteins could be identified as targets of Akt phosphorylation in rat mesangial cells (Barati et al., 2006). The serine-threonine kinase Akt plays a role in mesangial cell apoptosis, proliferation and hypertrophy. Cells were treated with Akt, and their proteins were afterwards separated by 2D PAGE and identified by mass spectrometry. Data suggest that Akt phosphorylation of stress-induced chaperones may contribute to mesangial cell proliferation or hypertrophy during glomerular diseases. S-Nitrosylation, another post translational modification, had been the focus for a proteomic analysis of s-nitrosylated proteins in murine cultured mesangial cells (Kuncewicz et al., 2003). Mesangial cells were treated with nitric oxide (NO), s-nitrosylated proteins were isolated with a method called “biotin-switch” and a 2D-based proteomic analysis followed. Target proteins could be identified by MALDI-TOF MS.

A differential proteomic analysis was performed of control and dexamethasone-treated cultured murine podocytes treated with dexamethasone in order get an insight into the mechanisms of glucocorticoids as primary treatment in the nephrotic syndrome (Ransom et al., 2005). Cultured murine podocytes were chosen as target, because the podocyte is the most affected kidney cell during the development of nephrotic syndrome. Six differentially abundant proteins, three of which were known to play roles in protection of cells from injury, were revealed. This led the authors to the conclusion that glucocorticoids could have a direct effect on podocytes.

A different approach in analyses of glomerular proteomics is the use of mass spectrometry without 2DE. One study focused on IgA nephropathy (IgAN), which is one of the most common glomerular diseases in human beings worldwide. Mass spectrometry was applied to analyse the O-glycan structure in IgAN and an underglycosylation of IgA1 deposited in glomeruli could be shown, which might play an essential role in glomerular deposition of IgA1 molecules (Yasuda et al., 2004).

In another study, in which mass to charge ratio (m/z) profiles originating from non-digested proteins of glomeruli isolated by lasercapture microdissection were directly acquired by MALDI-TOF mass spectrometry (Xu et al., 2005). Glomeruli were obtained from a 5/6 nephrectomy (Nx) rat model of focal segmental glomerulosclerosis. A comparison of the different m/z profiles revealed clearly distinguishable patterns of glomeruli taken at the day of nephrectomy versus

nonsclerotic glomeruli and sclerotic glomeruli. A close relation between patterns of sclerotic and nonsclerotic glomeruli suggested an early activation of prosclerotic mechanisms in seemingly intact glomeruli.

Taken together, there is still an enormous need for further studies to reveal mechanisms involved in pathophysiology and pathogenesis of glomerulosclerosis. Transgenic mouse models and the recent progresses in proteomic technologies are excellent tools for the performance of a differential analysis of the glomerular proteome. Therefore, the aim of the present study was to identify changes in the glomerular proteome of two murine models of nephropathy at early stages of glomerulosclerosis by performing a 2D-DIGE based proteomic analysis.

3. Animals, material and methods

3.1 Experimental design

In order to reveal, whether common characteristic patterns of morphological and functional glomerular alterations, displayed by both GIPR^{dn} or GH transgenic mice (refer to chapters 2.4.1 and 2.4.2), would result in common changes in the abundance of proteins, a quantitative differential proteomic analysis was performed on samples of isolated kidney glomeruli. The glomeruli were derived from male GH transgenic as well as GIPR^{dn} transgenic mice and their corresponding sex-matched wild-type littermate controls. Sample materials were generated from pairs of animals, consisting of one transgenic mouse of the respective mouse model and its corresponding control animal. For the generation of sample material, both animals of one pair were dissected at the same day of age. Investigations were performed at two defined stages of early glomerular alterations. These were glomerular hypertrophy (stage 1) and glomerular hypertrophy together with a beginning albuminuria (stage 2), respectively. GH transgenic and control mice were analysed at both stages. GIPR^{dn} transgenic and control mice were only analysed at stage 2. In order to enable a meaningful interpretation of the results of the proteomic analysis the setting of stringent criteria for the assignment of mice/glomerulus samples to stage 1 as well as stage 2 was a crucial prerequisite. Before the glomerulus isolation the absence (stage 1) or presence (stage 2) of albuminuria in mice of both mouse models had to be determined. This was done by recurrent performance of sodium dodecyl sulphate (SDS) polyacrylamide gel electrophoresis (PAGE)-based urine protein analysis. GH transgenic animals in stage 1 as well as the control animals for both groups in stage 1 and 2 had to show an absence of albuminuria. For stage 2 transgenic mice had to exhibit persistent albuminuria. These results were confirmed by Western blot and ELISA experiments. All mice fulfilling these criteria were taken for glomerulus isolation. Transgenic animals in stage 1 and 2 had to further display a significant increase of the mean glomerular volume as compared to their corresponding controls. The mean glomerular volume was estimated by methods of quantitative stereology, using histologic samples of kidney tissue that were taken before glomerulus isolation. Transgenic mice fulfilling the respective criteria and their corresponding controls were selected for differential proteomic analysis. Because the

determination of the glomerular hypertrophy was performed after glomerulus isolation, more mice were dissected than finally were taken for the proteomic analysis. From the glomerulus samples of the selected mice protein was extracted and a proteomic analysis was performed using the 2D-DIGE technique. Differentially abundant proteins were determined by DeCyder software analysis. Identification of the proteins was carried out by applying MALDI-TOF/TOF mass spectrometry analysis. The summarised experimental design of the study is displayed in **Fig. 3.1**.

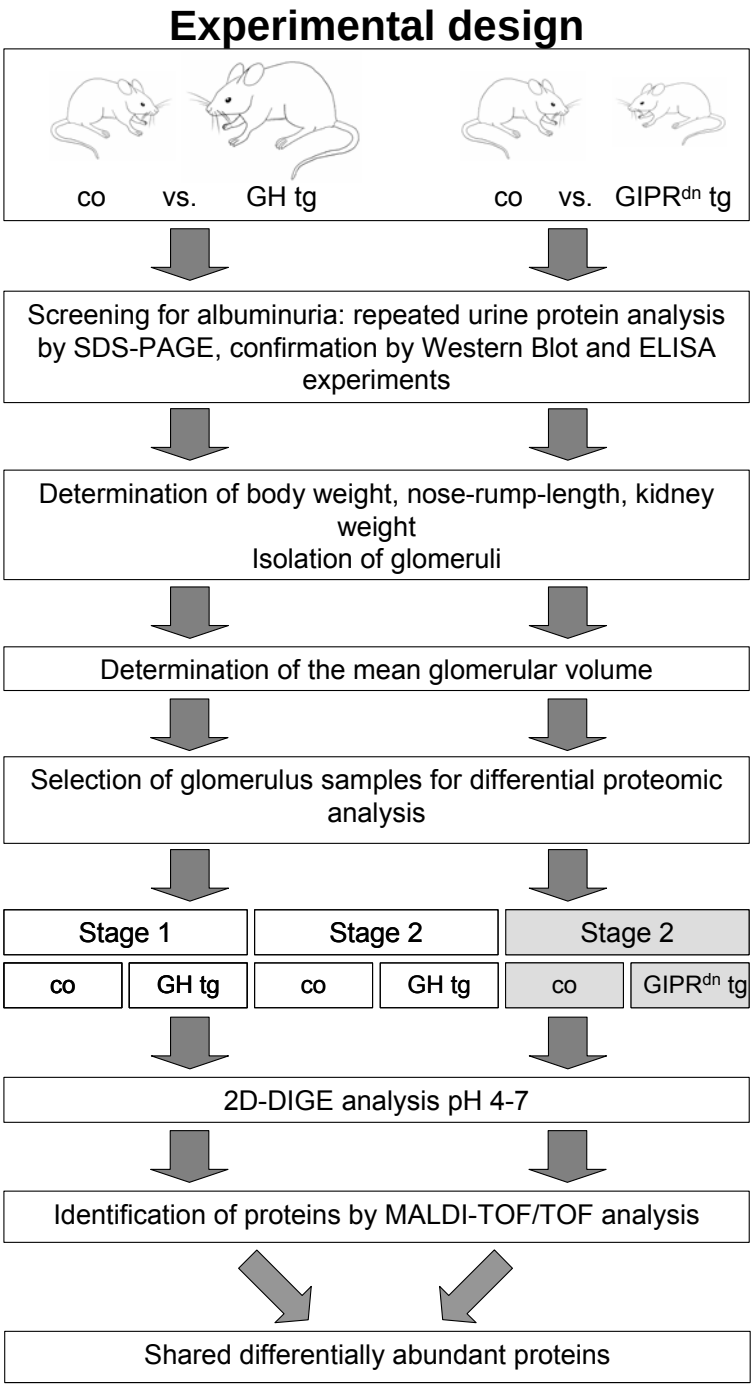

Fig. 3.1: Experimental design of the study

3.2 Animals

3.2.1 Breeding, animal husbundary and numbers of mice used for analyses

The generation of PEPCKbGH transgenic mice is described elsewhere in detail (McGrane et al., 1988; Wolf et al., 1993). PEPCKbGH transgenic mice were maintained on a NMRI genetic background. They will refered to as GH transgenic mice in the following sections. GIPR^{dn} transgenic mice were generated as previously described (Herbach, 2002; Herbach et al., 2005; Volz, 1997) and maintained on a CD1 genetic background. In both groups male hemizygous transgenic mice were mated to female wild-type mice (Charles River Laboratories, Germany) of the respective genetic background (NMRI and CD1, respectively). For all investigations in this study only male transgenic mice and age-matched wild-type littermate controls were used. All mice were maintained under standard (non-barrier) conditions (21±1°C, 55±3% relative humidity; 12/12-hours light/dark cycle) and were fed standard rodent chow (Altromin C1324, Germany) and tap water ad libitum. All animal experiments were performed in accordance with institutionally approved and current animal care guidelines. At an age of three weeks, animals were weaned, separated according to gender, marked by piercing the ears, and tail tip biopsies were taken for genetic analysis. All male mice in a litter were screened for albuminuria which included repeated taking of spot urine samples and determination of their creatinine concentration. On the whole, 36 litters were screened, 15 in the group of GH tg and co mice, representing 37 tg and 40 co mice, and 21 in the group of GIPR^{dn} tg and co mice, representing 49 tg and 53 co mice, respectively. All 102 mice in the group of GIPR^{dn} tg mice and controls were used for determination of glucosuria. Glomeruli were isolated from 55 of 77 screened animals in the group of GH tg mice and controls (29 tg and 26 co mice) and of 45 of 102 screened animals in the group of GIPR^{dn} tg mice and controls (23 tg and 22 co mice), respectively. All mice used for glomerulus isolation were also used for the determination of body weight, nose-rump length and kidney weight and quantitative stereological analysis was performed to determine the mean glomerular volume. Of these mice 20 in the group of GH tg mice and controls (5 tg and 5 co in stage 1; 5 tg and 5 co in stage 2) and 18 in the group of GIPR^{dn} tg mice and controls (9 tg and 9 co in stage 2) were used for the proteomic analysis. Glomerulus isolates from additional two GIPR^{dn} tg and two co mice were used to run preparative gels. Only the animals, that were taken

for the analytical gels in the proteomic analysis, are included in the results presentation.

3.2.2 PCR-Analysis

Transgenic mice were identified by polymerase chain reaction (PCR) as previously described (Herbach et al., 2005; Hoeflich et al., 2001). For detection of the bGH transgene oligonucleotide primers with the following sequence were used:
5'-GGG ACA GAG ATA CTC CAT CC-3' sense (bGH #1)
5'-ATG CGA AGC AGC TCC AAG TC-3' anti-sense (bGH #2)
These primers bind to the bGH transgene. The PCR-product of the bGH consists of 343 base pairs (~pos. 1379-1722 of the bGH-transgene) (Hoeflich et al., 2001). For the identification of $GIPR^{dn}$ transgenic mice oligonucleotide primers with the following sequence were used:
5´-ACA GNN TCT NAG GGG CAG ACG NCG GG-3´ sense (Tra1)
5´-CCA GCA GNC NTA CAT ATC GAA GG-3´ anti-sense (Tra3)
These primers bind to both the human cDNA of the mutated GIP receptor and the endogenous murine GIP receptor. The primers were chosen from areas where the known DNA sequence of the human, rat, mouse and hamster GIP receptor is highly conserved. The mutated human GIP receptor and the endogenous murine receptor can be distinguished in the PCR by their number of base pairs. The PCR product of the murine GIP receptor contains about 500 base pairs, whereas the PCR-product of the mutated human GIP receptor consists of about 140 base pairs (Herbach et al., 2005).

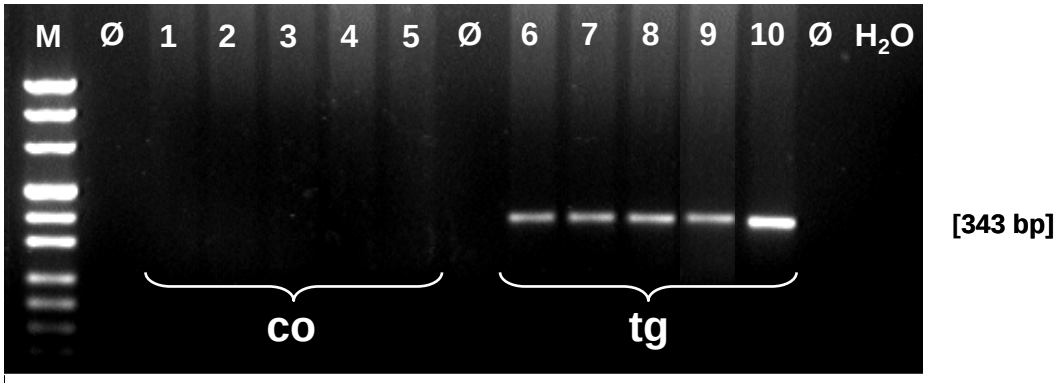

Fig. 3.2: PCR result of GH transgenic (tg) and control (co) mice. Samples of wild-type control animals show no PCR-product (lanes 1-5). GH transgenic animals exhibit a DNA-fragment of 343 base pairs (lanes 6-10). M: Fragment size marker (Puc Mix Marker 8, Fermentas, USA). Visible marker bands indicate fragment sizes of 1118, 881, 692, 489, 404, 331, 242, 190 and 147 base pairs from top to bottom. Ø: spacing line. H_2O: no template control.

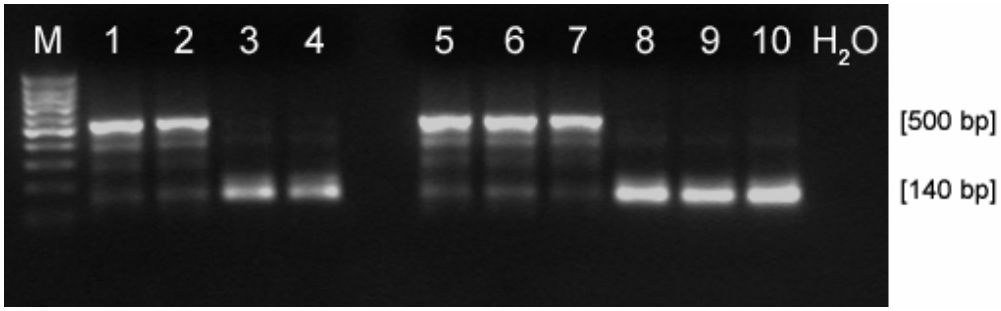

Fig. 3.3: PCR result of $GIPR^{dn}$ transgenic (tg) and control (co) mice. Samples from wild-type control mice show a PCR-product of 500 base pairs (endogeneous GIP receptor, lanes 1, 2, 5-7). $GIPR^{dn}$ transgenic mice exhibit a PCR-product of 140 base pairs (mutated GIP receptor, $GIPR^{dn}$, lanes 3, 4, 8-10). M: Fragment size marker (Puc Mix Marker 8, Fermentas, USA). Visible marker bands indicate fragment sizes of 1118, 881, 692, 489, 404, 331, 242, 190 and 147 base pairs from top to bottom. H_2O: no template control.

a) Method

Tail tip biopsies of approximately 0.4 cm length were taken at weaning and stored at -80°C until assayed. For DNA extraction, the tail tip was incubated in 400 µl Mastermix over night in a heating block at 55°C.

Master Mix:

375 µl Cutting Buffer

20 µl 20 % SDS

5 µl Proteinase K (20 mg/ml)

Thereafter, undigested components were separated by centrifugation for two minutes at 15,000 rpm. The supernatant was poured into another Eppendorf cup, and 400µl isopropanol were added to precipitate DNA. The DNA pellet was washed twice with 900 µl 70% EtOH, the liquid phase was discarded and the DNA pellet was dried at room temperature. DNA was suspended in 100 – 200 µl 1*TE buffer, according to the size of the pellet when dried. To make sure that the DNA was dissolved completely, it was stored at 4°C for at least 24h before proceeding with the PCR.

19 µl of the Master Mix and 1 µl of the suspended DNA were mixed carefully in PCR-analysis cups (Eppendorf, Germany), which were then placed in a Mastergradient thermocycler (Eppendorf, Germany) and the program was run. DNA of a transgenic mouse was used as positive control, DNA of a wild-type control mouse was used as negative control, H_2O served as quality control. If needed, PCR samples were stored at -20°C until further use.

After amplification, 4 µl of 6* loading dye (MBI Fermentas, Germany) was added to each sample. Then the samples were transferred into the sample wells of a 2 % agarose gel containing 0.9 µl ethidium bromide per 100 ml (0.1 %), and was positioned in an Easy Cast™ gel chamber (PeqLab, Germany) filled with 1*TAE running buffer. At the beginning of the row 6 µl PUC Mix Marker # 8 (MBI Fermentas, Germany) was placed in a well in order to allow estimation of amplified fragment size. Electrophoresis was run for 45 minutes at 90 volt. The amplified products were visualised (Eagle Eye II, Stratagene, Germany) under UV light (306 nm) and a digital picture was taken to document the result (see **Fig. 3.2** and **Fig. 3.3**).

b) Materials

Cutting Buffer:

2.5 ml 1 M Tris-HCl (pH 7.5; Roth, Germany)
5.0 ml 0.5 M EDTA (pH 8.0)
1.0 ml 5 M NaCl (Applichem, Germany)
250 µl 1 M DTT (Roth, Germany)
127 µl Spermidine (500 mg/ml; Sigma, Germany)
Ad 50 ml aqua bidest

1*TE buffer:

10 mM Tris-HCl (pH 8.0) (Roth, Germany)

1 mM EDTA (Sigma, Germany)

Proteinase K (Roche, Germany): 20 mg/ml diluted in aqua bidest.

Primer concentration:

Tra 1, Tra 3: 10 pmol/µl each (Genzentrum/DNSynthese, Germany)

bGH 1, bGH 2: 2 µmol/µl each (Genzentrum/DNSynthese, Germany)

dNTP (Eppendorf, Germany): dATP, dGTP, dTTP, dCTP, 100 mM each

Master Mix for GH transgenic and control mice: PCR kit (Quiagen, Germany)

10* buffer	2.00 µl
$MgCl_2$	1.25 µl
Q-solution	4.00 µl
dNTP 1mM	4.00 µl
Primer sense	1.00 µl
Primer antisense	1.00 µl
H_2O	5.65 µl
Taq polymerase	0.10 µl

Master Mix for $GIPR^{dn}$ transgenic and control mice: PCR kit (Quiagen, Germany)

10* buffer	2.00 µl
$MgCl_2$	1.25 µl
Q-solution	4.00 µl
dNTP 1mM	4.00 µl
Primer sense	2.00 µl
Primer antisense	2.00 µl
H_2O	3.65 µl
Taq polymerase	0.10 µl

EDTA 0.5 M pH 8.0

146.1 g EDTA (Sigma, Germany)

Ad 1000 ml aqua bidest, adjust to pH 8.0 with NaOH (Merck, Germany)

50* TAE buffer

242 g Tris base (Roth, Germany)

57.1 ml glacial acetic acid (Roth, Germany)

100 ml 0.5 M EDTA pH 8.0

Ad 1000 ml aqua bidest.

1* TAE buffer

10 ml 50* TAE buffer

Ad 500 ml with aqua bidest.

Agarose gel (GIBCO BRL, Germany)

2 g Agarose / 100 ml 1* TAE buffer, add 9 µl/l ethidium bromide (0.1 %) (Merck, Germany)

Program for DNA amplification of GH transgenic and control mice

denaturation	94°C	4 min	
denaturation	94°C	1 min	35 cycles
annealing	58°C	1 min	
extension	72°C	1 min	
final extension	72°C	10 min	
cooling	4°C	∞	

Program for DNA amplification of GIPR^{dn} transgenic and control mice

denaturation	94°C	4 min	
denaturation	94°C	1 min	39 cycles
annealing	60°C	1 min	
extension	72°C	2 min	
final extension	72°C	10 min	
cooling	4°C	∞	

3.2.3 Detection of glucosuria

The diabetic phenotype of GIPR^{dn} transgenic mice was reconfirmed by detection of glucose in urine samples, using Ratiomed EASY Screen Glucose® sticks (Megro, Germany). Spot urine samples were recurrently taken from GIPR^{dn} transgenic mice

as well as from their non-transgenic wild-type littermate controls from day 21 on (time point of weaning) and investigated until glucosuria was detected in samples of $GIPR^{dn}$ transgenic mice.

3.3 Urine protein analysis

Repeated urine protein analysis was performed in order to document the absence of albuminuria in stage 1 and the onset of albuminuria in stage 2. For stage 1, one urine sample was collected on the day before sacrifice. In the group of GH transgenic and control mice stage 2 urine samples were collected every two days from 26 days of age onwards. In the group of $GIPR^{dn}$ transgenic and control mice urine samples were collected weekly from six weeks of age onwards. In both groups 24 hours after the first detection of albuminuria a second urine sample was collected and glomeruli were isolated from these animals and their corresponding wild-type controls, if albuminuria could be confirmed. All urine samples were always taken between four and five o'clock in the afternoon and immediately stored at -80°C until assayed. For qualitative analysis a sodium dodecyl sulphate polyacrylamide gel electrophoresis (SDS-PAGE) was performed. Gels with samples of $GIPR^{dn}$ transgenic mice were stained with silver staining and gels with samples of GH transgenic mice with Coomassie staining. In order to demonstrate the comparable results, additional SDS-PAGEs of urine samples taken the day before glomerulus isolation from GH transgenic mice and their corresponding controls, which were used for proteomic analysis, were run and stained with silver staining. A quantitative analysis of albuminuria of urine samples of animals used in the proteomic analysis was performed by using an enzyme linked immunosorbent assay (ELISA).

3.3.1 Sodium dodecyl sulphate polyacrylamide gel electrophoresis (SDS-PAGE)

a) Methods

Urine creatinine concentration was measured, using an automated analyzer technique (Hitachi, Merck, Germany). Urine samples were standardised by dilution with sample buffer to a constant creatinine content of 1.5 mg/dl for silver staining and 3 mg/dl for coomassie staining, respectively. A mouse albumin standard (1 mg/ml;

Biotrend, Germany) was diluted 1:50 for silver staining and 1:25 for coomassie staining, respectively, in sample buffer. A 12 % separating SDS-polyacrylamide gel was casted in a Mini-Protean III gel-casting chamber (Biorad, Germany), overlayed with distilled water and allowed to polymerise for 45 minutes. The 5 % stacking gel was cast on top of the separation gel and a comb for forming sample wells was inserted. The stacking gel was allowed to polymerise for 45 minutes. The comb was removed and the gel was placed into a Protean III electrophoresis cell (Biorad, Germany), which next was filled with running buffer. Protein was denatured by heating the diluted samples and the mouse albumin standard in a thermoblock TB1 (Biometra, Germany) for 10 min at 96°C. The samples, an additional broad range molecular weight standard (Biorad, Germany), and the mouse albumin standard were then loaded onto the gel and electrophoresis was run for 60 min at 200 volt. Subsequently, either a silver staining or a Coomassie blue staining was performed. Silver staining was performed due to a standard protocol (see 10.1 in the Attachment). For Coomassie staining the gel was at first stained with the Coomassie blue staining solution for 30 min and destained in the Coomassie destaining solution for approximately 1.5 hours until clear background. Visible protein bands were registered and gels were scanned for documentation (HP Office Jet G55, Germany). Finally, gels were dried for long-term storage using the DryEase™ Mini-gel Drying System (Invitrogen, Germany) according to the manufacturer's protocol.

b) Materials

Tris/HCl 0.5 M pH 6.8

6.075 g Tris base (Roth, Germany)

Ad 100 ml distilled water, adjust pH with 1N HCl (Merck, Germany)

Tris/HCl 1.5 M pH 8.8

18.5 g Tris base

Ad 100 ml distilled water, adjust pH with 1N HCl

Sample buffer

1 ml Distilled water

0.25 ml Tris/HCl 0.5 M pH 6.8

0.2 ml Glycerol (Merck, Germany)

0.4 ml SDS (Sigma, Germany) 10 %

0.125 ml Bromphenol blue (Sigma, Germany) 0.05 %

12 % SDS-polyacrylamide gel

3.5 ml distilled water

2.5 ml Tris/HCl 1.5 M, pH 8.8

100 µl SDS 10 %

4.0 ml Acrylamide 30 % (Roth, Germany)

50 µl Ammonium persulfate (Biorad, Germany) 10 %

10 µl Tetraethylethylenediamine TEMED (Roth, Germany)

5 % SDS-polyacrylamide gel

6.1 ml distilled water

2.5 ml Tris/HCl 0.5 M, pH 6.8

100 µl SDS 10 %

1.3 ml Acrylamide 30%

50 µl Ammonium persulfate 10 %

10 µl Tetraethylethylenediamine TEMED

Running buffer (stock)

30.3 g Tris base

144 g Glycine (Merck, Germany)

Ad 1 l distilled water

Running buffer (ready to use)

40 ml Stock solution

4 ml SDS 10 %

Ad 400 ml distilled water

Coomassie staining solution

625 mg Coomassie brilliant blue G250 (Merck, Germany)

12.5 ml 100 % acetic acid (AppliChem, Germany)

125 ml 100 % ethanol

Ad 250 ml distilled water

Coomassie destaining solution

17.5 ml 100 % acetic acid

12.5 ml 100 % ethanol

Ad 250 ml distilled water

3.3.2 Western blot analysis

In order to clarify whether a lane of approximately 67 kDa in the SDS-PAGE reflects albumin, Western blot analysis was performed from urine samples of two transgenic animals and corresponding controls of both groups investigated in stage 2, according to a standard protocol detailed below.

a) Method

Materials used are listed below.

For Western blot analysis, a 12 % SDS polyacrylamide gel was run as described above. After electrophoresis, gels were placed on a pre-wetted nitrocellulose membrane (Schleicher & Schüll, Germany) between three layers of absorbent paper imbibed with buffer, and fiber pads each side, and the Sandwich was set in the gel holder cassette. Two cassettes were placed into the electrode module, which was then inserted in the buffer lank along with a frozen cooling unit (Mini Trans-Blot Cell, Biorad, Germany). After filling the tank with Towbin buffer, the transfer was run over night at 30 Volt (Biorad Power PAC 300, Biorad, USA). The membranes were dyed with ponceau S solution (Sigma, Germany) to confirm blotting was sucessful. After washing in Tris-buffered saline (TBS, pH 8.3), blocking was performed in 1% bovine serum albumin (BSA, Sigma, Germany) for one hour to avoid non-specific binding of the antibody probe to the membrane. Incubation with rabbit anti-mouse albumin antibody probe (Biotrend, Germany; 1:300 in TBS-Tween and 1 % BSA) was performed for three hours. The membrane was incubated with horseradish

peroxidase conjugated goat anti-rabbit antibody (DAKO Diagnostika, Germany, 1:1000 in TBS-Tween and 1% BSA) for one hour. After washing three times in TBS-Tween for ten minutes, immunoreactivity was visualized using 3,3' diaminobenzidine tetra hydrochloride dihydrate (Biotrend, Germany) as chromogen. The membranes were scanned, dried and stored in a cassette.

b) Materials

Towbin buffer

3.03 g Tris base (Roth, Germany)
14.4 g Glycine (Merck, Germany)
200 ml Methanol (Roth, Germany)
800 ml distilled water
Storage at 4°C

Tris buffered saline (TBS) 10* stock solution

60.6 g Tris base (Roth, Germany)
87.6 g Sodium chloride (AppliChem, Germany)
Ad 1 l distilled water, adjust to pH 8.3 with 1N HCl (Merck, Germany)
Storage at 4°C

TBS-Tween

1* TBS (10* TBS stock solution diluted 1:10)
0.05 % Tween 20 (Sigma, Germany)

DAB (3,3’ diaminobenzidine tetrahydrochloride dihydrate)

5 ml DAB (Biotrend, Germany)
25 ml Tris/HCl 50 mM pH 7.3
10 µl Hydrogen peroxide, 30 % (Roth, Germany)

3.3.3 Determination of urinary albumin concentration by ELISA

In order to confirm the results obtained by SDS-PAGE analysis the concentration of urinary albumine in urine samples of all animals used in the proteomic analysis was determined by the Mouse Albumin Enzyme Linked Immunosorbent Assay (ELISA) Quantitation Kit Bethyl E90-134 (Bethyl, USA). All steps were performed at room

temperature. Nunc C bottom immunoplates (Kirkegaard and Perry, USA) were coated with 100 µl / well of the provided capture antibody for 60 min. After washing for three times with the wash solution 200µl blocking solution was added to each well and incubated for 30 min, followed by three washing steps. In the meantime the murine albumin standard dilutions were prepared according to manufacturer's protocol with sample diluent. The proper dilution of urine specimens ranged from 1:60 – 1:6000 (GH tg: 1:300 – 1:6000, GH co: 1:300 - 1:1500, $GIPR^{dn}$ tg: 1:60 – 1:1600, $GIPR^{dn}$ co: 1:300 – 1:600). Standards, samples and blanks were analysed in duplicates. For the first incubation step (60 min), 100 µl of the standard solutions and the diluted specimens were added to the coated wells of the ELISA plate. Then, the plate was washed for five times by aspiration. In a second incubation step (60 min), 100 µl of the provided horseradish peroxiase-conjugated detection antibody (diluted 1:100,000 in sample diluent) were added to each well. Next, the plate was washed as described above. Subsequently, the antibody-conjugate that bound to the albumin, which was bound to the capture antibody, was detected through a chromogenic reaction. Enzyme substrate solution (TMB/H_2O_2, Kirkegaard and Perry, USA) was prepared according to manufacturers recommendations and 100 µl were added to each well and incubated for 7 min. To stop the substrate reaction 100 µl of stopping solution were added. The colour intensitiy was measured by determining the absorbance at 450 nm using a computer-assisted (Magellan; Tecan AG, Germany) microplate reader (Sunrise; Tecan AG, Germany). The values of the specimen wells were in the linear segment of the calibration curve. Materials used are listed below.

Materials

Coating buffer

0.05 M Carbonate-bicarbonate (Sigma, Germany)
Adjust to pH 9.6

Wash solution pH 8.0

50 mM Tris (Roth, Germany)
0.14 M NaCl (AppliChem, Germany)
0.05 % Tween 20 (Roth, Germany)
Adjust to pH 8.0

Blocking solution pH 8.0

50 mM Tris (Roth, Germany)

0.14 M NaCl (AppliChem, Germany)

1 % Bovine serum albumin in Tris buffered saline (Sigma, Germany)

Adjust to pH 8.0

Sample diluent pH 8.0

50 mM Tris (Roth, Germany)

0.14 M NaCl (AppliChem, Germany)

1 % Bovine serum albumin in Tris buffered saline (Sigma, Germany)

0.05 % Tween 20 (Roth, Germany)

Adjust to pH 8.0

Stopping solution

1 M H_3PO_4 (Roth, Germany)

3.4 Determination of body weight and nose-rump-length

All mice were weighed prior to sacrifice. Body weight was determined to the nearest 0.1 g (Kern KB 5000-1, Kern & Sohn GmbH, Germany). Additionally, the nose-rump-length was determined.

3.5 Glomerulus isolation

Murine glomeruli were isolated using a modified version of a recently published method for large scale isolation of glomeruli from murine kidneys perfused with spherical superparamegnetic beads (Takemoto et al., 2002). These beads embolize the glomerular capillaries. After collagenase treatment of the kidney tissue, glomeruli containing beads can be isolated in a magnetic field.

In order to produce optimal defined sample material glomeruli of only one pair of a transgenic mice and its corresponding control were isolated per day between nine and eleven o'clock in the morning. Transgenic and control mice were ordered strictly random each time. Mice were anesthetised by intraperitoneal injection of ketamine (Ketanest®, 80 mg/kg 80 mg/kg, Bayer, Germany) and xylacin (8 mg/kg, Rompun®, Bayer, Germany). Approximately $8x10^7$ (a volume of 200 µl, respectively)

Dynabeads® M-450 Epoxy (Invitrogen, Germany) were diluted in 40 ml of 38°C warm phosphate buffered saline pH 7.4 (PBS) and perfused through the left heart ventricle. As perfusion technique had pointed out to be the most important prerequisite for the method's success, a perfusion device developed by Andreas Blutke (German utility patent no. DE 202006001542 U1) was used, which allows for uncomplicated perfusion of nearly all glomeruli in the adult mouse kidney with sufficient numbers of magnetic beads under adjustable pressure conditions (Blutke et al., 2005). Perfusion was performed using a perfusion pressure of 70 mm Hg. An incision in the inferior vena cava, cranial of the diaphragm provided outflow of the perfusate. The kidneys were removed, decapsulated and weighed to the nearest 0.1 mg (BP 61 S, Sartorius AG, Germany).

For histology and morphometric analysis, immunohistochemistry and electron microscopy, a sagittal slice of approximately 1 mm thickness was carefully cut from the middle of each kidney, using a razor blade. Pieces of 1 mm^3 were taken from each slice of the renal cortex for electron microscopy and were fixed in 6.25 % glutaraldehyde. One and a half kidney slices were taken for histology, fixed by immersion in 4% paraformaldehyde (VWR international, Germany), and embedded in plastic. The remaining half kidney slice was taken for eventual immunhistochemistry, fixed in 4 % paraformaldehyde, and embedded in paraffine.

The remaining kidney tissue designated for glomerulus isolation was then cut into small pieces of approximately 1 mm^3 and digested with collagenase (1 mg/ml collagenase A, Roche, Germany) in Hanks' balanced salt solution (Invitrogen, Germany) in a 2 ml cup (Eppendorf, Germany) at 37°C for 30 min in a thermoblock TB1 (Biometra, Germany) with gentle agitation. The digested tissue was gently pressed through a 100-µm cell strainer (BD Biosciences, Germany) in a 50 ml Falcon tube (BD Biosciences, Germany), using a flattened pestle and the cell strainer was then washed with 6 ml of 4°C cold PBS. The cell suspension was then transferred to a 12 ml tube (Techno Plastic Products AG, Switzerland) adding another 3 ml PBS and placed into the magnetic field of a strong permanent magnet (BDI Magnet™ Cell Separation Magnet, BD Biosciences, Germany) for 5 min. The liquid was removed and the isolated tissue containing Dynabeads was resuspended in 9 ml of 4°C PBS and placed in the magnetic field for another 5 min. After removing the liquid tissue was resuspended in 2 ml PBS and filtered through a new 100-µm cell strainer without pressing into a 50 ml tube. The cell strainer was washed with 6 ml of 4°C cold PBS

and the suspension was transferred to a 12 ml tube adding 2 ml PBS. From this volume an aliquot of 1.5 ml was transferred to a 1.5 ml cup (Eppendorf, Germany) for transcriptomic analysis. The remaining volume was placed again into the magnetic field for 5 min. After removing the liquid, isolated glomeruli were resuspended in 1.5 ml PBS, transferred to a 1.5 ml cup and placed into the magnetic field for 2 min. Washing steps were repeated for three to four times depending on the grade of purity of the isolated glomeruli which was estimated by the control of the wash fluids under a photomacroscope (Stemi DV4, Zeiss, Germany). After the last removal of liquid the cup with isolated glomeruli was immediately stored at -80°C until further use. During the procedure, kidney tissues were kept at 4°C except for the collagenase digestion at 37°C. Isolation time, calculated from the animal's death to the storage of isolated glomeruli at -80°C, averaged 100 minutes.

Phosphate-buffered saline (PBS) (pH 7.4)

0.25 g Potassium dihydrogen phosphate (AppliChem, Germany)
8.0 g Sodium chloride (AppliChem, Germany)
1.46 g Di-sodium hydrogen phosphate dehydrate (AppliChem, Germany)
Ad 1 l aqua bidest, adjust to pH 7.4

3.6 Histological technique

3.6.1 Plastic histology

For histology and morphometric analysis 1 ½ slices of kidney tissue of each animal were fixed by immersion in 4% paraformaldehyde (VWR international, Germany) in phosphate buffered saline (PBS pH 7.4) for 24 hours at 8°C and then routinely processed for plastic embedding in a Citadel 1000 (Shandon, Germany). In order to avoid distortion the kidney slices were fixed with a piece of foam-rubber sponge in the tissue-embedding capsules. Subsequently, the kidney slices were processed in a hydroxymethylmethacrylate (Fluka Chemie, Germany)/methylmethacrylate (Riedel de Haën, Germany) solution at 4°C on a shaker for 18 hours. The kidney slices were then shifted into "solution 1", composed of benzoylperoxide (338 mg; Merck, Germany), methylmethacrylate (20 ml), hydroxymethylmethacrylate (60 ml), ethyleneglycol monobutylether (16 ml; Merck, Germany), and polyethylene glycol 400 (2 ml; Merck, Germany). After immersion at 4°C on a shaker for four hours, the

kidney slices were placed in plastic cups and embedded using 60 µl of dimethylanilin (Merck, Germany) in 40 ml of “solution 1” as starter for polymerisation. Embedding cups were immediately placed into a water bath (4°C) and polymerisation took place at 4°C over night (Hermanns et al., 1981). Sections of 1.5 µm thickness were cut from the casted blocks on a Reichert-Jung 2050 rotary microtome (Cambridge Instruments, Germany). The sections were routinely processed and stained with Hemalaun-Eosin (H&E) and Periodic Acid Schiff (PAS). Staining procedures are listed in the attachment (10.2).

3.7 Determination of the mean glomerular volume

The mean glomerular volume was estimated using a model-based method, as previously described in detail (Hirose et al., 1982; Wanke, 1996; Weibel and Gomez, 1962). In this model-based stereological approach, the glomeruli were considered as rotation ellipsoids. The mean glomerular area was obtained from planimetric measurements of glomerular profile areas. In the calculation, a shape coefficient and a size distribution coefficient were considered. The results were corrected for embedding shrinkage. The values for the shape and size distribution coefficient as well as for the shrinkage correction factor for plastic embedded murine renal tissue were taken from Wanke (1996). Morphometric evaluation was carried out on a Videoplan® image analysis system (Zeiss-Kontron, Germany) coupled to a light microscope (Orhoplan; Leitz, Germany) via a color video camera (CCTV WV-CD132E; Matsushita, Japan). Images of PAS stained GMA/MMA sections were displayed on a color monitor using a Videoplan® image analysis system (Zeiss-Kontron, Germany). The final magnification on the monitor was 400 x. An object micrometer (Zeiss) served for calibration. All glomerular profiles present in the sections of one animal (mean 123 ± 25) were sampled according to the unbiased counting rule (Horlyck et al., 1986). Glomeruli were sampled by moving the visual field along the two lateral lines of a frame displayed on the monitor. Glomeruli between the lines or touching the left-hand line were sampled, and those touching the right-hand line were excluded to give an unbiased sample. The contours of the sampled glomerular profiles were circled with a cursor. The mean glomerular volume was calculated using the following equation (Hirose et al., 1982; Wanke, 1996):

$$\hat{\bar{v}}_{(glom)(s)} = \frac{\beta}{k} \cdot \bar{a}_{(glom)}^{1.5}$$

$\hat{\bar{v}}_{(glom)(s)}$: stereologically estimated mean glomerular volume (referring to GMA/MMA embedded tissue)

β : shape coefficient

k : size variation coefficient

$\bar{a}_{(glom)}$: arithmetic mean of areas of glomerular profiles

The values for the shape coefficient (β =1.40) and the size variation coefficient (κ = 1.04) were taken from Wanke (1996). Results were corrected for embedding shrinkage, using the linear tissue shrinkage correction factor (fs = 0.91) for murine kidney tissue embedded in GMA/MMA (Wanke, 1996):

$$\bar{v}_{(glom)} = \hat{\bar{v}}_{(glom)(s)} / f_s^3$$

$\hat{\bar{v}}_{(glom)}$: stereologically estimated mean glomerular volume (prior to embedding)

f_s : linear tissue shrinkage correction favtor for murine kidney tissue embedded in GMA/MMA

3.8 Lysis of glomerulus samples for proteomic analysis

Cups with isolated glomeruli were centrifuged at 18,000 rcf for 10 min at 4°C in a GS-15R centrifuge (Beckman, Germany). 80 – 90 µl of cell lysis buffer per 11,000 glomeruli were added at the wall and spun down for 1 min. Samples were homogenized in an iced ultrasonic bath for 5 – 7 min (Sonorex RK 100; Bandelin, Germany). The lysates were centrifuged for 2 min at 18,000 g through QIAshredder columns (Qiagen, Germany). In order to remove Dynabeads cups were exposed to a magnet on ice for 1 min and supernatant was recovered. Protein concentration of lysates was assessed by Bradford assay (Bradford, 1976). Lysates were stored at -80°C until further use.

Cell lysis buffer pH 8.5

2 M Thiourea (Sigma, Germany)
7 M Urea (Roth, Germany)
30 mM Tris (Roth, Germany)
4 % (w/v) CHAPS (3-[Cholamidopropyl]dimethylammonio)-1-propanesulfonate) (Sigma, Germany)
Adjust to pH 8.5 with 25 % HCl (Merck, Germany)

Bradford reagent

0.01 % (w/v) Coomassie brilliant blue G-250 (Sigma, Germany)
5 % (v/v) Ethanol (Roth, Germany)
10 % (v/v) Phosphoric acid (85 %) (Merck, Germany)

3.9 Minimal labeling of proteins with fluorescent dyes

Lyophilised fluorescent dyes (CyDyes) were reconstituted according to the manufacturer's protocol with dimethylformamid (DMF) to give a 1mM solution and stored at -20°C. CyDyes were used undiluted from the 1 mM stock solution. Labeling reaction for minimal labelling was performed according to the manufacturer's protocol. Labeled samples were stored at -80°C until further processing.

3.10 2D Difference gel electrophoresis (2D-DIGE)

3.10.1 Isoelectric focussing (IEF)

Gel strips (Immobiline™ DryStrips, pH 4-7, 18 cm, GE Healthcare Bio Sciences, Germany) were rehydrated in a reswelling tray (GE Healthcare Bio Sciences, Germany) in 350 µl rehydration buffer covered with mineral oil (DryStrip Cover Fluid; GE Healthcare Bio Sciences, Germany) overnight. Isoelectric focussing was done for a total of 44 kVh using anodic cup loading with a Multiphor II device (GE Healthcare Bio-Sciences). For the preparative gels, unlabeled protein samples were applied by in-gel rehydration and IEF was run for 51 kVh. Focussed gel strips were stored at -80 °C until further processing.

Rehydration buffer

2M Thiourea (Sigma, Germany)

7 M Urea (Roth, Germany)

4 % (w/v) CHAPS (Sigma, Germany)

13 mM 1,4-dithioerythritol (DTE; Roth, Germany)

1 % (v/v) Pharmalyte 3-10 (GE Healthcare Bio Sciences, Germany)

0.8 % (v/v) saturated bromphenol blue solution (Merck, Germany)

3.10.2 SDS-PAGE

For SDS-PAGE a separation gel (18 cm x 16 cm x 1 mm) was cast, overlayed with ddH_2O and allowed to polymerise overnight. The stacking gel (3 cm x 16 cm x 1 mm) was cast on top of the separation gel and a comb providing for IPG strip application was inserted. The stacking gel was allowed to polymerise for one hour.

IPG-strips were equilibrated two times for 15 min in 15 ml equilibration buffer containing 1 % DTE in the first and 2.5 % iodacetamide + 200 µl saturated bromphenol blue solution in the second step on a shaker (100 rpm). Afterwards strips were shortened to 14.5 cm, placed onto the stacking gel and fixed with 0.5 % agarose (Serva, Germany) in SDS running buffer. Gels were run for 30 min at 30 mA/gel and 3 hours at 40 mA/gel in SDS running buffer at a temperature of 9 °C using a Protein™ II xi device (Bio-Rad, Hercules, CA, USA). The gels in the group of GH transgenic mice vs. their controls were processed by the Toplab GmbH (Martinsried, Germany), had a dimension of (23 cm x 19.5 cm x 1 mm) and were run in an ISO Dalt Tank (Höfer, Germany).

Separation gel (12 % polyacrylamide) (2 gels)

26.8 ml ddH_2O

20 ml 1.5 M TrisHCl pH 8.8 (Roth, Germany)

32 ml Acrylamide / bisacrylamide (37.5:1) (Serva, Germany)

800 µl SDS 10 % (Serva, Germany)

400 µl Ammonium persulfate 10 % (Merck, Germany)

40 µl N,N,N’,N’-Tetramethylethylendiamine (TEMED) (Roth, Germany)

Stacking gel (4 % polyacrylamide) (2 gels)

6.1 ml ddH_2O

2.5 ml 0.5 M TrisHCl pH 6.8 (Roth, Germany)

1.3 ml Acrylamide / bisacrylamide (37.5:1) (Serva, Germany)

100 µl SDS 10 % (Serva, Germany)

50 µl Ammonium persulfate 10 % (Merck, Germany)

10 µl N,N,N',N'-Tetramethylethylendiamine (TEMED) (Roth, Germany)

Equilibration buffer

6 M Urea (Roth, Germany)

30 % (v/v) Glycerol (Roth, Germany)

2 % (w/v) SDS (Serva, Germany)

50 mM TrisHCl pH 6.8

SDS running buffer

25 mM Tris (Roth, Germany)

192 mM Glycine (Roth, Germany)

0.1 % (w/v) SDS (Serva, Germany)

3.10.3 Scanning and analyzing the gels

Fluorescence scanning of the separated proteins was performed using a Typhoon 9400 Variable Mode Imager (GE Healthcare Bio Sciences, Germany). Parameters were set according to the manual, the photomultiplier tube (PMT) parameters were set to 570 V (Cy 3), 560 V (Cy 5), and 800 V (Cy 2), respectively. The group of GH tg vs co was scanned using the Ettan™ DIGE Imager (GE Healthcare Bio Sciences, Germany) at Toplab GmbH, Martinsried. Exposure was set to 0.500 (Cy3), 0.800 (Cy 5), and 1.250 (Cy 2), respectively. The resulting images in both groups were analyzed with the DeCyder™ Differential Analysis Software v6.5 (GE Health Care Bio Sciences, Germany). Pre-matched spot maps created by the software, were each inspected and rematched manually to obtain the best possible match quality.

3.10.4 Staining of gels

After fluorescence scanning the analytical gels of the group of $GIPR^{dn}$ transgenic and corresponding control mice were stained for total protein using Roti®-Blue colloidal

coomassie stain. All preparative gels were stained with Roti®-Blue colloidal coomassie stain. Staining was performed according to the supplier's manual.

3.11 Identification of proteins of interest

3.11.1 Spot excision and tryptic hydrolysis

Differentially abundant spots were excised from preparative gels using OMX-S® devices (OMX GmbH, Germany) which were used according to the manufacturer's protocol. Briefly a gel spot was selected with the integrated picker, the gel spot was centrifuged in the device to crush the matrix into tiny pieces and a volume of 20 µl trypsin-digestion buffer (200 ng modified Trypsin sequencing grade porcine (Promega, Germany)) was added for the tryptic hydrolysis of proteins (at 50 °C for 45 min). After tryptic hydrolysis of proteins, peptides were eluted in the same device in a clean peptide sample container and dried in a vacuum concentrator (Bachhofer, Germany). They were stored at -80°C until further processing.

3.11.2 Desalting of peptides

Peptides for subsequent MALDI TOF/TOF mass spectrometry were desalted using $ZipTip_{\mu\text{-}C18}$® pipette tips (Millipore, Germany). Peptides were reconstituted in 10 µl 0.5 % trifluoroacetic acid (TFA; Fluka, Germany) and sonicated for three minutes. ZipTips were wetted with 50 % acetonitrile (ACN; Merck, Germany), 0.1 % TFA and equilibrated with 0.1 % TFA. Peptides were bound to the ZipTip by pipetting up and down ten times, followed by two washing steps (first 0.5 % methanol , 0.1% TFA and second 0.1 % TFA). Peptides were then directly eluted from the ZipTip with 2 µl Matrix solution (5 mg/ml α-cyano-4-hydroxycinnamic acid (Bruker Daltonik, Germany) in 50 % acetonitrile, 0.1 % TFA) and spotted on an Opti-TOF™ MALDI target (Applied Biosystems, Germany).

3.11.3 Mass spectrometry and database search

Peptide mass fingerprint (PMF) spectra were acquired by 1600 laser shots (ND:Yag laser, 355 nm) in a mass range between 800 Da and 4500 Da on a 4800 MALDI-TOF-TOF mass spectrometer (Applied Biosystems). Peak lists were generated using

a minimum signal to noise ratio of 10 and prominent human keratin and porcine trypsin autolysis peaks were excluded. The ten most intense precursor signals were selected for MS/MS fragmentation. MS/MS analysis was performed by 500 laser shots and air as collision gas. Peak finding within the MS/MS spectra was performed using a signal to noise ratio of 10. Data were transferred to the GPS Explorer Software V 3.6 (Applied Biosystems) and searched against the Mus musculus subset of the Swissprot database (241365 sequences, date 23112006) using the Mascot (Matrix Science Ltd.) search engine with the following parameters: “Enzyme” = Trypsin; “Fixed modification” = Carbamidomethyl (C); “Variable modification” = Oxidation (M); “Max. missed cleavages” = 1; “Precursor tolerance” = 200 ppm; “MS/MS fragment tolerance” = 0.5 Da

3.11.4 LC-ESI-MS/MS analysis

LC-ESI-MS/MS analysis was performed with an Ettan MDLC chromatographic device coupled to a linear ion trap mass spectrometer. The lyophilized peptides were resuspended in 40 µl 0.1 % formic acid (Fluka, Germany) and applied to the device. A C18 trap column was utilized for peptide desalting and concentration including a 15 minute sample application period at a flow rate of 10 µl/min using 0.1 % formic acid. Reversed-Phase chromatography to separate the peptides was performed on a C18 PepMap 100 nano-LC column at a flow rate of 240 nl/min. For mobile phase A, water containing 0.1 % formic acid and for mobile phase B, 84 % ACN containing 0.1 % formic acid were used. As LC method the following gradient was applied:
30 min ramp increasing to 30 % mobile phase B, 20 min ram up to 60 % mobile phase B, 10 min at 100 % mobile phase B. For application to mass spectrometry, ESI ionization was achieved with a needle voltage of 1.4 kV on distal-coated SilicaTips. Cycles of one MS scan over the mass range m/z 400-1600 followed by three data dependent MS/MS scans were performed in the “dynamic exclusion™ activated” mode. Collision energy was set to 35 %. Mascot search of the results includes MS/MS data comparing data of the Swiss-Prot database and IPI database for murine entries. The search parameters were set as follows: (i) Enzyme: Trypsin; (ii) Variable modification: Oxidation (M); (iii) Peptide tolerance: 2 Da; (iv) MS/MS tol.: 0.8 Da; (v) Peptide charge: 1+, 2+, 3+; (vi) Instrument: ESI-Trap; (vii) Maximum missed cleavages: 2.

3.12 Statistical evaluation and data presentation

Comparisons between the different groups were carried out by performance of two-tailed Student's t-tests (type 2), using the MS Excel® software (Microsoft®, USA), performed on a personal computer. P values < 0.05 were considered significant. Data are presented as means and standard deviation (SD) throughout the study.

4. Results

Differential proteomic analysis was performed on isolated murine glomeruli of two different mouse models of glomerulopathy – GH transgenic and GIPR^{dn} transgenic mice vs. their wild-type littermate controls – at the defined disease stage of glomerular hypertrophy with beginning albuminuria (stage 2). In addition isolated glomeruli in the earlier disease stage of glomerular hypertrophy without detectable albuminuria (stage 1) were analysed in GH transgenic mice and corresponding controls. Only glomerular samples of transgenic mice that fulfilled the stage specific criteria and samples of their corresponding age-matched controls were taken for proteomic analysis. Therefore, before proteomic analysis a stage- and not age-specific selection of the samples was made. Urine protein analysis was performed regularly in order to determine the presence (stage 2) or absence (stage 1) of albuminuria. When this criterium was fulfilled glomeruli were isolated of the transgenic and the corresponding control animal. Afterwards the mean glomerular volume was determined by quantitative stereology. To be taken for proteomic analysis, transgenic mice in both stages had to show glomerular hypertrophy, defined as an increase of the mean glomerular volume by at least 30 % as compared to the corresponding wild-type littermate control. Subsequently, a 2D-DIGE analysis in the pH range 4-7 was performed.

4.1 Urine protein analysis

4.1.1 SDS-PAGE

Urine samples of mice were screened regularly for albuminuria prior to glomerulus isolation by SDS-PAGE. On the whole, about 1152 urine samples (391 in the group of GH transgenic and control mice and 761 in the group of GIPR^{dn} transgenic and control mice, respectively) were taken from 179 animals in both mouse models. With these samples about 250 SDS-PAGEs were run for screening purposes. In stage 1 one urine sample was taken on the day before glomerulus isolation of transgenic (tg) and control (co) mice. There was no detectable albumin in the urine of transgenic mice as compared to their controls that were taken for proteomic analysis as shown in **Fig. 4.1**. Urine samples of GH tg and wild-type controls (co) stage 2 were screened every two days from an age of 26 days onwards and those of GIPR^{dn} tg and co stage

2 weekly from an age of six weeks onwards, respectively. 24 hours after the first positive result for the presence of albumin a second urine sample which had also to be positive was taken one day prior to glomerulus isolation of both GH and GIPR^{dn} tg and co mice. All tg animals that were taken for proteomic analysis showed a beginning albuminuria as compared to their controls (**Fig. 4.2**). Intensities of albumin bands in urine samples of GH tg animals approximately conformed to those of GIPR^{dn} tg mice. In **Fig. 4.3** the onset of albuminuria of an exemplary GIPR^{dn} tg mouse and its corresponding control as well as an exemplary GH tg mouse and its corresponding control is demonstrated: a negative result ten (GIPR^{dn}) / five (GH) days prior to glomerulus isolation followed by two positive results for the presence of albumin in the urine three and one day prior to glomerulus isolation. Albuminuria was confirmed in exemplary GH tg and GIPR^{dn} tg mice as compared to their controls by Western blot analysis (see **Fig. 4.4**).

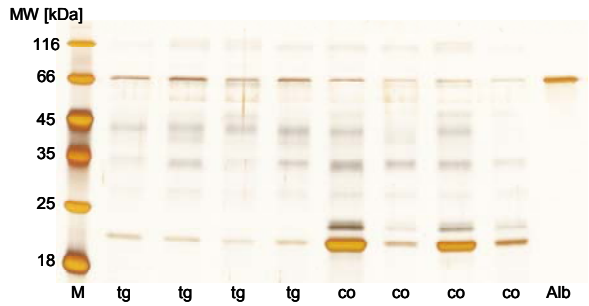

Fig. 4.1: SDS-PAGE of urine samples of GH transgenic (tg) mice in stage 1 and their corresponding wild-type controls (co) No albuminuria is detectable in GH transgenic mice as compared to their controls on the day before glomerulus isolation. MW molecular weight; M Molecular weight marker; Alb Mouse albumin standard

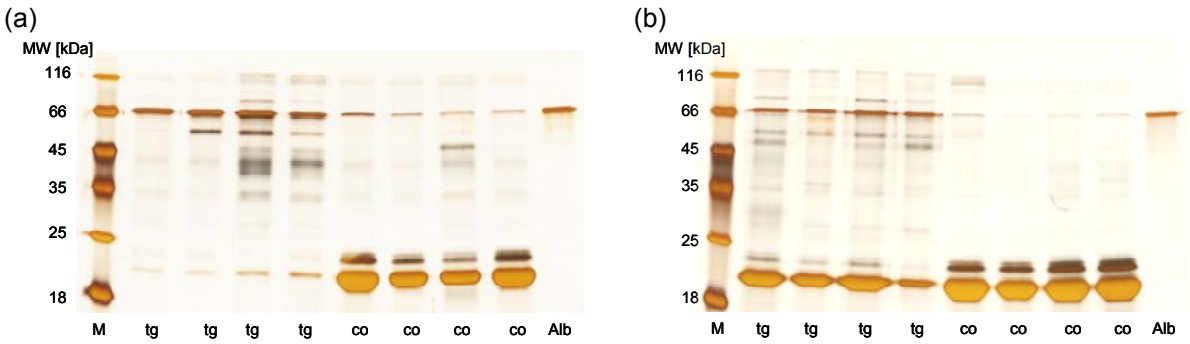

Fig. 4.2: SDS-PAGE of urine samples of (a) GH and (b) GIPR^{dn} transgenic (tg) mice in stage 2 and their corresponding wild-type controls (co). Transgenic mice of both groups exhibit albuminuria as compared to their controls on the day before glomerulus isolation. MW molecular weight; M Molecular weight marker, Alb Mouse albumin standard

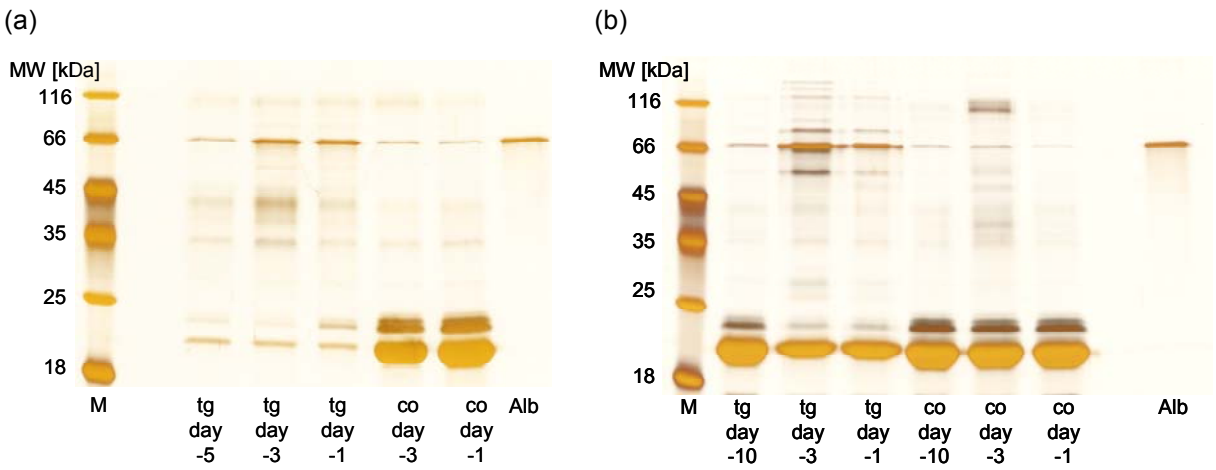

Fig. 4.3: SDS-PAGE demonstrating the onset of albuminuria two days prior to glomerulus isolation. (a) GH transgenic (tg) and corresponding wild-type control (co) mouse; (b) GIPR^{dn} tg and corresponding co mouse; MW molecular weight; M Molecular weight marker, Alb Mouse albumin standard; day -10, -5, -3, -1 urine samples 10, 5, 3, 1 days before glomerulus isolation.

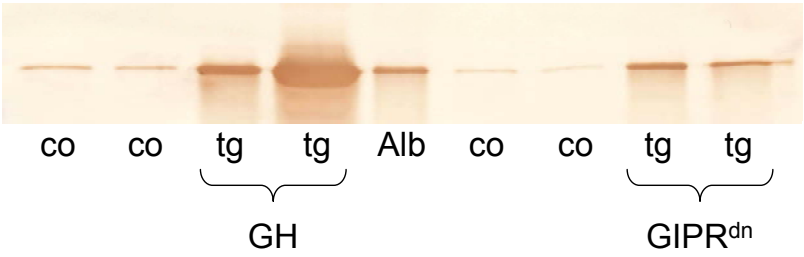

Fig. 4.4: Western blot analysis of urine samples of GH as well as GIPR^{dn} transgenic (tg) and corresponding wild-type control (co) mice. Alb: Mouse albumin standard

4.1.2 Quantification of albuminuria

Results of the SDS-PAGE analysis give a good impression, whether albuminuria is detectable in an urine sample or not, but quantification of the results cannot be made. Furthermore, comparisons of urine samples from transgenic vs. those from control mice can only be made within one gel and not between different gels. In order to confirm and quantify the results obtained by SDS-PAGE, the concentration of albumin in the urine of all animals that were taken for proteomic analysis was measured by ELISA and the albumin-creatinine-ratio was calculated. In urine samples of GH transgenic mice vs. wild-type control mice there was no significant difference in the concentration of urine creatinine, whereas in GIPR^{dn} transgenic mice the urine creatinine concentration was significantly decreased as compared to their

controls (see **Fig. 4.5** (a)). In the group of GH transgenic mice in stage 1 there was no significant difference in the albumin-creatinine-ratio between transgenic and corresponding control animals. In the groups of GH transgenic mice in stage 2 as well as GIPR^{dn} transgenic mice in stage 2 the albumin-creatinine-ratio was significantly increased in transgenic animals as compared to their controls (see **Fig. 4.5** (b)).

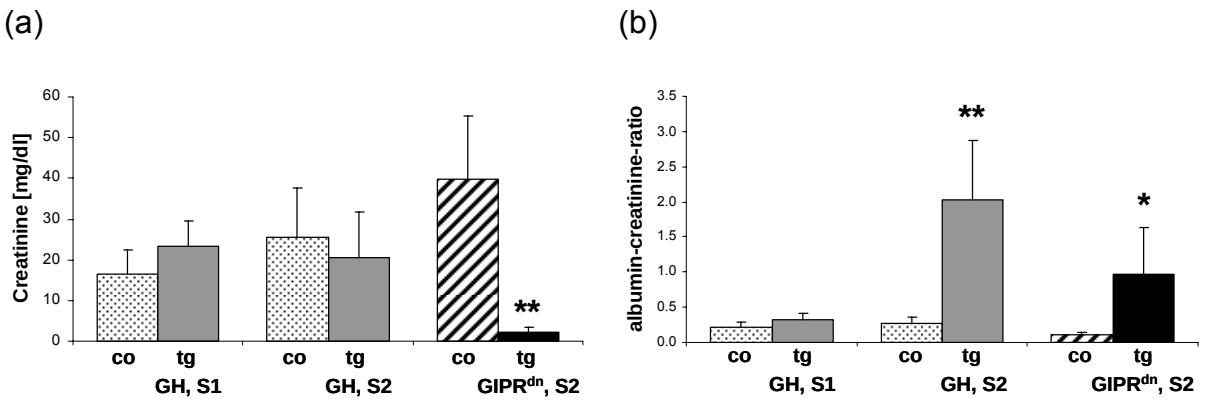

Fig. 4.5: Urinary creatinine concentration (a) and albumin-creatinine-ratio (b). (a) GIPR^{dn} transgenic (tg) mice exhibit a significantly decreased urine creatinine concentration as compared to their controls (co). GH as well as GIPR^{dn} transgenic mice in stage 2 show a significantly increased albumin-creatinine-ratio as compared to their wild-type controls (co). S1 stage 1, S2 stage 2. Data are presented as means ± SD. *$p<0.05$, **$p<0.01$

4.2 Body weight, kidney weight and nose-rump-length

Right before glomerulus isolation additional parameters (body and kidney weight, nose-rump-length) were determined for each animal (see **Table 4.1**). GH transgenic mice in stage 2 showed a significantly increased body weight as compared to their controls. Kidney weight and nose-rump-length in GH transgenic mice in stage 1 and 2 as well as the body weight in GH transgenic animals in stage 1 were increased as compared to their control mice, but these differences did not reach statistical significance. GIPR^{dn} transgenic mice in stage 2 showed significant changes in all analysed parameters as compared to control mice. Body weight and nose-rump-length were significantly decreased, whereas the kidney weight was significantly increased in GIPR^{dn} transgenic animals as compared to their controls.

Group	Body weight [g]	Kidney weight [mg]	Nose-rump-length [cm]
Co (GH, S1)	20 ± 4	339 ± 53	8.7 ± 0.5
GH tg, S1	22 ± 1	361 ± 15	9.1 ± 0.4
Co (GH, S2)	26 ± 2	436 ± 53	9.6 ± 0.3
GH tg, S2	29* ± 2	485 ± 48	10.2 ± 0.5
Co ($GIPR^{dn}$, S2)	37 ± 3	635 ± 86	11.0 ± 0.3
$GIPR^{dn}$ tg, S2	32** ± 3	815** ± 100	10.2** ± 0.4

Table 4.1: Body weight, kidney weight, nose-rump-length of all mice used for proteomic analysis. Differences in of body weight, kidney weight and nose-rump-length of GH transgenic mice in stage 1 (GH tg, S1) do not reach statistical significance as compared to their controls (Co (GH, S1)). GH transgenic mice in stage 2 (GH tg, S2) show a significantly increased body weight as compared to their controls (Co (GH, S2)). $GIPR^{dn}$ tg mice in stage 2 ($GIPR^{dn}$ tg, S2) have a significantly reduced body weight and nose-rump-length as compared to controls (Co ($GIPR^{dn}$, S2)). Their kidney weight is significantly higher than that of controls. Data are shown as means ±SD; *$p<0.05$; **$p<0.01$

4.3 Mean glomerular volume

Animals in both stages had to exhibit glomerular hypertrophy, which was defined by a significant increase of the mean glomerular volume by at least 30 %. The mean glomerular volume was determined by quantitative stereology using plastic sections of the kidney slices that had been taken prior to glomerulus isolation in order to select the animals for proteomic analysis. The mean glomerular volume ($v_{(Glom)}$, corrected for embedding shrinkage) was increased by 58 % on the average in GH transgenic animals in stage 1 and by 63 % on the average in stage 2 as compared to their control animals. $v_{(Glom)}$ in $GIPR^{dn}$ transgenic mice stage 2 was increased by 42 % as compared to their controls as summarized in **Fig. 4.6**.

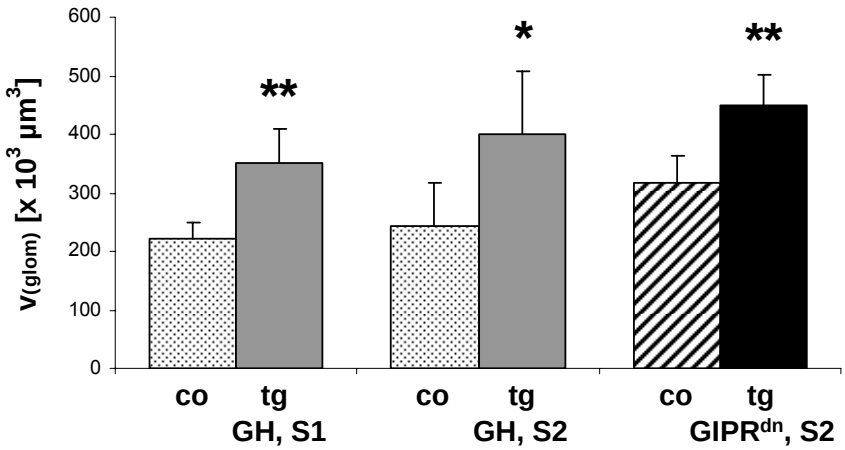

Fig. 4.6: Mean glomerular volume. S1 stage 1; S2 stage 2; co, wild-type control mice; tg transgenic mice. Tg mice show a significant increase in the mean glomerular volume as compared to their controls. Data are presented as means ±SD. *p<0.05, **p<0.01

Examplary cross sections of glomeruli demonstrating glomerular hypertrophy are shown in **Fig. 4.7**.

All mice that were taken for proteomic analysis exhibited a significant glomerular hypertrophy and no albuminuria (GH tg mice in stage 1 vs. corresponding controls) or glomerular hypertrophy plus the onset of albuminuria (GH and $GIPR^{dn}$ tg mice in stage 2 as compared to their controls). Mice without a sufficient increase in the mean glomerular volume did not fulfil the criteria and were excluded from proteomic analysis.

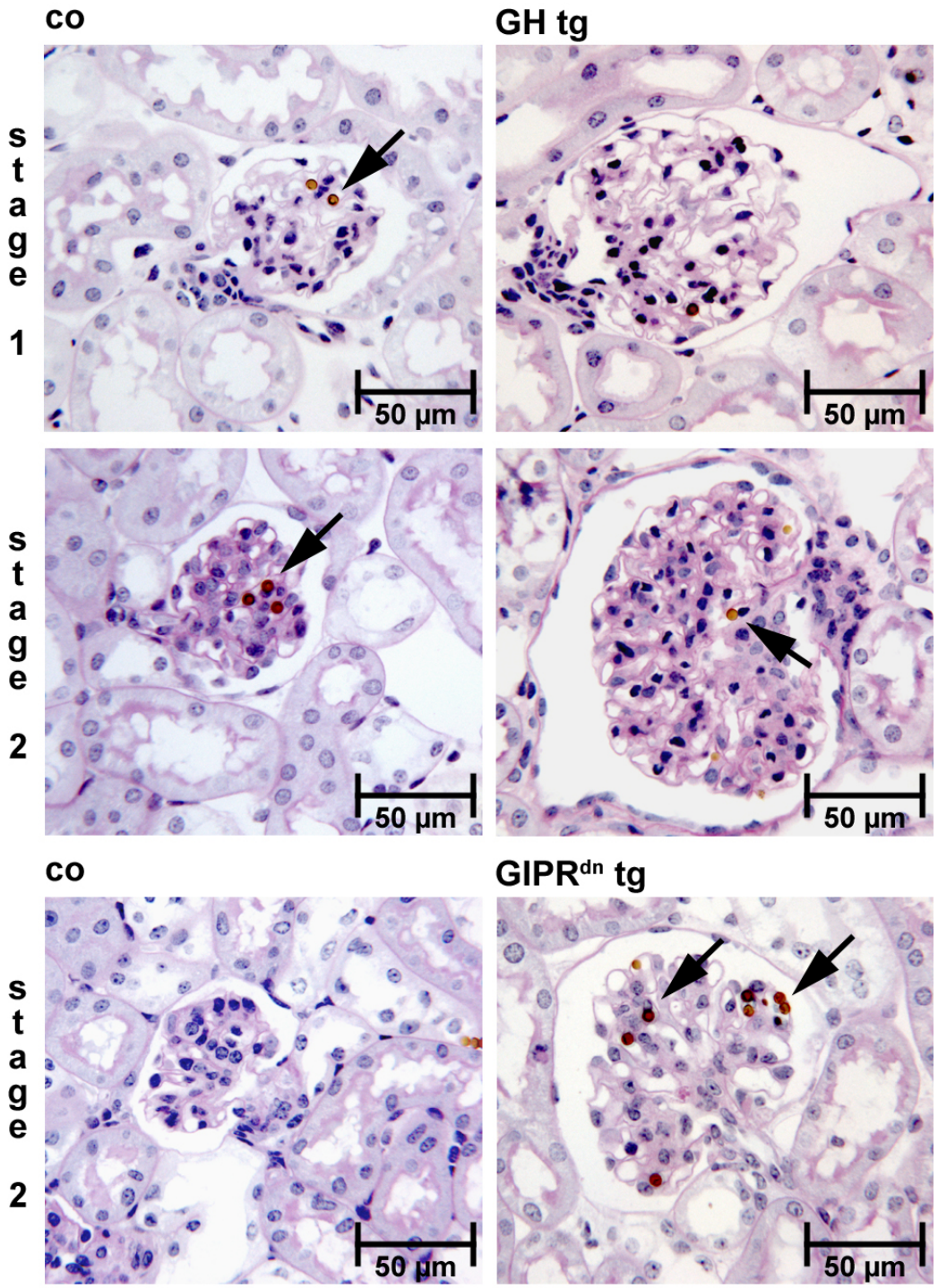

Fig. 4.7: Glomerular hypertrophy. Glomeruli in histological kidney sections of transgenic (tg) as compared to their wild-type control (co) mice demonstrating glomerular hypertrophy; magnetic beads are marked by arrows; plastic sections, PAS-staining

4.4 Glomerulus isolation

Glomeruli were isolated from mice with (stage 2) or without albuminuria (stage 1). In order to achieve sufficient results concerning quantity and quality a recently published method for large scale isolation of glomeruli perfused with spherical superparamagnetic beads (refer to 3.5) was modified and optimized for the purpose of this study. During the optimization process beads of different size and manufacturer were tested for their suitability and the results were very different in quantity and quality of the isolated glomeruli. Beads with a diameter of approximately 1 µm (BeadMAG-55, Chemicell, Germany) lead to very high numbers of isolated glomeruli. But beads not only precipitated within the glomerular capillaries (see **Fig. 4.8** (a)), but also in peritubular capillaries. Therefore, a high percentage of non-glomerular tissue like tubulus fragments was isolated. Other beads (SiMAG-Oxiran/20), Chemicell, Germany) turned out to have very heterogeneous diameters which lead to an obstruction of the afferent arterioles by very large beads and only few glomeruli could be isolated (see **Fig. 4.8** (b)).

(a) (b)

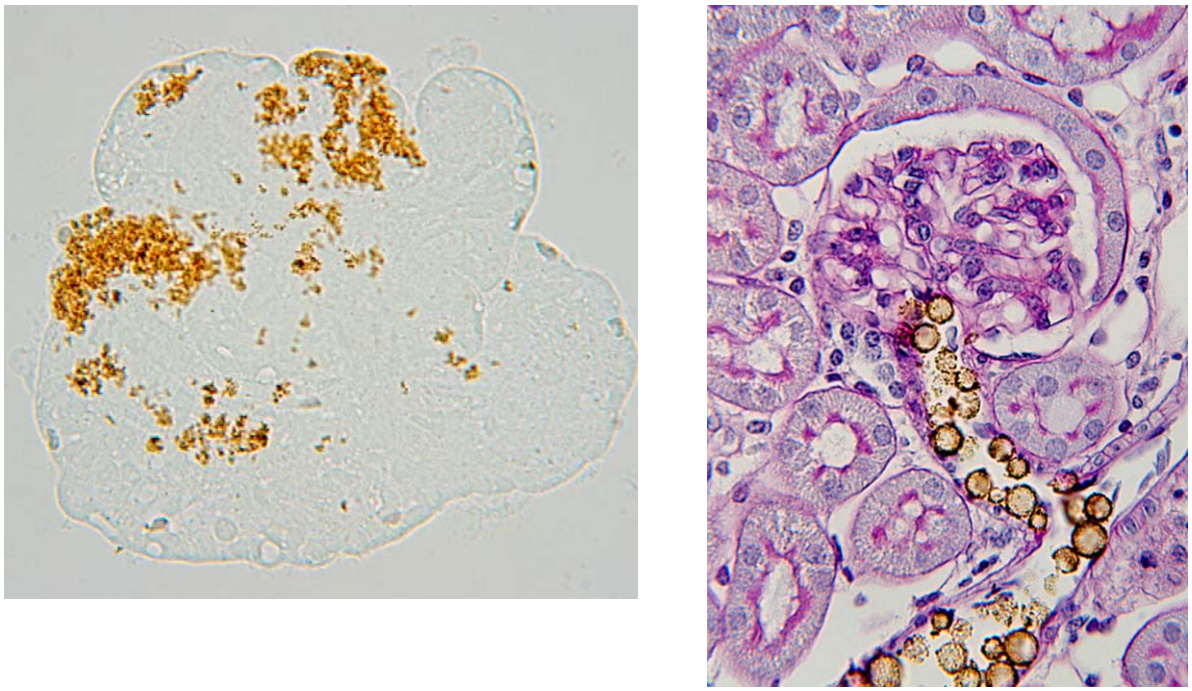

Fig. 4.8: Beads with different diameters. (a) Native sample of a glomerulus perfused with beads with a diameter of 1 µm. Precipitated beads are of yellowish colour; magnification 250 x. (b) Histological kidney section showing a profile of a glomerulus after perfusion with beads of very heterogeneous size. Beads with very large diameter obstruct the vas afferens of the glomerulus preventing beads from entering the glomerular capillaries. PAS-staining, magnification 250 x.

The best results could be achieved using DynaBeads® M-450 Epoxy with a diameter of 4.5 µm (see **Fig. 4.9**). Out of one murine kidney approximately 10,000 glomeruli could be isolated with ~97 % purity. Taking into account that one slice from the middle of each kidney was removed prior to and an aliquot for transcriptomic analysis during the glomerulus isolation, approximately 11,000 to 13,000 glomeruli per mouse could be isolated to be used for the proteomic analysis.

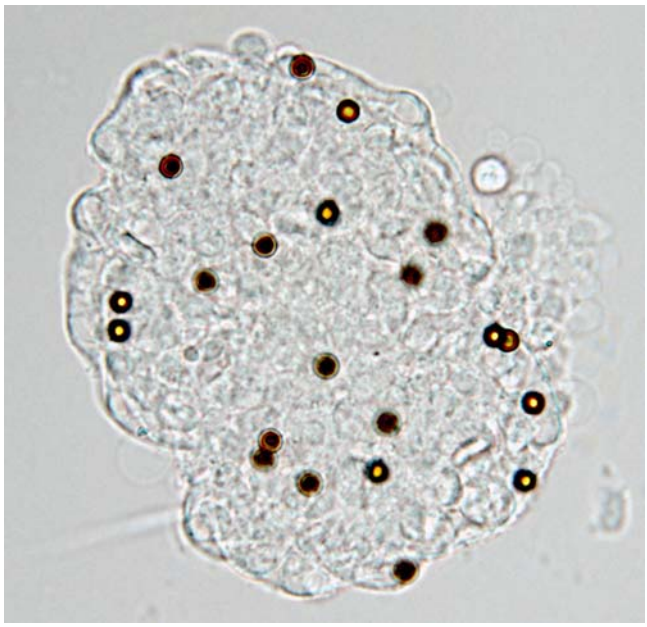

Fig. 4.9: Optimal perfusion of a glomerulus with DynaBeads. Native preparation of a glomerulus perfused with DynaBeads® Epoxy. A homogeneous size and distribution of the beads within the glomerulus can be observed. Magnification 250 x

Another critical point in the process of glomerulus isolation turned out to be constant and not too high pressure of perfusion. Therefore, perfusion was performed with a constant pressure of 70 mm Hg.

4.5 2D-DIGE analysis of glomerulus preparations

Glomerulus isolates for proteomic analysis were selected by the criteria glomerular hypertrophy (stage 1) and glomerular hypertrophy together with onset of albuminuria (stage 2), respectively. Samples of isolated glomeruli were lysed and an average of 250 µg protein could be extracted from ~12,000 glomeruli isolated per mouse. For differential quantitative analysis of the glomerular proteomes of GH transgenic (tg) as well as $GIPR^{dn}$ tg mice vs. their corresponding wild-type littermate controls (co) the

“2D DIGE minimal labeling” technique was applied. The experimental design of the study for one pair – one transgenic mouse and its corresponding wild-type littermate control – of each analysed group is outlined in **Fig. 4.10**.

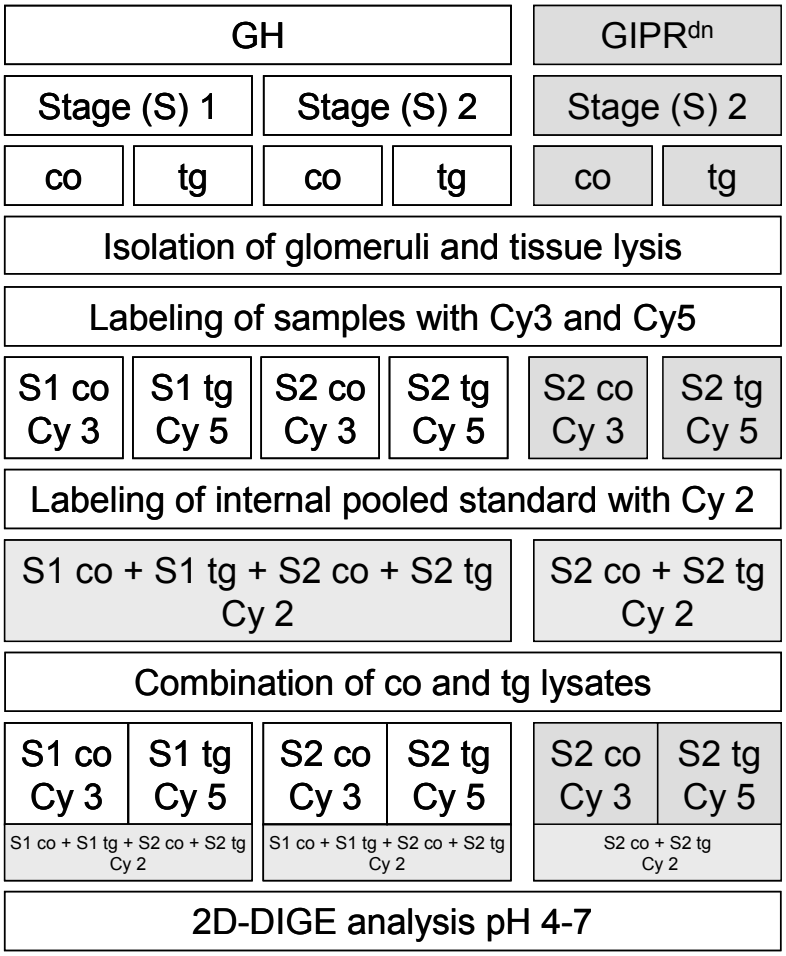

Fig. 4.10: Experimental design of the study demonstrated for one transgenic mouse and its corresponding control of each analysed model. co wild-type control; tg transgenic

The “internal pooled standards (IPS)”, labeled with Cy 2, consisted of protein aliquots from each analysed GH tg mouse and corresponding control and from each analysed GIPR^{dn} tg mouse and its corresponding control, respectively. Glomerlus lysates from control mice were labelled with Cy 3 and those of transgenic mice with Cy 5. Per 2D-gel, 50 µg aliquots of glomerular samples from transgenic mice, from corresponding control mice and IPS were analysed (150 µg protein in total) on a pH 4-7 gradient. Due to relatively low protein amounts in some of the glomerular samples from GIPR^{dn} transgenic and control mice 40 µg instead of 50 µg aliquots were analysed (120 µg protein in total). After scanning the 2D-DIGE gels, the images were transferred to the

DeCyder software for gel matching, internal standardization and statistical analysis. Each group was analysed separately. Spots were considered differentially abundant, if they fulfilled the following criteria: (i) spot present in each gel of the analysed group, (ii) average abundance ratio of spot volumes ± 1.5, (iii) *p*-value of the Student's t-test $p < 0.01$.

4.5.1 GH transgenic (tg) mice vs. wild-type controls (co)

In total five biological replicates, representing five GH transgenic mice in stage 1 as well as in stage 2 and their corresponding wild-type littermate controls were run. In the group of stage 1 one biological replicate was not possible to be analysed. Therefore, only four biological replicates were taken for software analysis. After the DeCyder software analysis five spots were considered as differentially abundant in glomeruli of GH transgenic mice in stage 1 as compared to their controls (see **Fig. 4.11** and **Table 4.2**), two of which were increased (Spots 1 and 2) in their abundance and three were decreased (Spots 3-5) in their abundance. Average abundance ratios ranged from – 4.9 (spot 3) to + 2.22 (spot 2). Spot 3 showed the lowest p-value of 1.9×10^{-4}. 22 spots were differentially abundant in the glomeruli of GH transgenic mice in stage 2 as compared to controls with average abundance ratios from - 4.25 (spot 17) up to + 4.17 (spot 14) (**Fig. 4.12** and **Table 4.3**). P-values ranged from 1.2×10^{-6} (spot 6) to 9.3×10^{-3} (spot 4). Ten spots (spots 1, 2, 6, 7, 10, 13, 14, 15, 19, 20) were increased in their abundance and 12 spots (spots 3, 4, 5, 8, 9, 11, 12, 16, 17, 18, 21, 22) were decreased. In **Fig. 4.11** and **Fig. 4.12** exemplary Cy 3 images which represent the samples of the wild-type controls are shown. Differentially abundant spots are marked by circles and indicated by numbers. Spot 2 in stage 1 and spot 14 in stage 2, which represent the same spot in the gels are better visible in the corresponding Cy 5 images. Therefore the corresponding areas of both, Cy 3 and Cy 5 images are shown in frames on the right of the gel image (**Fig. 4.11** and **Fig. 4.12**).

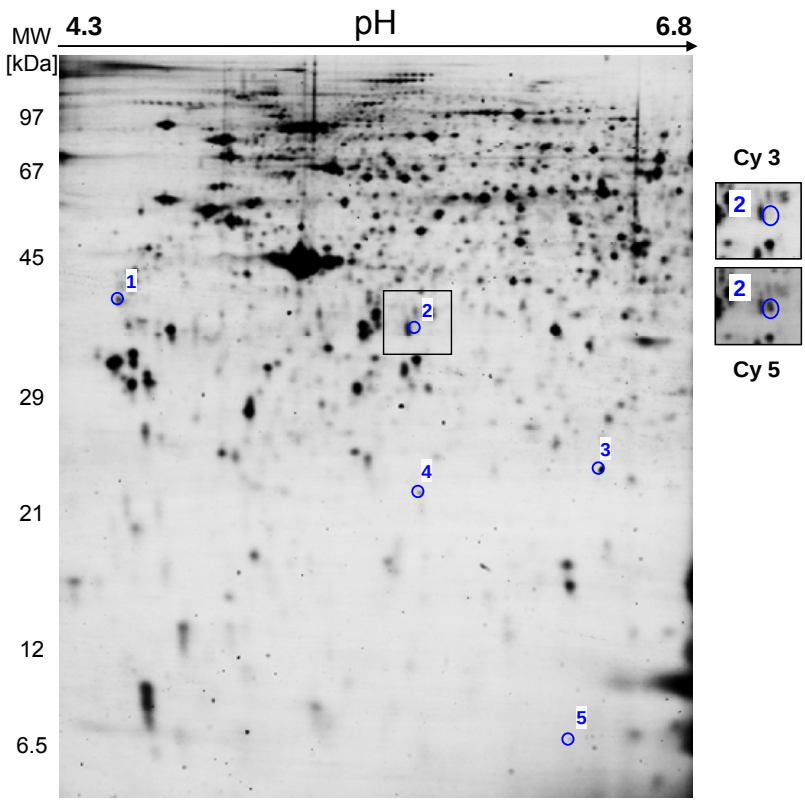

Fig. 4.11: Cy 3 image of a gel in the group of GH transgenic mice in stage 1 vs. their controls in the pH 4.3 – 6.8. Differentially abundant protein spots are marked by circles and indicated by numbers corresponding to the numbers in **Table 4.2**. Spot 2 is better visible in the Cy 5 image as shown in the lower frame on the right. MW molecular weight.

Spot	DeCyder No.	Average Ratio	p-value
1	1186	1.56	0.0053
2	1289	2.22	0.0062
3	1641	-4.90	1.9×10^{-4}
4	1712	-2.49	0.0014
5	2259	-2.13	0.0054

Table 4.2: Intensity ratios and significance values of the five differentially abundant spots in the group of GH transgenic mice in stage 1 vs. their controls. The first column indicates the spots outlined in **Fig. 4.11**. The second column shows the corresponding spot number given by the DeCyder software. A positive algebraic sign indicates an increase of intensity in the transgenic sample; a negative algebraic sign indicates a decrease of intensity.

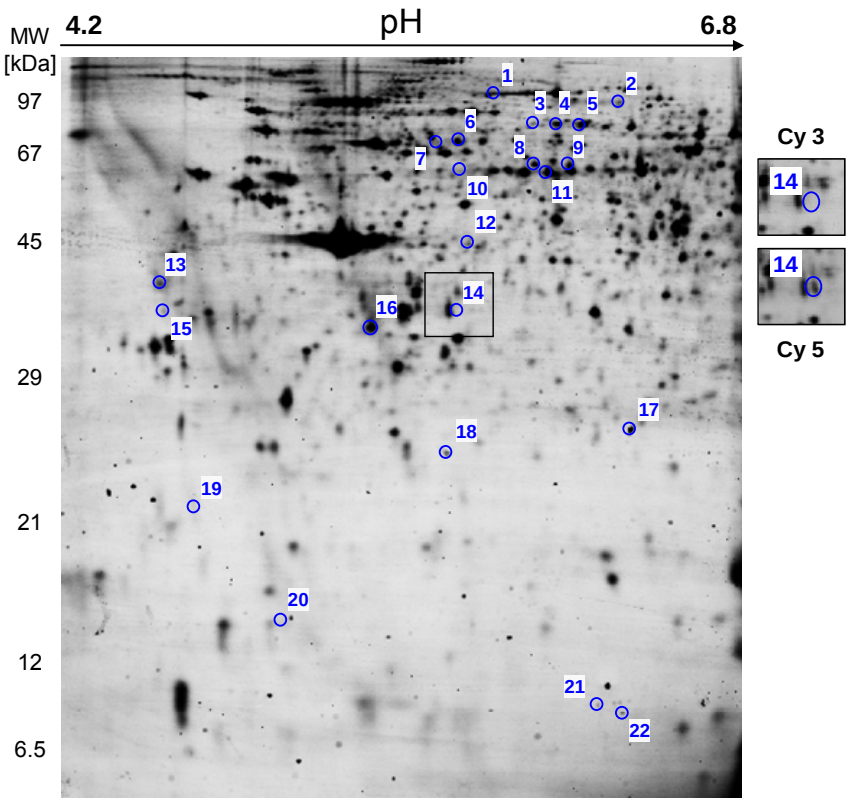

Fig. 4.12: Cy 3 image of a gel in the group of GH transgenic mice in stage 2 vs. their controls in the pH 4.2 – 6.8. Differentially abundant protein spots are marked by circles and indicated by numbers corresponding to the numbers in **Table 4.3**. Spot 14 is better visible in the Cy 5 image as shown in the lower frame on the right. MW molecular weight.

Spot	DeCyder No.	Average Ratio	p-value
1	184	1.51	0.0087
2	252	1.52	0.0054
3	371	-1.59	0.0018
4	372	-1.59	0.0093
5	375	-1.59	0.0031
6	448	2.06	1.2×10^{-6}
7	459	1.99	0.00018
8	562	-1.59	8.5×10^{-5}
9	566	-1.51	0.0004
10	587	1.56	0.001
11	600	-1.52	0.0013
12	930	-1.70	0.0014
13	1097	1.79	0.0019
14	1168	4.17	0.0011
15	1183	2.13	0.0011
16	1235	-1.74	0.00035
17	1556	-4.25	2.2×10^{-6}
18	1633	-2.00	0.00053

Spot	DeCyder No.	Average Ratio	p-value
19	1746	1.54	0.0083
20	2044	1.62	0.0025
21	2240	-1.56	0.0074
22	2250	-2.22	0.00023

Table 4.3: Intensity ratios and significance values of the 22 differentially abundant spots in the group of GH transgenic mice in stage 2 vs. their controls. The first column indicates the spots outlined in **Fig. 4.12**. The second column shows the corresponding spot number given by the DeCyder software. A positive algebraic sign indicates an increase of intensity in the transgenic sample; a negative algebraic sign indicates a decrease of intensity.

In order to demonstrate the reproducibility of the analysis, the line charts of the identified spots and the corresponding 3D volume plots of the protein spot intensities of each biological replicate in the group of GH transgenic mice in stage 2 and their controls are shown in **Fig. 4.13**. The line charts display graphically the altered abundance between samples from transgenic and their corresponding control animals. The spot abundancies are normalized between the gels on the basis of the IPS and are plotted as the abundance in a logarithmic scale (standardized log abundance) on the y-axis. The degree of difference in the standardized abundance between the two protein spot groups (tg and co) is expressed as the average ratio (AR). The line charts are created automatically by the software and the scale on the y-axis is not identical for all spots. Normalized abundancies of control samples are represented by the left dots, those of transgenic samples on the right. Corresponding abundance values from one transgenic mouse and its corresponding control are connected by dashed lines. Averages are indicated by crosses and connected by a blue line. Dots positioned very close to each other within the protein spot groups and parallel dashed lines indicate a very reproducible result and give rise to a low p-value. For example, in spot 6 (serum albumin) the values for the standardized abundance are distributed in a narrower range than in spot 11 (DRP-2), resulting in a lower p-value of spot 6 as compared to spot 11. Beneath the line charts, the corresponding spots are displayed as 3D-illustrations for each of the five biological replicates. In the 3D volume plots the fluorescence intensity of each spot over an area is depicted as 3D structur in dependency of the location. X- and y-axis represent the spot area of the gel and the z-axis represents the spot intensity of each pixel in this ares. Analysed spots are encircled by violet boundaries. These boundaries were

created by the algorithm of the software program and could not be influenced by the user. Blue and green colour tags show the orientation of the gel, as the coloured border indicates the location of the upper edge of the gel. 3D volume plots allow a visual comparison of the intensity changes within a sample pair (tg and co sample) as well as within the series of the five 2D-DIGE gels. Additionally, they provide information about the quality of a spot, e.g. protein spots have a characteristic distinguishable appearance as compared for example with peaks caused by dust particles on the glass plate, so-called speckles. Protein spots appear as slightly rounded peaks that descend fluently into the surrounding area as can be seen e.g. in the 3D volume plots of spots 11 (DRP-2) or 16 (Annexin A4). During image analysis special care was taken to filter speckles and spots that included speckles, thus making quantitation more precise.

In the subsequent **Fig. 4.13** the line charts and 3D volume plots of selected spots from the group of GH transgenic mice in stage 2 vs. their controls are shown. These spots could be identified (vinculin, filamin-A, serum albumin, dihydropyrimidinase related protein 2 (DRP-2), tropomyosin, annexin A4, myosin regulatory light chain (RLC) 2, and galectin-1). Some spots contained more than one protein as a consequence of comigration and are therefore referred to as multiple IDs. Average abundance ratios (AR) were increased for the spots identified as vinculin (+1.51), filamin-a (+1.52), serum albumin (+2.06 and +1.99), tropomyosin (+2.13), myosin RLC 2 (+1.54), and galectin-1 (+1.62) as well as spot 14 (multiple IDs; +4.17). Average abundance ratios were decreased for the spots identified as DRP-2 (-1.59, -1.51, -1.52), annexin A4 (-1.74) and spots 4 and 5 (multiple IDs; -1.59).

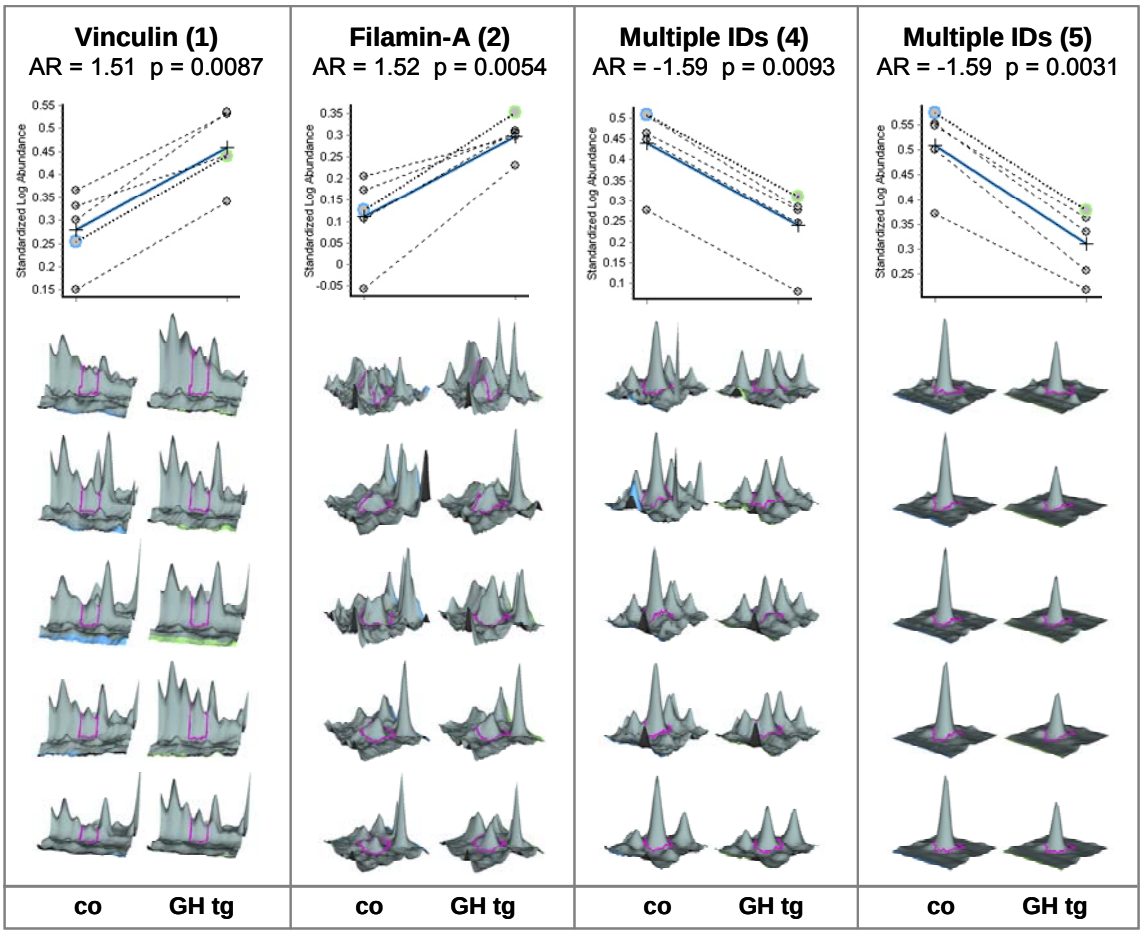
Vinculin (1)
AR = 1.51 p = 0.0087
Filamin-A (2)
AR = 1.52 p = 0.0054
Multiple IDs (4)
AR = -1.59 p = 0.0093
Multiple IDs (5)
AR = -1.59 p = 0.0031
Standardized Log Abundance
co GH tg
co GH tg
co GH tg
co GH tg

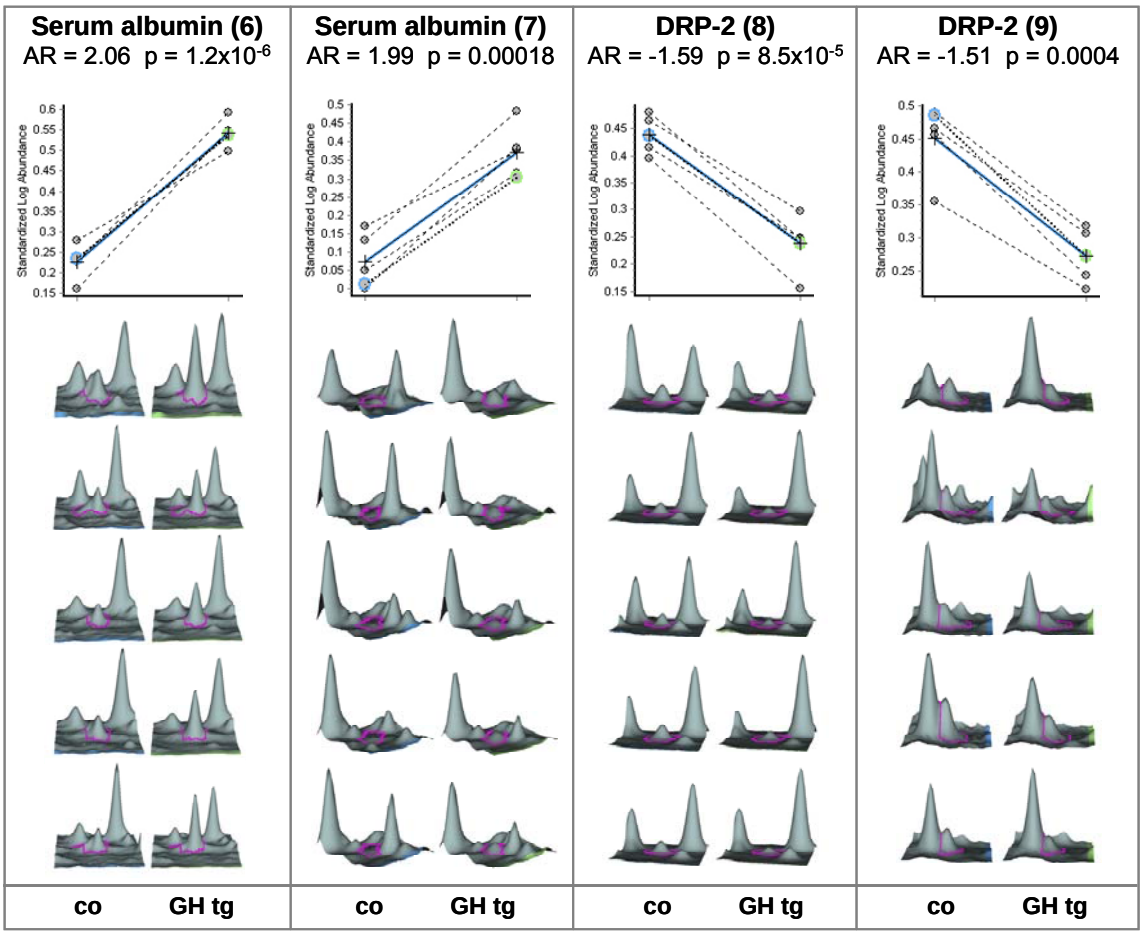
Serum albumin (6)
AR = 2.06 p = 1.2x10-6
Serum albumin (7)
AR = 1.99 p = 0.00018
DRP-2 (8)
AR = -1.59 p = 8.5x10-5
DRP-2 (9)
AR = -1.51 p = 0.0004
Standardized Log Abundance
co GH tg
co GH tg
co GH tg
co GH tg

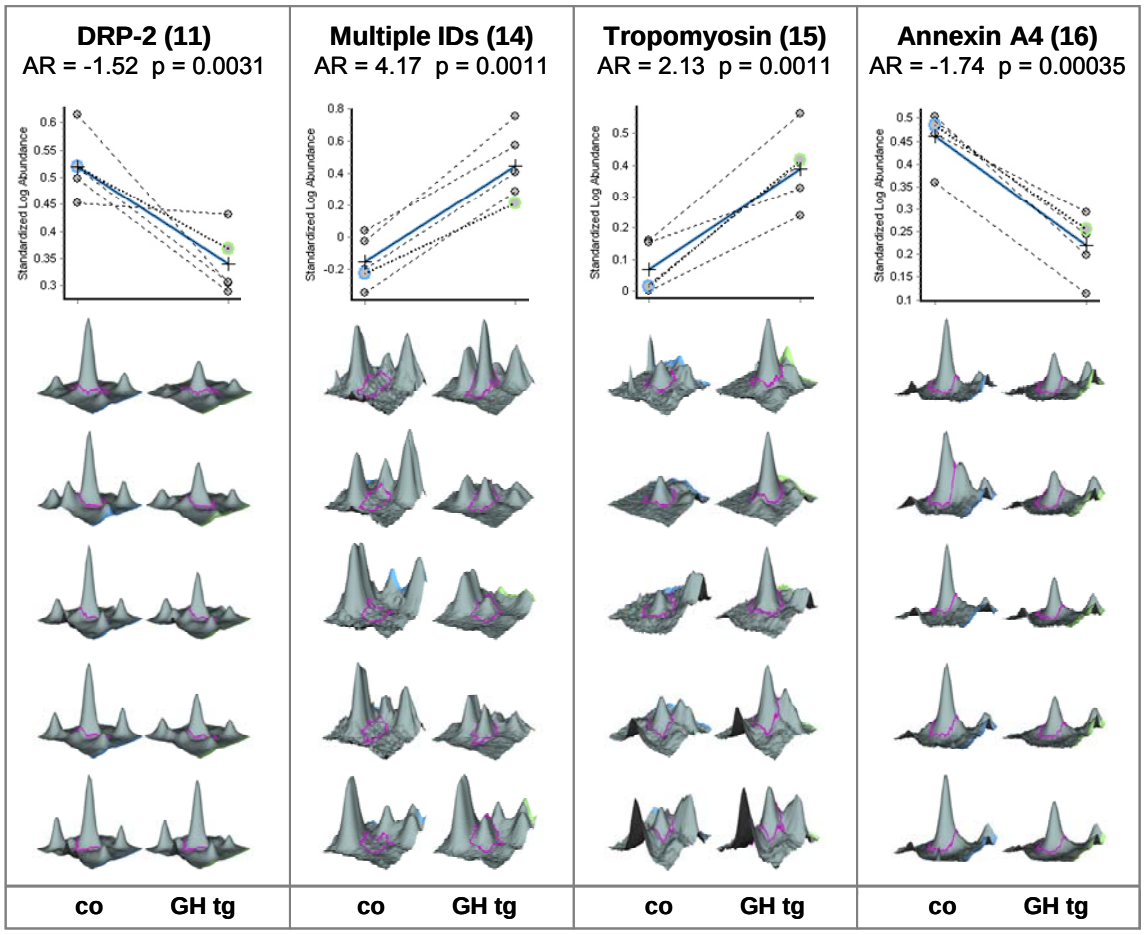

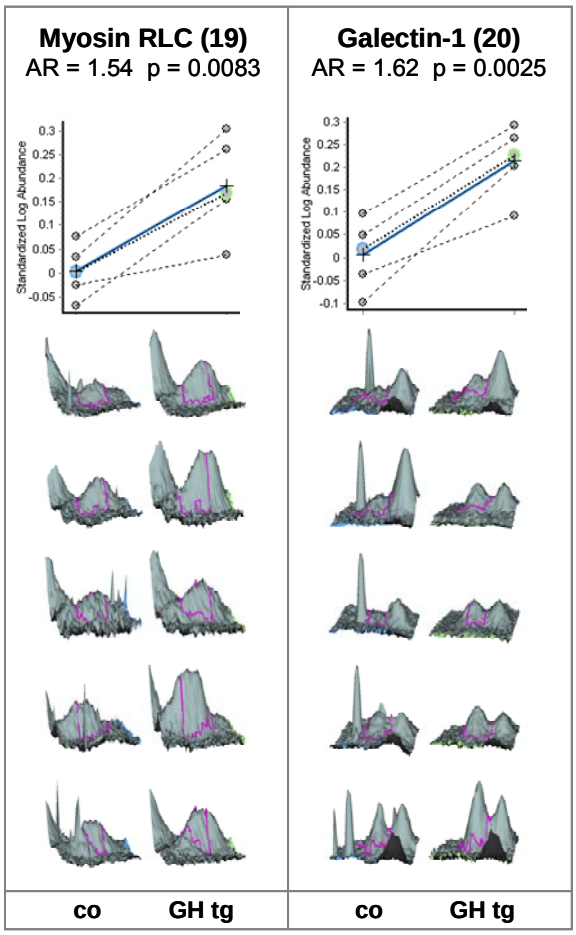

Fig. 4.13: GH transgenic mice in stage 2 vs. their controls: Line charts and 3D volume plots of protein spot intensities. For each protein, names (spot numbers are enclosed in brackets), abundance ratios (AR) and the p-values of the Student's t-test are assigned. Individual intensities from each of the six replicates are represented as dots (control left and transgenic right). Values of corresponding samples are connected by dashed lines. Averages are indicated by crosses and connected by a blue line. For each of the five biological replicates, all 3D volume plots of the corresponding spots are represented below.

4.5.2 GIPR^{dn} transgenic (tg) mice vs. wild-type controls (co)

The first subset of gels with five biological replicates representing five transgenic and five wild-type littermate controls had to be excluded from software analysis, because the Cy 2 images in all gels were not appropriate due to labelling problems. Therefore, eight glomerulus samples from another four pairs of GIPR^{dn} transgenic and control mice were taken for a new subset of gels. These samples fulfilled all criteria for stage 2, but not all of the pairs were littermates. In total four biological replicates, representing four trangenic mice and their corresponding wild-type controls, were analysed.

The internal pooled standard (IPS) of an analysis is represented by the Cy 2 images of the gels. Because in each gel an aliquot of the IPS is loaded, the comparison of the Cy 2 images allows a judgement about the quality and reproducibility of the analysed gels. The Cy 2 images of the four biological replicates in the group of GIPR^{dn} transgenic mice in stage 2 and their controls, shown **Fig. 4.14**, demonstrate the good reproducibility of the present analysis. Spot patterns as well as the spot intensities look almost identical in each replicate.

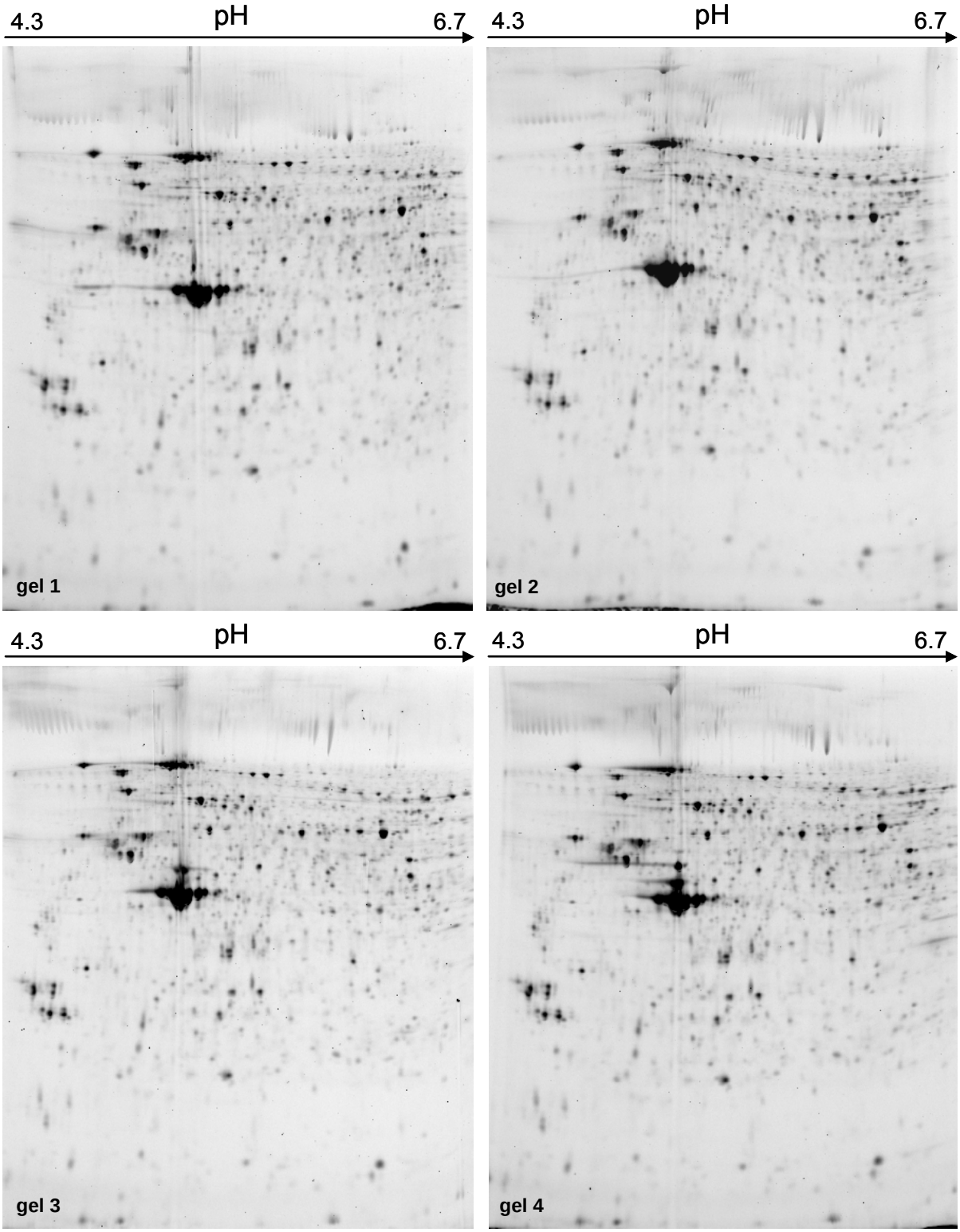

Fig. 4.14: Cy 2 images representing the IPS of the four biological replicates in the group of GIPR^{dn} transgenic mice in stage 2 vs. their controls.

After DeCyder software analysis 42 spots fulfilled the criteria mentioned in chapter 4.5 and were considered as differentially abundant. p-values of the student's t-test ranged from 8.7 x 10^{-5} (spot 13) to 9.8 x 10^{-3} (spot 32). 34 spots (spots 1-3, 7, 9, 10, 12, 14-26, 28-37, 39-42) were increased in the glomeruli of GIPR^{dn} transgenic mice in stage 2 as compared to their controls with average abundance ratios from 1.50 (spot 15) to 5.88 (spot 29). Eight spots (spots 4-6, 8, 11, 13, 27, 38) were decreased in the glomeruli of GIPR^{dn} transgenic mice in stage 2 vs. their controls with average ratios from -1.51 (spot 5) to -2.90 (spot 38). In **Fig. 4.15** a Cy 5 image, representing a glomerulus sample from a GIPR^{dn} transgenic animal, is shown and the positions of differentially abundant spots are marked by circles and indicated by numbers. The intensity ratios and significance values of the respective spots are listed in **Table 4.4**.

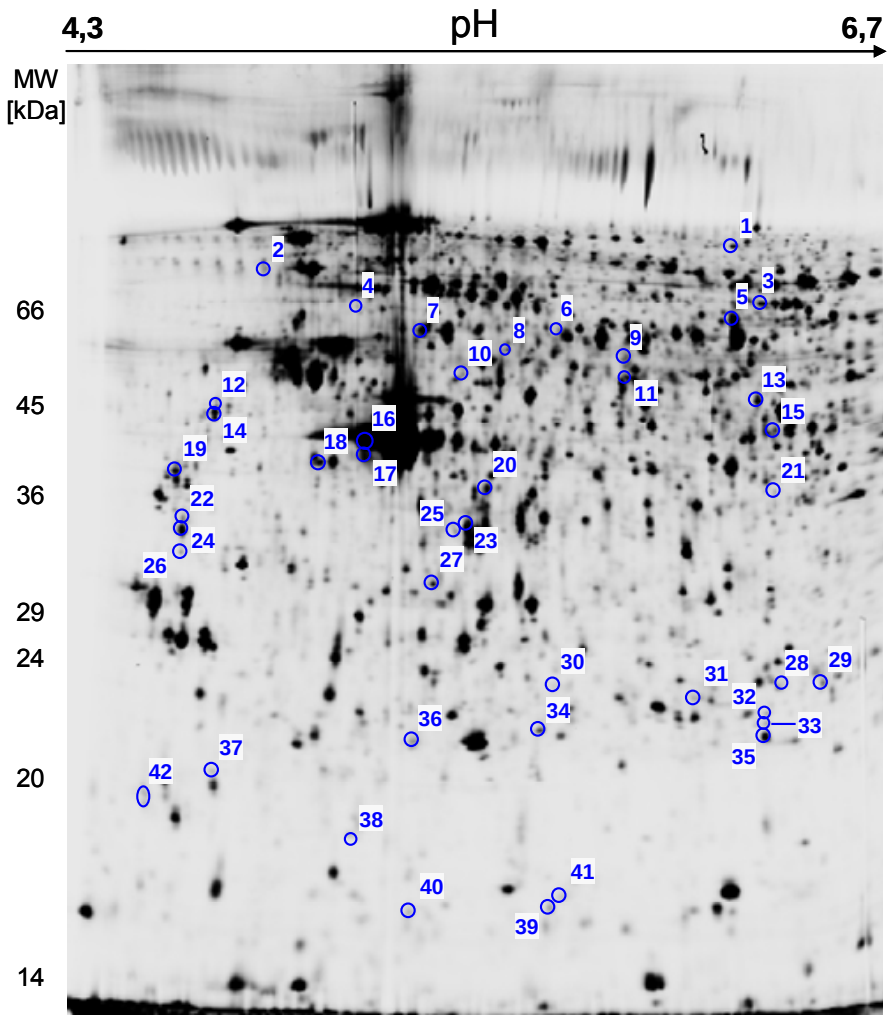

Fig. 4.15: Cy 5 image of a gel in the group of GIPR^{dn} transgenic mice in stage 2 vs. their controls in the pH 4.3-6.7. Differentially abundant spots are marked by circles and indicated by numbers corresponding to the numbers in **Table 4.4**. MW molecular weight

Spot	DeCyder No.	Average Ratio	p-value
1	467	1.55	0.0083
2	575	1.80	0.001
3	740	1.62	0.0063
4	747	-1.90	0.006
5	802	-1.51	0.0045
6	840	-1.64	0.0014
7	852	1.77	0.0027
8	937	-1.58	0.0011
9	969	1.61	0.0031
10	1045	1.72	0.0094
11	1057	-1.54	0.0072
12	1132	1.79	0.0054
13	1143	-1.85	$8.7x10^{-5}$
14	1192	1.67	0.0094
15	1263	1.50	0.0003
16	1305	1.53	0.0099
17	1378	1.63	0.00094
18	1395	1.64	0.0025
19	1425	1.77	0.003
20	1489	1.65	0.0039
21	1501	1.76	0.0027
22	1590	1.51	0.0045
23	1618	1.96	0.0012
24	1628	1.81	0.0016
25	1632	1.84	0.0064
26	1697	1.52	0.0051
27	1784	-1.58	0.0089
28	2066	5.05	0.0026
29	2072	5.88	0.0044
30	2077	2.98	0.0028
31	2102	3.00	0.0005
32	2138	2.42	0.0098
33	2165	2.56	0.0021
34	2173	2.32	0.0094
35	2187	2.20	0.0053
36	2198	1.74	0.0051
37	2242	1.54	0.0021
38	2308	-2.90	0.0001
39	2382	3.69	0.0064
40	2387	1.67	0.0018
41	2519	1.92	0.00012
42	2528	1.78	0.001

Table 4.4: Intensity ratios and significance values of the 42 differentially abundant spots in the group of $GIPR^{dn}$ transgenic mice in stage 2 vs. their controls. The first column indicates the spots outlined in **Fig. 4.15**. The second column shows the corresponding spot number given by the DeCyder software. A positive algebraic sign indicates an increase of intensity in the transgenic sample; a negative algebraic sign indicates a decrease of intensity.

As described in 4.5.1 the line charts and the 3D volume plots of the spot intensities show the reproducibility of the analysis. For the group of GIPR^{dn} transgenic mice in stage 2 vs. their controls they are shown for identified spots in each of the four biological replicates in **Fig. 4.16** The average abundance ratios (AR) were increased in glomeruli of GIPR^{dn} transgenic mice compared to those of controls in the spots identified as sarcosine dehydrogenase (SarDH; +1.55), succinate dehydrogenase (DHSA; +1.62), heat shock protein 60 (HSP 60; +1.77), fibrinogen gamma chain (FIBG; +1.72), actin (+1.53, + 1.63, + 1.64, +1.67), eukaryotic translation initiation factor 3 subunit 1 (eIF-31 alpha; +1.51), tropomyosin (+1.81), Ig kappa light chain (KAC; + 5.05), complement C4-B (CO4B; + 2.20), myosin regulatory light chain 2 (myosin RLC; +1.78) as well as spots 9, 14, 15, 20, 21, 29, 34 and 36 (multiple IDs). A decreased average abundance ratio in samples of GIPR^{dn} transgenic mice compared to their controls could be detected in the spots identified as dihydropyrimidinase related protein 2 (DRP-2; -1.51), bleomycin hydrolase (BLM hydrolase; -1.51), annexin A4 (-1.58) as well as spot 11 (multiple IDs). Comparing the spot identified as BLM hydrolase with the spot identified as CO4B, differences in the line charts can be observed. In the spot identified as BLM hydrolase the values of the standardized abundance are very similar within the transgenic as well as within the control samples. In contrast, in the spot identified as CO4B especially the abundance values of the transgenic samples appear more widely distributed, but are nevertheless significantly higher than in the control samples, giving rise to a higher p-value ($p = 5.3 \times 10^{-3}$) as compared to the spot identified as BLM hydrolase ($p = 8.7 \times 10^{-5}$).

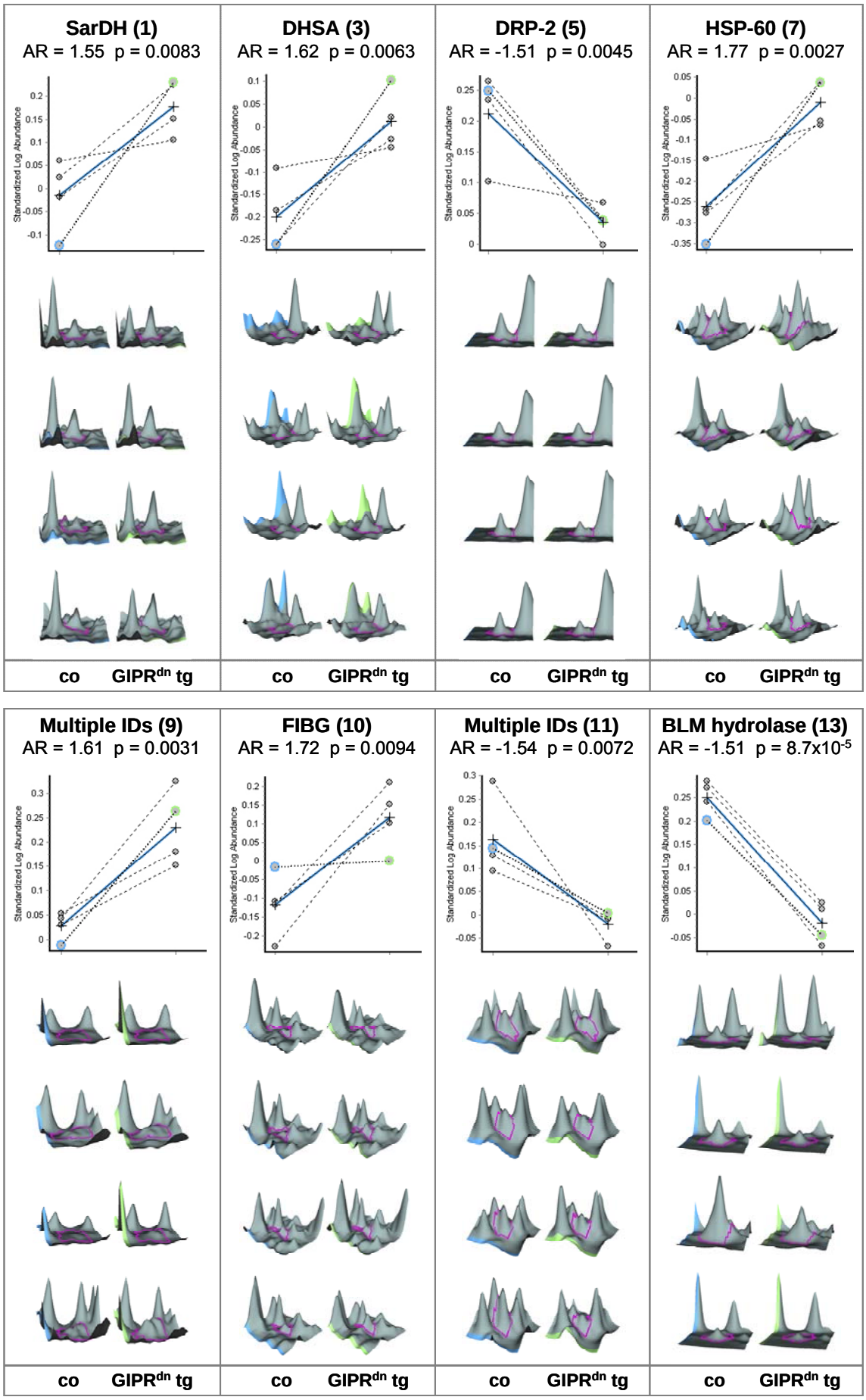
SarDH (1)
AR = 1.55 p = 0.0083
DHSA (3)
AR = 1.62 p = 0.0063
DRP-2 (5)
AR = -1.51 p = 0.0045
HSP-60 (7)
AR = 1.77 p = 0.0027
Multiple IDs (9)
AR = 1.61 p = 0.0031
FIBG (10)
AR = 1.72 p = 0.0094
Multiple IDs (11)
AR = -1.54 p = 0.0072
BLM hydrolase (13)
AR = -1.51 p = 8.7x10-5
Standardized Log Abundance
co GIPRdn tg

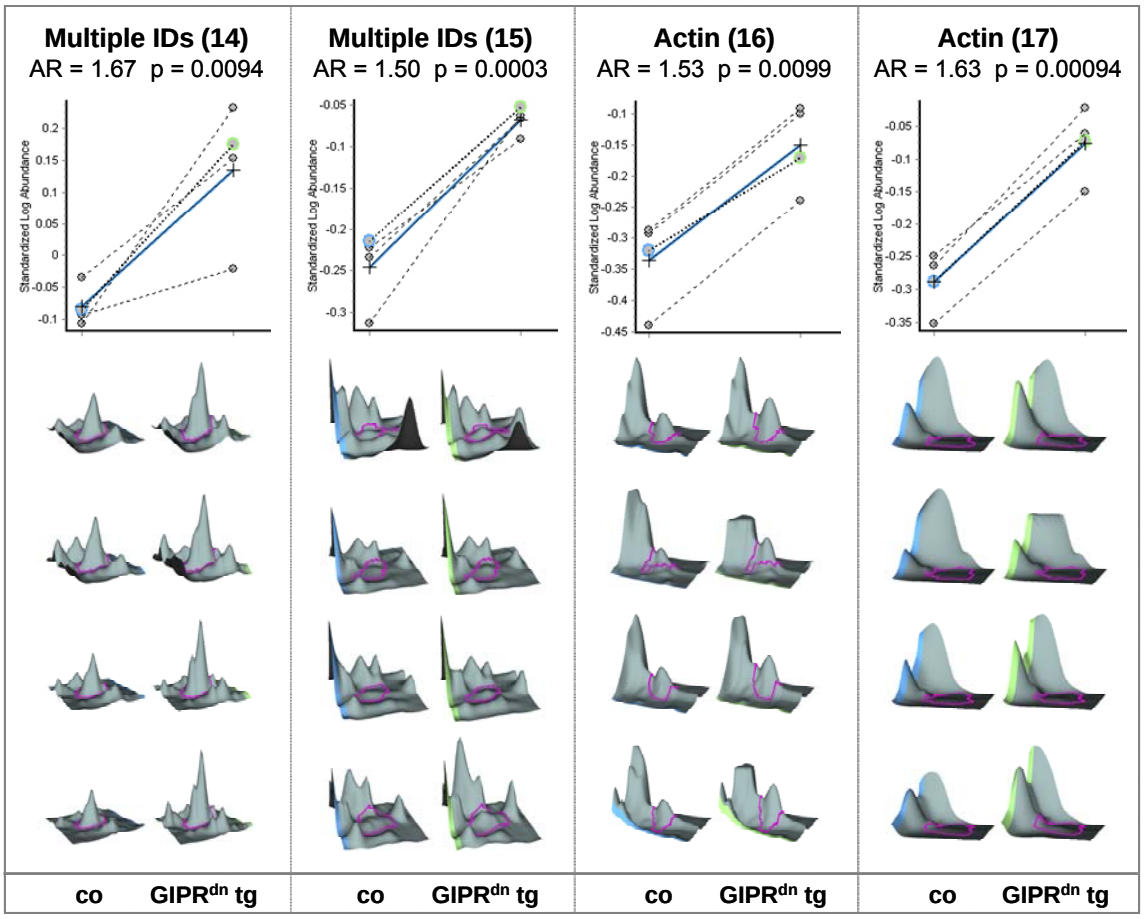
Multiple IDs (14)
AR = 1.67 p = 0.0094
Multiple IDs (15)
AR = 1.50 p = 0.0003
Actin (16)
AR = 1.53 p = 0.0099
Actin (17)
AR = 1.63 p = 0.00094
Standardized Log Abundance
co GIPRdn tg
co GIPRdn tg
co GIPRdn tg
co GIPRdn tg

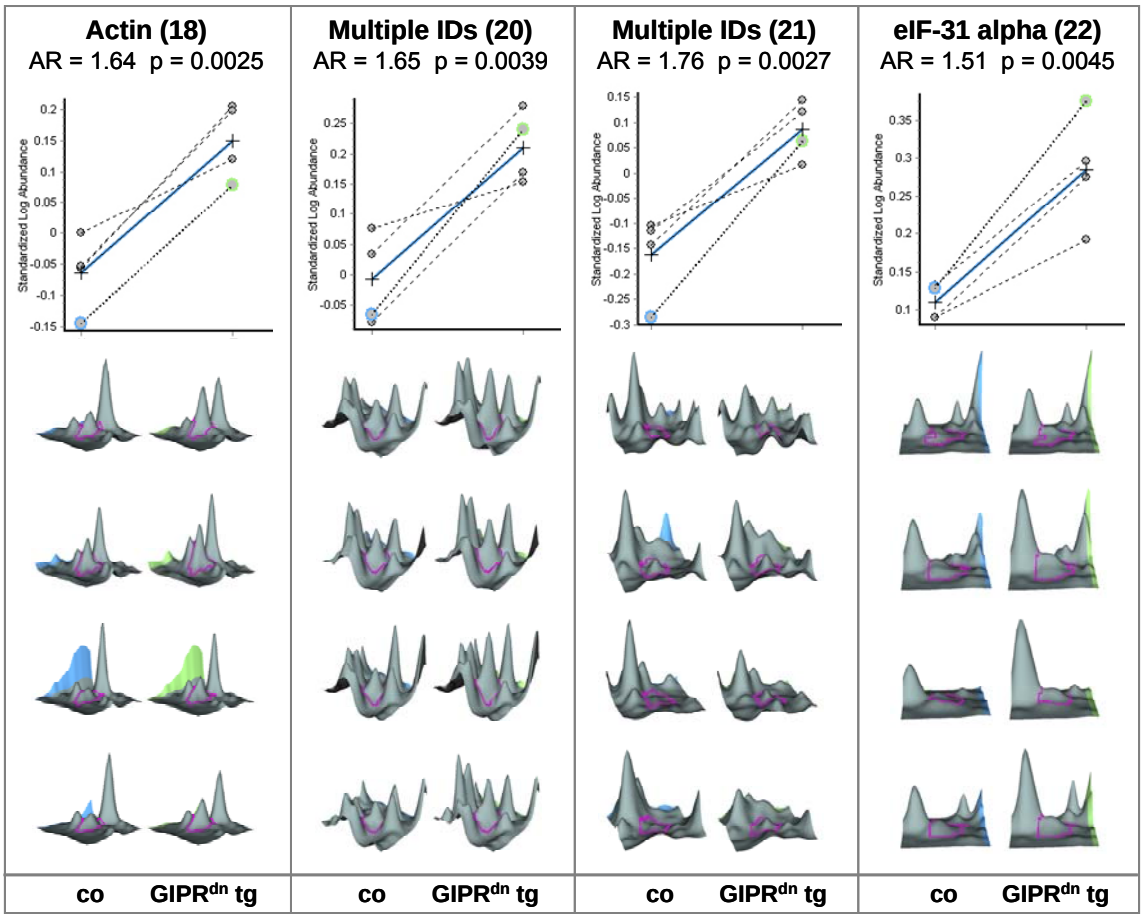
Actin (18)
AR = 1.64 p = 0.0025
Multiple IDs (20)
AR = 1.65 p = 0.0039
Multiple IDs (21)
AR = 1.76 p = 0.0027
eIF-31 alpha (22)
AR = 1.51 p = 0.0045
Standardized Log Abundance
co GIPRdn tg
co GIPRdn tg
co GIPRdn tg
co GIPRdn tg

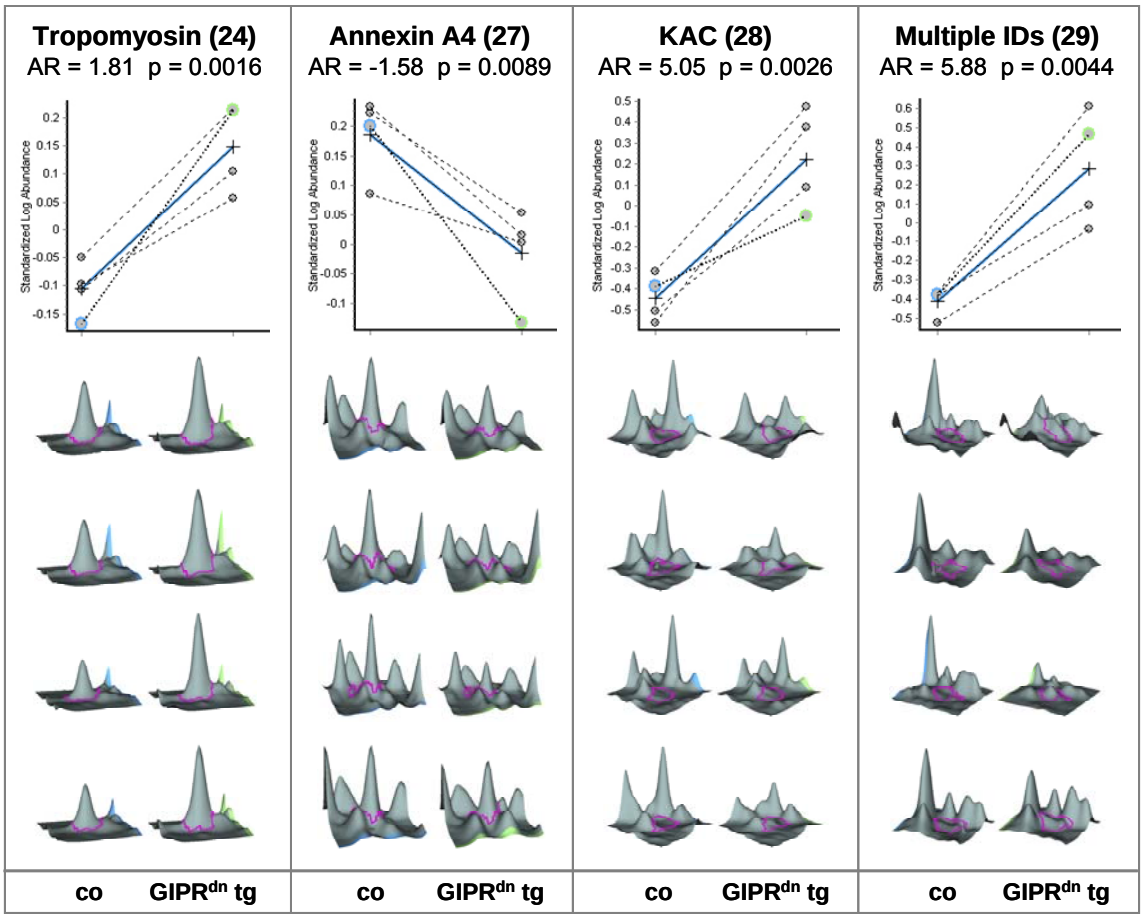
Tropomyosin (24)
AR = 1.81 p = 0.0016
Annexin A4 (27)
AR = -1.58 p = 0.0089
KAC (28)
AR = 5.05 p = 0.0026
Multiple IDs (29)
AR = 5.88 p = 0.0044
Standardized Log Abundance
co GIPRdn tg
co GIPRdn tg
co GIPRdn tg
co GIPRdn tg

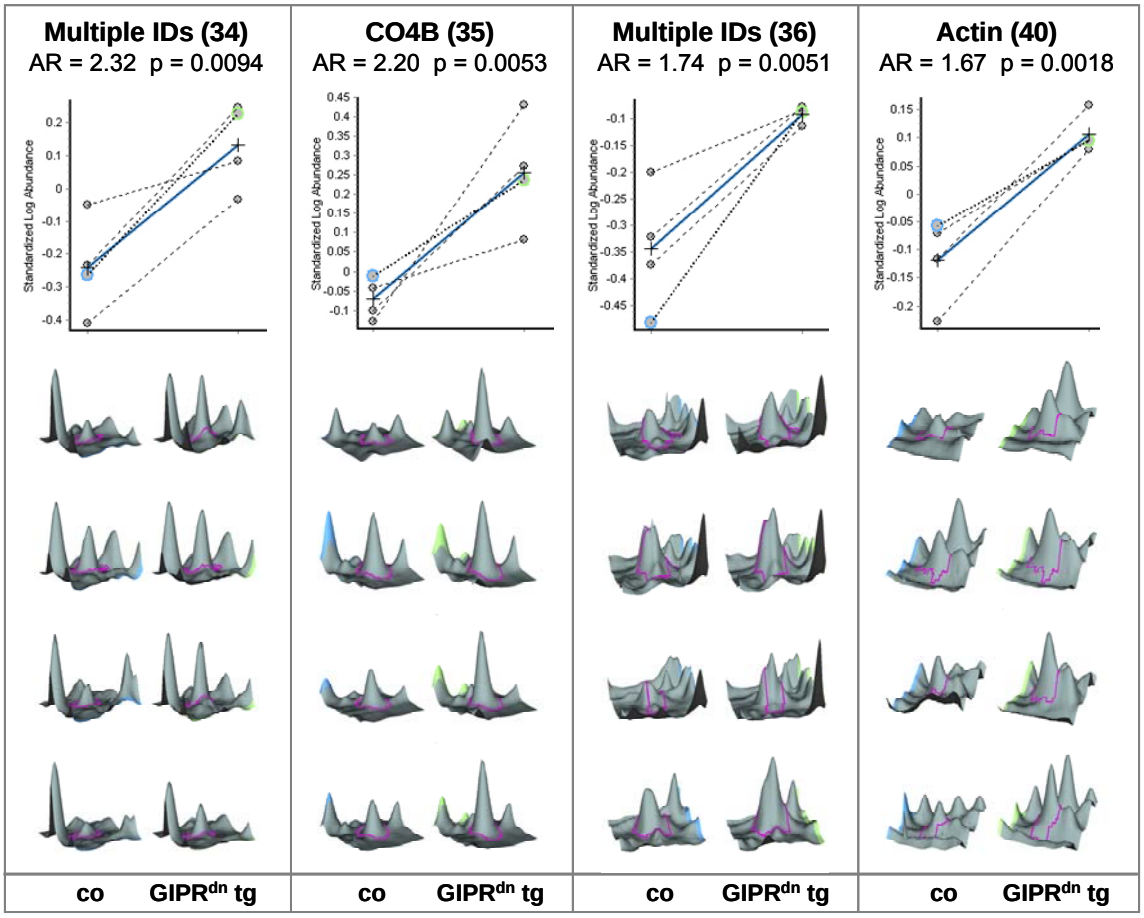
Multiple IDs (34)
AR = 2.32 p = 0.0094
CO4B (35)
AR = 2.20 p = 0.0053
Multiple IDs (36)
AR = 1.74 p = 0.0051
Actin (40)
AR = 1.67 p = 0.0018
Standardized Log Abundance
co GIPRdn tg
co GIPRdn tg
co GIPRdn tg
co GIPRdn tg

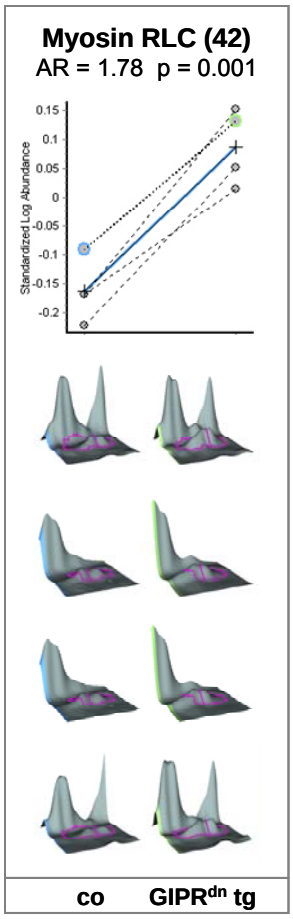

Fig. 4.16: GIPR^{dn} transgenic mice in stage 2 vs. their controls: Line charts and 3D volume plots of protein spot intensities. For each protein, names (spot numbers are enclosed in brackets), abundance ratios (AR) and the p-values of the Student's t-test are assigned. Individual intensities from each of the six replicates are represented as dots (control left and transgenic right). Values of corresponding samples are connected by dashed lines. For each of the four biological replicates, all 3D volume plots of the corresponding spots are represented below.

4.6 Identification of proteins of differentially abundant proteins

For identification of the differentially abundant spots, preparative 2D-gels in the pH range 4-7 were loaded with a total amount of 500 µg protein from glomerulus lysates. In the group of GH transgenic mice vs. their controls a pool of glomerular lysates from transgenic and control mice was used for the preparative gel (see **Fig. 4.17**). In the group of GIPR^{dn} transgenic mice vs. their controls one preparative gel was prepared with glomerulus samples from transgenic mice and another one with glomerulus samples from control mice (see **Fig. 4.18**). Preparative gels were stained for total protein with colloidal Coomassie. Differentially abundant spots were excised from the preparative gels and subsequently a tryptic hydrolysis was performed using the OMX-S® device.

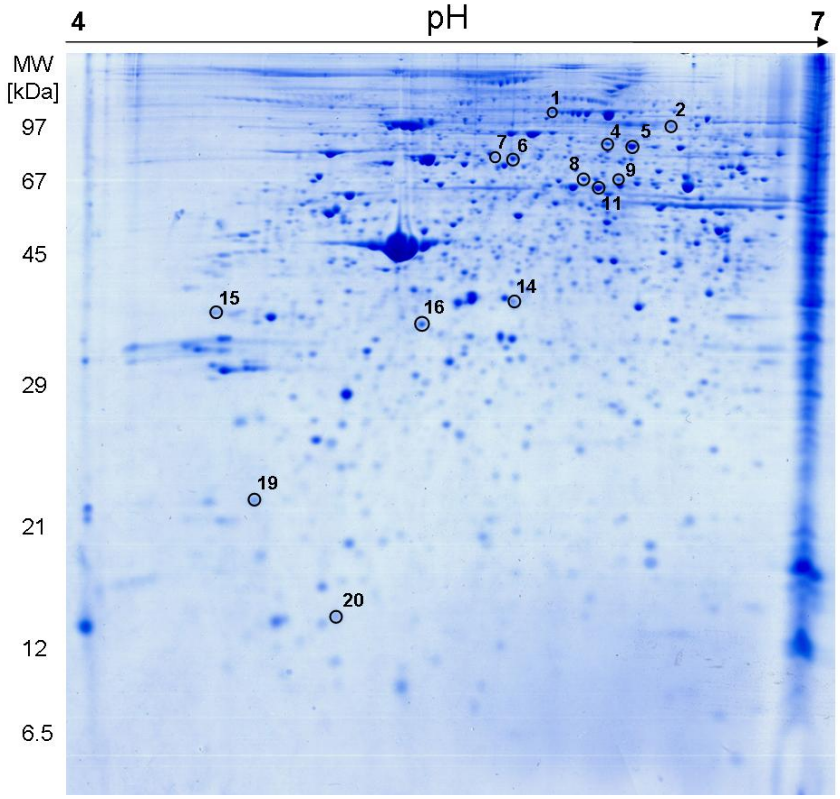

Fig. 4.17: Preparative gel of glomerulus samples from GH transgenic and control mice in pH 4-7. Gel contains 500 µg protein. All identified spots are marked by circles and indicated by numbers corresponding to the numbers in **Table 4.6** MW molecular weight.

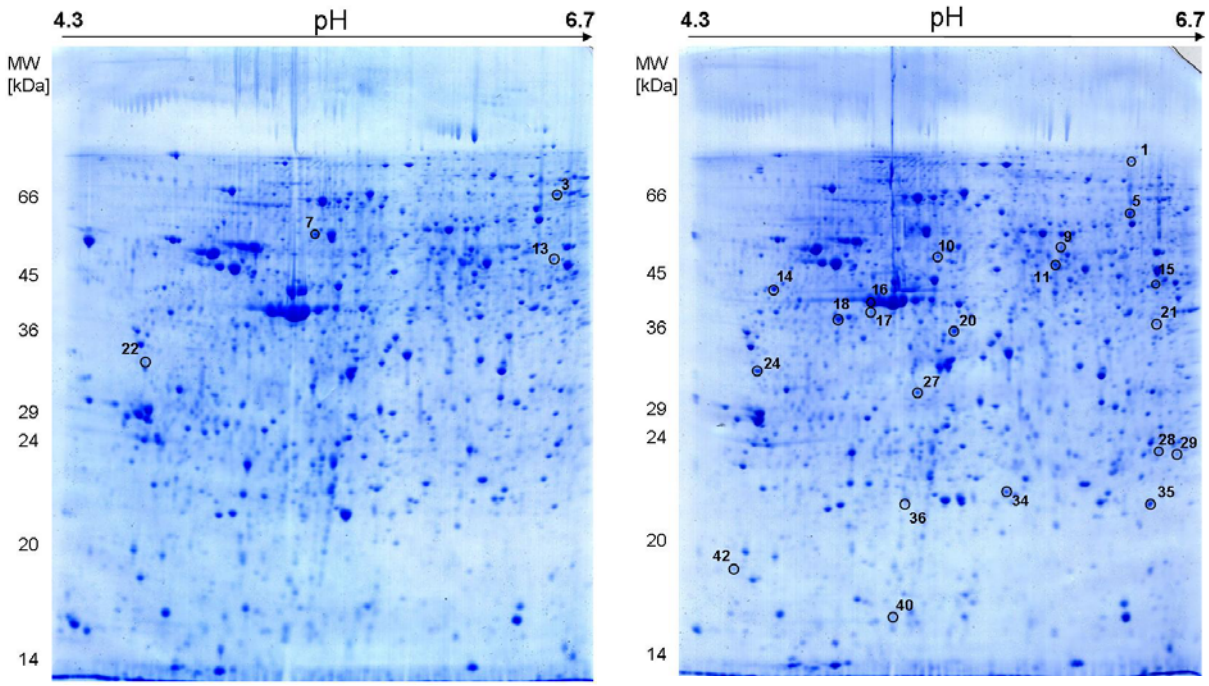

Fig. 4.18: Preparative gels of glomerulus samples from control mice (a) and from GIPR^{dn} transgenic mice (b) in pH 4-7. Gels contain 500 µg protein each; all identified spots are marked by circles and indicated by numbers corresponding to the numbers in **Table 4.7**. MW molecular weight.

14 spots could be excised from the preparative gel of samples from GH tg and co mice and 28 from the gels of samples from GIPR^{dn} transgenic and control mice, respectively. After tryptic hydrolysis spots were subjected to MALDI-TOF/TOF mass spectrometry analysis. Five of the 29 spots from the group of GIPR^{dn} transgenic mice in stage 2 vs. their controls were analysed by LC-ESI-MS/MS analysis, because they appeared to be very weak spots in the preparative gels. In the groups of GH transgenic mice in stage 1 and 2 vs. their controls all 14 excised spots could be identified. In the group of GIPR^{dn} transgenic mice in stage 2 vs. their controls 23 of 24 excised spots could be identified by MALDI-TOF/TOF analysis and 3 of 5 excised spots by LC-ESI-MS/MS analysis.

Peptide mass fingerprint (PMF) spectra of four spots that were unambiguously identified by MALDI-TOF/TOF analysis – two in the group of GH transgenic mice stage 2 vs. their controls and two in the group of GIPR^{dn} transgenic mice stage 2 vs. their controls – are shown in **Fig. 4.19** and **Fig. 4.20**. The PMF spectra of the remaining unambiguously identified spots are shown in the attachment. The m/z ratio for the precursor ions that are formed during the PMF step is plotted on the x-axis. The relative intensities of the peaks in the PMF spectra are plotted on the y-axis. Overall the PMF spectra had adequate intensities and for each spot the maximum of 10 precursor ions were processed by Collision induced dissociation (CID), resulting in 10 MS/MS spectra per PMF spectrum.

Fig. 4.21 – **Fig. 4.23** show exemplary MS/MS spectra of three precursor ions derived from the PMF spectrum of spot 27 in the group of GIPR^{dn} transgenic mice in stage 2 vs. their controls (**Fig. 4.20** (b)) that could be identified as annexin a4. The respective precursor ions are indicated by red stars in **Fig. 4.20** (d). The peptides identified from the three MS/MS spectra could be matched to the sequence of annexin a4. In **Fig. 4.21** the matched b- and y-ions are annotated. Ten of eleven y-ions as well as four of eleven b-ions could be positively matched, indicating an unequivocal identification of the peptide.

(a)

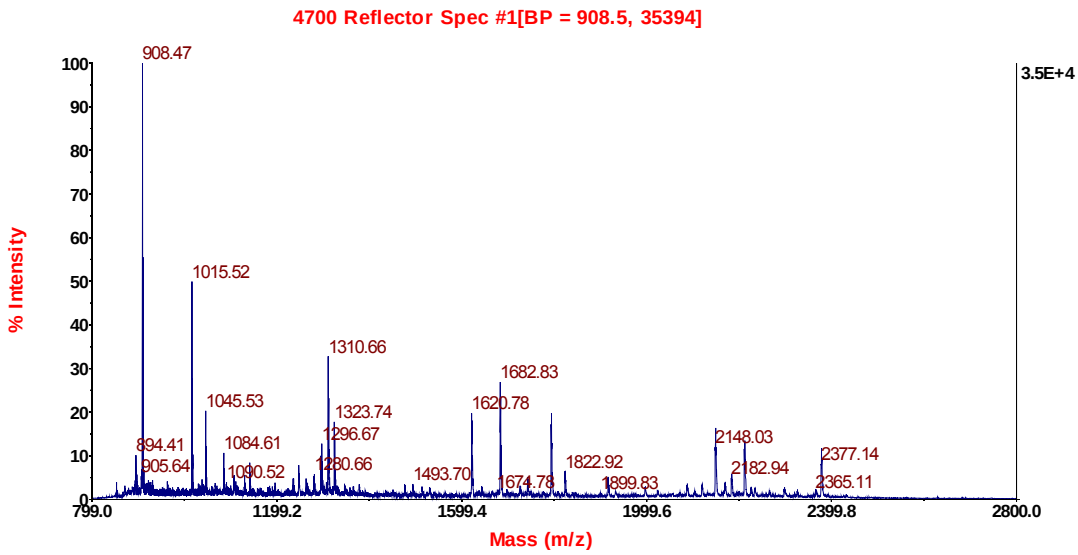

Spot 9 in the group of GH tg mice in stage 2 vs. their controls

(b)

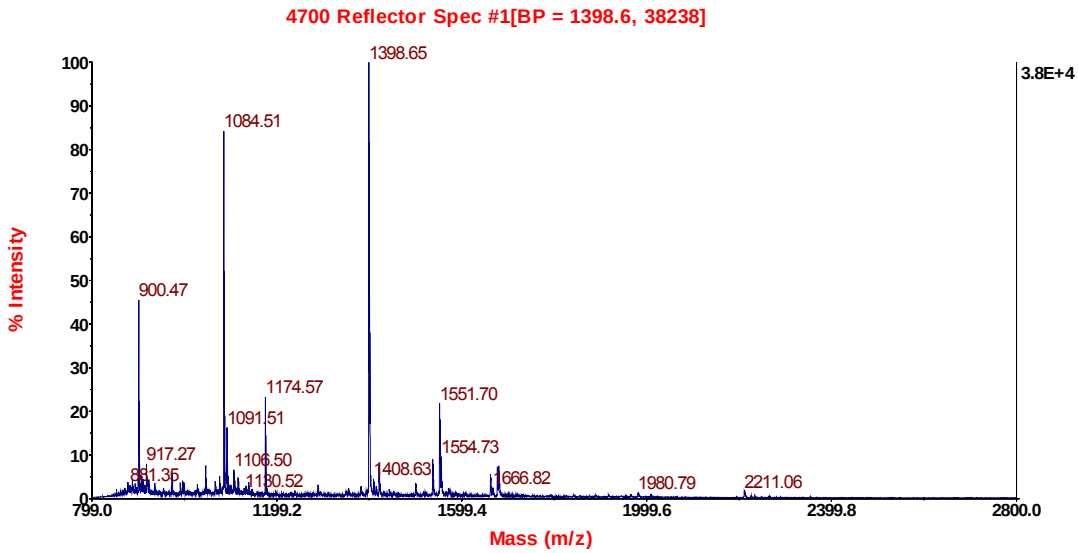

Spot 16 in the group of GH tg mice in stage 2 vs. their controls

Fig. 4.19: PMF spectra of spots 9 (a) and 16 (b) in the group of GH transgenic mice in stage 2 vs. their controls The mass to charge ratio (m/z) is plotted on the x-axis and the peak intensity is plotted on the y-axis.

(a)

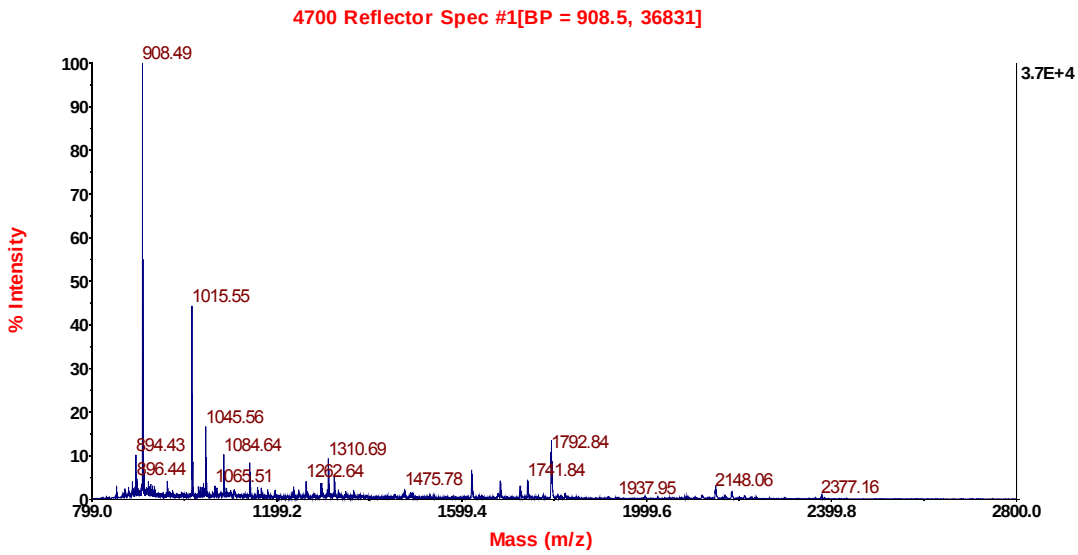

Spot 5 in the group of GIPR^{dn} tg mice in stage 2 vs. their controls

(b)

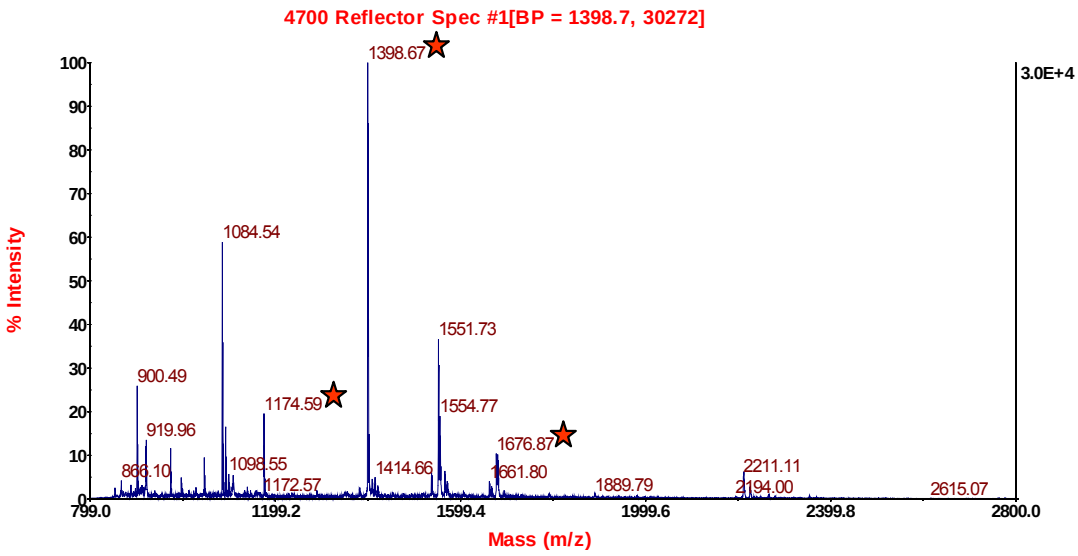

Spot 27 in the group of GIPR^{dn} tg mice in stage 2 vs. their controls

Fig. 4.20: PMF spectra of spots 5 (a) and 27 (b) in the group of GIPR^{dn} transgenic mice in stage 2 vs. their controls. The mass to charge ratio (m/z) is plotted on the x-axis and the peak intensity is plotted on the y-axis. Precursor ions for MS/MS spectra in **Fig. 4.21** – **Fig. 4.23** are indicated by red stars in (b).

(A)

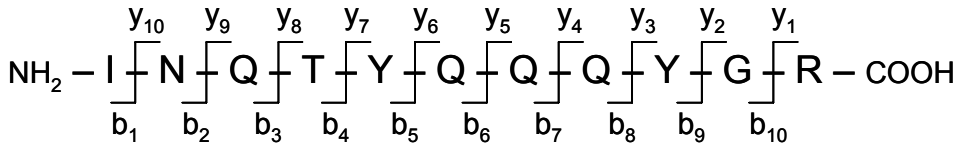

(B)

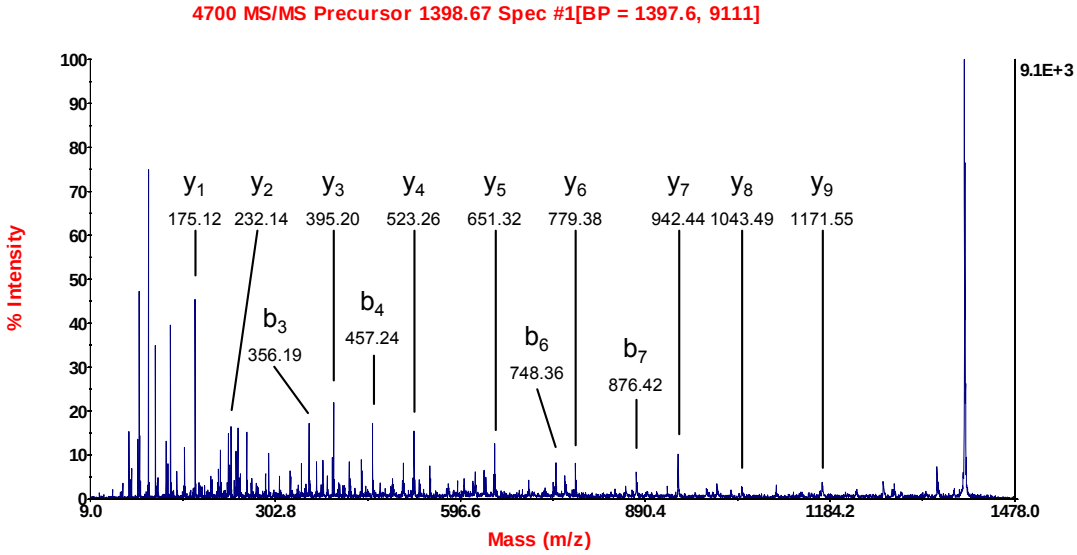

Fig. 4.21: MS/MS analysis of the 1398.67 precursor ion of the protein annexin A4. (A) Amino acid sequence of the 1398.67 precursor ion and schematic representation of all possible b- and y- ions (B) MS/MS spectrum of the peptide. The peaks of the measured b- and y-ions are annotated with the corresponding m/z-values.

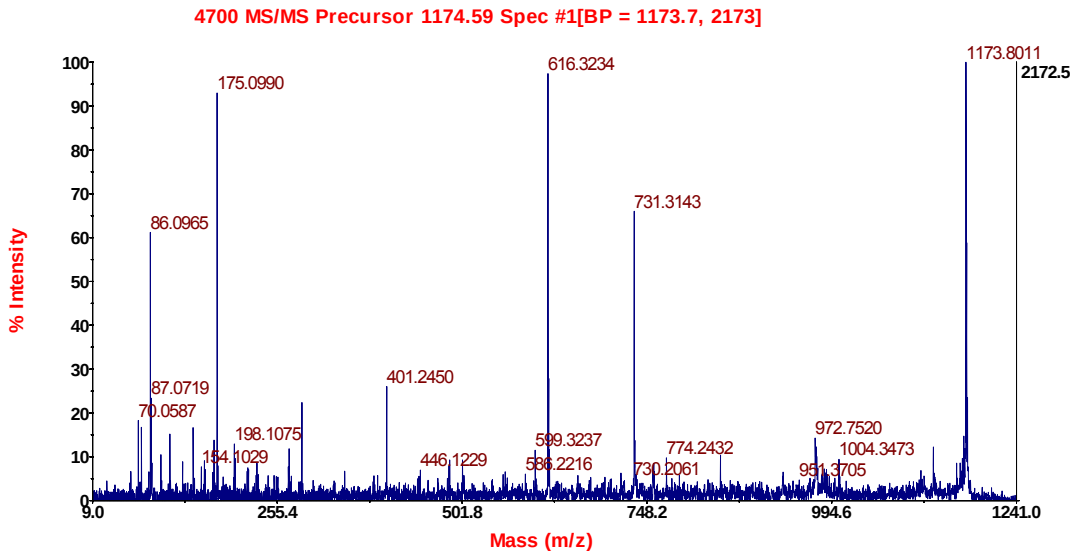

Fig. 4.22: MS/MS spectrum of the 1174.59 precursor ion of the protein annexin A4. The detected peptide had the amino acid sequence GLGTDDNTLIR.

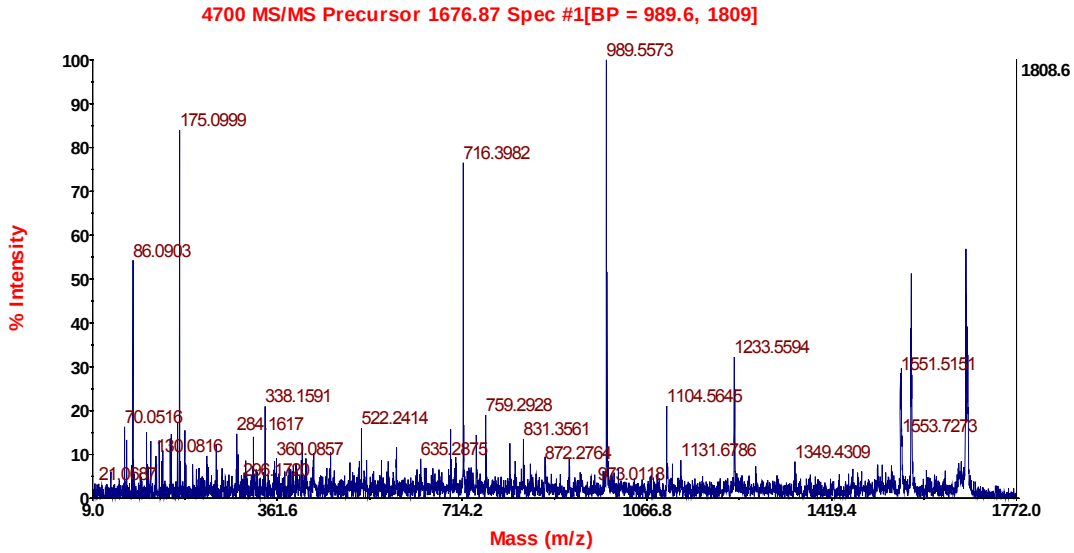

Fig. 4.23: MS/MS spectrum of the 1676.87 precursor ion of the protein annexin A4. The detected peptide had the sequence GLGTDEDAIIGILAYR.

Data from the analysis were searched against the mus musculus subset of the swiss prot database using the Mascot search engine. One of the parameters used to describe the quality of the database identification is the Mascot Protein Score (also called Mowse Score). This score is a measure of significance of a protein identification. The absolute value for the minimum score value necessary for a valid identification depends on the individual parameters of the search. The protein score is based on MS and MS/MS data, and represents a combination of the peptide mass fingerprinting (MS data) results and the MS/MS data (Ion Scores). Mascot Ion Scores reflect the quality of the MS/MS spectra, and the total Ion Score is based on weighted Ion Scores (MS/MS data) for the individual peptides. The Mascot algorithm presents this score as a number and a diagram. For valid results of MALDI TOF/TOF MS analysis, the score had to be above 54 under the conditions and parameters of this study. The area of insignificance is indicated by the green hatched area. Red bars indicate a hit in the database. As an example, **Fig. 4.24** lists three possibilities for what this diagram can look like. This helps to immediately distinguish between unambiguously identified, unidentified and ambiguously identified proteins. An unambiguously identified protein is represented by only one significant hit, that is shown as a red bar outside the green hatched area of insignificance (Fig. 4.24 (a)). An ambiguous identification is characterised by two or more significant hits in the database, shown as several red bars outside the green hatched area (Fig. 4.24 (b)).

If a spot remains unidentified, all red bars are located within the green hatched area of insignificance (**Fig. 4.24** (c)).

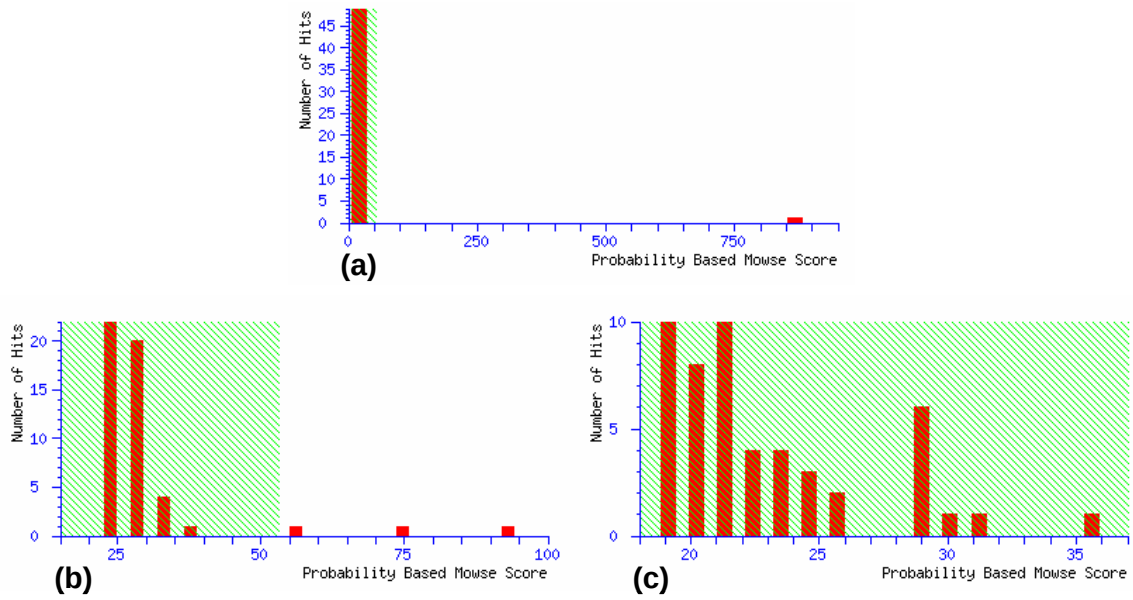

Fig. 4.24: Possible results of a database search as displayed in the Mascot result. Database hits are indicated as red bars. Hits in the green hatched area are not significant. Red bars outside the green hatched area indicate significant search results. Unambiguously identified protein (a) (only one significant hit), ambiguously identified protein, containing two or more significant hits (b) and the result for an unidentified protein spot (c) (no significant hits outside the green hatched area).

The so-called sequence coverage indicates, how many percent of the amino acid sequence of the protein could be covered by positively matched peptides. The matched peptides are highlighted in an illustration of the sequence. **Fig. 4.25** shows as an example the amino acid sequence of the protein annexin a4 identified with a protein score of 442 and a sequence coverage of 48 % out of spot 27 in the group of GIPR^{dn} transgenic mice in stage 2 vs. their controls, indicating matched peptides by red highlighting. This type of sequence representation facilitates a simple visualisation of the protein parts identified by MS/MS analysis.

```
  1 MEAKGGTVKA ASGFNATEDA QTLRKAMKGL GTDEDAIIGI LAYRNTAQRQ
 51 EIRSAYKSTI GRDLIEDLKS ELSSNFEQVI LGLMTPTVLY DVQELRRAMK
101 GAGTDEGCLI EILASRTPEE IRRINQTYQQ QYGRSLEEDI CSDTSFMFQR
151 VLVFLSAAGR DEGNYLDDAL MKQDAQELYE AGEKRWGTDE VKFLSILCSR
201 NRNHLLHVFD EYKRISQKDI EQSIKSETSG SFEDALLAIV KCMRSKPSYF
251 AERLYKSMKG LGTDDNTLIR VMVSRAEIDM LDIRASFKRL YGKSLYSFIK
301 GDTSGDYRKV LLILCGGDD
```

Fig. 4.25: Amino acid sequence of the protein annexin a4. Matched peptides are shown in bold red. Sequence coverage was 48%.

4.6.1 GH transgenic mice vs. their controls

In the group of GH transgenic mice in stage 1 vs. their controls only one of five differentially abundant spots could be identified by MALDI-TOF/TOF analysis, but contained a mixture of three different proteins as a consequence of comigration. This spot 2 in stage 1 conforms to the spot 14 in stage 2. In stage 2, 11 out of 22 differentially abundant spots could be unambiguously identified and three were identified with an ambiguous result of two or more proteins by MALDI-TOF/TOF analysis. Protein scores ranged from 81 up to 867. Among the 11 unambigous results were eight unique proteins and five isoforms. Serum albumin was found in spots 6 and 7 and dihydropyrimidinase-related protein 2 was found in spots 8, 9, 11. The data of all identified spots are listed in **Table 4.5** (stage 1) and **Table 4.6** (stage 2). Spot 15 in stage 2 was identified as tropomyosin, but a definite statement about the isoform cannot be made from the database result.

Spot	DeCyder No.	Protein	Swiss Prot Entry name	PS	SC [%]	Number of peptides identified by MS/MS	Mass [Da]		pI	
							Data-base	gel	Data-base	gel
2	1289	1) Serum albumin precursor	ALBU_MOUSE	230	25	3	70700	38000	5.75	5.68
		2) Guanine nucleotide-binding protein subunit beta 4	CBB4_MOUSE	81	24	0	37965		5.74	
		3) BTB/POZ domain-containing protein KCTD12	KCD12_MOUSE	96	11	0	36155		5.63	

Table 4.5: Most important parameters of the identified spots in the group of GH transgenic mice in stage 1 vs. their controls. SC = sequence coverage; PS = Mascot protein score; pI = Isoelectric point.

Spot	DeCyder No.	Protein	Swiss Prot Entry name	PS	SC [%]	Number of peptides identified by MS/MS	Mass [Da]		pI	
							Data-base	gel	Data-base	gel
1	184	Vinculin	VINC_MOUSE	343	38	1	117083	115000	5.77	5.87
2	252	Filamin-A	FLNA_MOUSE	305	17	2	283738	99000	5.68	6.30
4	372	1) Ezrin	EZRI_MOUSE	408	39	3	69347	76000	5.83	6.05
		2) Moesin	MOES_MOUSE	199	21	3	67708		6.24	
		3) Radixin	RADI_MOUSE	182	20	3	68672		5.85	
5	375	1) Ezrin	EZRI_MOUSE	716	57	8	69347	76000	5.83	6.15
		2) Moesin	MOES_MOUSE	336	27	4	67708		6.24	
		3) Radixin	RADI_MOUSE	313	22	5	68672		5.85	
6	448	Serum albumin precursor	ALBU_MOUSE	601	50	5	70700	71000	5.75	5.68
7	459	Serum albumin precursor	ALBU_MOUSE	384	42	4	70700	71000	5.75	5.62
8	562	Dihydropyrimidinase-related protein 2	DPYL2_MOUSE	570	50	6	62638	63000	5.95	5.97
9	566	Dihydropyrimidinase-related protein 2	DPYL2_MOUSE	633	58	5	62638	62000	5.95	6.10
11	600	Dihydropyrimidinase-related protein 2	DPYL2_MOUSE	867	54	9	62638	63000	5.95	6.02
14	1168	1) Serum albumin precursor	ALBU_MOUSE	230	25	3	70700	38000	5.75	5.68
		2) Guanine nucleotide-binding protein subunit beta 4	CBB4_MOUSE	81	24	0	37965		5.74	
		3) BTB/POZ domain-containing protein KCTD12	KCD12_MOUSE	96	11	0	36155		5.63	
15	1183	Tropomyosin 1 alpha chain *	TPM1_MOUSE	199	44	1	32718	37000	4.69	4.50
16	1235	Annexin A4	ANXA4_MOUSE	527	62	6	36121	36000	5.43	5.33
19	1746	Myosin regulatory light chain 2, smooth muscle isoform	MLRN_MOUSE	315	63	5	19767	22000	4.80	4.67
20	2044	Galectin-1	LEG1_MOUSE	302	61	4	15067	14000	5.33	4.97

Table 4.6: Most important parameters of the identified spots in the group of GH transgenic mice in stage 2 vs. their controls. SC = sequence coverage; PS = Mascot protein score; pI = Isoelectric point. * one of three possible isoforms

4.6.2 GIPR^{dn} transgenic mice in stage 2 vs. their controls

Of the 42 differentially abundant spots in the group of GIPR^{dn} transgenic mice in stage 2 vs. their controls 16 spots could be unambiguously identified and seven ambiguously with two or more proteins by MALDI-TOF/TOF MS analysis. Protein scores from 58 up to 789 could be observed. The 16 unambiguously identified spots corresponded to 13 unique proteins. With LC-ESI-MS/MS analysis three spots could be ambiguously identified. The nominal mass and pI were consistent with the

observed values in most the spots. The most important parameters of all identified spots are listed in **Table 4.7**. For spot 24 (Tropomyosin) and spots 16, 17, 18, 20 and 40 (Actin) the database result shows several possible isoforms with different protein scores. Taken into account that the result with the lowest protein score is identified by the same peptides like those hits with higher scores a definite statement about which isoform is exactly present cannot be made by the database results.

Spot	DeCyder No.	Protein	Swiss Prot Entry name	PS	SC [%]	Number of peptides identified by MS/MS	Mass [Da]		pI	
							Data-base	gel	Data-base	gel
1	467	Sarcosine dehydrogenase, mitochondrial precursor	SARDH_MOUSE	89	11	0	102644	97000	6.28	6.23
3	740	Succinate dehydrogenase [ubiquinone] flavoprotein subunit, mitochondrial precursor	DHSA_MOUSE	291	27	3	73623	78000	7.06	6.32
5	802	Dihydropyrimidinase-related protein 2	DPYL2_MOUSE	579	45	8	62638	63000	5.95	6.23
7	852	60 kDa heat shock protein, mitochondrial precursor	CH60_MOUSE	723	46	7	61088	58000	5.91	5.33
9	969	1) Lactadherin precursor	MFGM_MOUSE	71	15	0	53376	56000	6.10	5.92
		2) Nidogen-1 precursor	SPTB1_MOUSE	67	5	0	139387		5.25	
10	1045	Fibrinogen gamma chain precursor	FIBG_MOUSE	319	32	4	50044	50000	5.54	5.43
11	1057	1) Heterogeneous nuclear ribonucleoprotein H	HNRH1_MOUSE	287	37	3	49322	51000	5.89	5.92
		2) Heterogeneous nuclear ribonucleoprotein H'	HNRH2_MOUSE	174	23	2	49322		5.89	
		3) Cell cycle checkpoint protein RAD17	RAD17_MOUSE	70	15	0	77913		5.80	
13	1143	Bleomycin hydrolase	BLMH_MOUSE	61	22	0	53104	51000	6.04	6.32
14	1192	1) Vimentin	VIME_MOUSE	789	73	8	53581	45000	5.06	4.71
		2) Desmin	DESM_MOUSE	121	16	1	53391		5.21	
		3) Peripherin	PERI_MOUSE	71	16	1	54349		5.40	
15	*1263*	*1) BCKDH E1-alpha*	*ODBA_MOUSE*	*236*	*19*	*5*	*50624*	*45000*	*8.14*	*6.35*
		2) Elongation factor Tu, mitochondrial	*EFTU_MOUSE*	*234*	*35*	*4*	*49876*		*7.23*	
		3) hnRNP D0	*HNRPD_MOUSE*	*32*	*5*	*1*	*38501*		*7.62*	
16	1305	Actin, cytoplasmic 2 *	ACTG_MOUSE	773	56	8	42108	42000	5.31	5.17
17	1378	Actin, cytoplasmic 2 *	ACTG_MOUSE	207	26	2	42108	41000	5.31	5.17
18	1395	Actin, cytoplasmic 2 *	ACTG_MOUSE	600	41	6	42108	41000	5.31	5.03
20	1489	1) Isocitrate dehydrogenase [NAD] subunit alpha, mitochondrial precursor	IDH3A_MOUSE	316	38	3	40069	38000	6.27	5.52
		2) Actin, cytoplasmic 2 *	ACTG_MOUSE	272	26	4	42108		5.31	
21	*1501*	*1) Phosphotriesterase-related protein*	*PTER_MOUSE*	*50*	*10*	*1*	*39193*	*39000*	*6.18*	*6.35*
		2) S-Arrestin	*ARRS_MOUSE*	*36*	*2*	*1*	*44902*		*5.57*	
22	1590	Eukaryotic translation initiation factor 3 subunit 1	IF31_MOUSE	77	15	1	29582	35000	4.69	4.61
24	1628	Tropomyosin 1 alpha chain**	TPM1_MOUSE	211	35	2	32718	34000	4.69	4.61

Spot	DeCyder No.	Protein	Swiss Prot Entry name	PS	SC [%]	Number of peptides identified by MS/MS	Mass [Da]		pI	
							Data-base	gel	Data-base	gel
25	*1632*	*1) PDHE1-B*	*ODPB_MOUSE*	*62*	*8*	*1*	*39254*	*35000*	*6.41*	*5.45*
		2) Annexin A3	*ANXA3_MOUSE*	*39*	*8*	*1*	*36389*		*5.33*	
		3) SBCAD	*ACDSB_MOUSE*	*39*	*5*	*1*	*48300*		*8.00*	
27	1784	Annexin A4	ANXA4_MOUSE	442	48	5	36121	31000	5.43	5.36
28	2066	Ig kappa chain C region	KAC_MOUSE	65	35	1	11942	23000	5.23	6.37
29	2072	1) Heterogeneous nuclear ribonucleoprotein H	HNRH1_MOUSE	178	14	3	49322	23000	5.89	6.51
		2) Heterogeneous nuclear ribonucleoprotein H'	HNRH2_MOUSE	177	14	3	49533		5.89	
34	2173	1) Glutathione peroxidase 3 precursor	GPX3_MOUSE	241	32	3	25589	22000	8.26	5.66
		2) Glutathione peroxidase 1	GPX1_MOUSE	58	23	1	25553		6.74	
35	2187	Complement C4-B precursor	CO4B_MOUSE	82	8	0	194403	22000	7.54	6.44
36	2198	1) ATP synthase D chain, mitochondrial	ATP5H_MOUSE	164	35	3	18664	21000	5.52	5.27
		2) COMM domain-containing protein 8	COMD8_MOUSE	62	10	1	21067		5.38	
40	2387	Actin, cytoplasmic 2 *	ACTG_MOUSE	247		4	42052	16000	5.29	5.27
42	2528	Myosin regulatory light chain 2, smooth muscle isoform	MLRN_MOUSE	117	28	2	19767	19000	4.80	4.51

Table 4.7: Most important parameters of the identified spots in the group of GIPR^{dn} transgenic mice in stage 2 vs. their controls. SC = sequence coverage; PS = Mascot protein score; pI = Isoelectric point; italic = spots identified via LC-ESI-MS/MS. * one of six possible isoforms; ** one of three possible isoforms

4.6.3 Proteins with differential abundance in GH transgenic as well as GIPR^{dn} transgenic mice in stage 2 vs. their corresponding controls

Of the eight unique proteins identified in the group of GH transgenic mice in stage 2 vs. their controls and the 13 unique proteins identified in the group of GIPR^{dn} transgenic mice in stage 2 vs their controls an intersection of four identical proteins could be build (see **Table 4.8**). These proteins were consistent with the direction of the change in abundance as well as with the approximate level of the abundance ratio.

	GH tg vs. co		GIPR^{dn} tg vs. co	
Protein	**AR**	**Spot No.**	**AR**	**Spot No.**
Dihydropyrimidinase related protein 2	-1.59 -1.51 -1.52	8 9 11	-1.51	5
Annexin A4	-1.74	16	-1.58	27
Myosin regulatory light chain 2, smooth muscle isoform	1.54	19	1.78	42
Tropomyosin	2.13	15	1.81	24

Table 4.8: Overlap of identified proteins in the groups of GH transgenic mice and GIPR^{dn} transgenic mice in stage 2 vs. their corresponding controls. tg transgenic, co wild-type control; AR abundance ratio

5. Discussion

5.1 General aspects

In the present study a differential proteomic analysis of glomeruli from two different murine models of glomerulopathy was performed at defined disease stages. GH transgenic as well as GIPR^{dn} transgenic mice develop comparable early functional and morphological glomerular alterations. Glomeruli of transgenic mice and corresponding age-matched littermate controls were isolated at the stage of glomerular hypertrophy together with beginning albuminuria. Additionally, glomeruli of GH transgenic and control mice were isolated at the earlier stage of glomerluar hypertrophy without albuminuria. For glomerulus isolation a recently published method which bases on the perfusion of glomeruli with spherical superparamagnetic beads embolizing the glomerular capillaries was modified and optimized for the purposes of the present study (Takemoto et al., 2002). Subsequently, a 2D-DIGE based proteomic analysis was performed on the isolated glomeruli. This resulted in a number of differentially abundant proteins between transgenic and controls in each of the analyzed groups. Differentially abundant proteins were identified by MALDI-TOF/TOF analysis. The overall aim of the study was not only to identify differentially abundant proteins within one group, but to build up an intersection of the identified proteins between the group of GH transgenic mice in stage 2 and their controls and the group of GIPR^{dn} transgenic mice in stage 2 and their controls. This intersection represents a common pattern of identical proteins, independent of the transgene expression and the different genetic background (NMRI and CD1) of the two investigated mouse models.

5.2 Mouse models and analysed disease stages

Glomerular hypertrophy is considered to play a major role in the progression of chronic renal failure. In the concept of Fogo and Ichikawa it is postulated that disease-specific initial pathogenic insults lead to a reduced number of nephrons followed by glomerular hypertrophy (Fogo and Ichikawa, 1989; Ichikawa et al., 1991). The latter then leads to glomerular damage, further loss of nephrons and feeds the

vicious cycle that ends in the chronic renal failure. In primary focal segmental glomerulosclerosis and diabetes mellitus associated kidney lesions glomerular hypertrophy develops per se without a prior nephron loss. Nevertheless, the exact mechanisms of the pathogenesis of glomerulosclerotic alterations are yet to be found out. Albuminuria following glomerular hypertrophy is the earliest clinical evidence of glomerular damge and has been shown to be a sensitive marker for kidney disease as well as a renal risk factor (Ruggenenti and Remuzzi, 2006; Shumway and Gambert, 2002). Insights from animal models are still needed to enable an intervention at an early time point (Zoja et al., 2006). In order to find out proteins with potential relevance in the early steps of glomerulosclerosis development the early stage lesions, characterised by glomerular hypertrophy together with albuminuria, were chosen for this study. In GH transgenic mice glomerular hypertrophy without albuminuria was additionally analysed, because in these mice glomerular hypertrophy develops reliably four to five days before the onset of albuminuria. The two mouse models in this study were chosen, because they allowed the analysis of comparable morphological and functional glomerular lesions due to different reasons for their development of nephropathy. GH transgenic mice represent a model for progressive glomerulosclerosis (Wanke, 1996). $GIPR^{dn}$ transgenic mice develop severe diabetes mellitus and are a model for diabetes associated kidney lesions (Herbach, 2002; Herbach et al., 2003; Schairer, 2006). Both models show glomerular hypertrophy, albuminuria and glomerulosclerosis. The morphological and functional glomerular alterations are comparable, but they begin at totally different time points in the two models. In GH transgenic mice glomerular hypertrophy is already detectable at about 27 days of age and albuminuria starts about four to five days later. In $GIPR^{dn}$ transgenic mice the alterations develop from seven to eight weeks of age onwards. Therefore, an intersection of identified differentially abundant proteins between both groups is of particular interest.

In order to obtain reproducible and meaningful results in the proteomic analysis it is crucial to use optimally defined sample material. In the present study mice of which glomeruli were used for proteomic analysis were carefully selected by stringent criteria. These criteria were stage- but not age-specific. This was especially important for the selection of glomerular samples from $GIPR^{dn}$ transgenic and control mice, because the onset of albuminuria in $GIPR^{dn}$ transgenic mice varies in weeks. Out of the high number of screened mice only those were selected for proteomic analysis

which demonstrated a significant albuminuria as well as a glomerular hypertrophy as compared to their controls. In the stage of albuminuria transgenic mice in both models had to show two urine samples, which were taken in an interval of 48 hours, with a positive result for albuminuria in order to avoid choosing animals with only a transient albuminuria. Because GIPR^{dn} transgenic mice exhibited a severe diabetic polyuria, some aspects had to be considered during urine protein analysis to get comparable results. For SDS-PAGEs all urine samples were set to an identical creatinine concentration. The concentrations of albumin in the urine samples were determined by an ELISA experiment. Afterwards the measured albumin concentrations were set in relation to the creatinine concentrations and the albumin-creatinine-ratio was calculated. The comparability of the grade of albuminuria in GH transgenic and GIPR^{dn} transgenic mice could be demonstrated by both analyses.

The presence of glomerular hypertrophy was the prerequisite in both disease stages and mouse models. The mean glomerular volume was determined by quantitative stereology applying a model-based method frequently used for this purpose (Hirose et al., 1982; Wanke, 1996). Only mice that demonstrated an increase in the mean glomerular volume by at least 30 % as compared to the corresponding controls were chosen for the proteomic analysis. Early glomerular hypertrophy in GH transgenic mice is in line with previous results (Fisch, 2004; Wanke, 1996).

For a further characterisation of the analysed mouse models body and kidney weight as well as the nose-rump-length of each animal were determined prior to the process of glomerulus isolation. In GIPR^{dn} transgenic and control mice the results are consistent with earlier studies on these mice (Herbach, 2002; Herbach et al., 2005). GIPR^{dn} transgenic mice had a significantly reduced body weight and nose-rump-length as well as a significant increase of the kidney weight as compared to their controls. In GH transgenic mice in stage 2 only the body weight was significantly increased as compared to the control animals. The body weight of GH transgenic mice in stage 1 as well as kidney weight and nose-rump-length of GH transgenic mice in stage 1 and 2 were increased vs. the corresponding control animal data, but these differences did not reach statistical significance. This is probably due to the very young age when the growth hormone effect is not yet long enough to cause more profound alterations. As previously shown, differences in body and kidney weight between GH transgenic and control mice become significant at an age of 38 days (Fisch, 2004). Creating well defined sample material is crucial for a good

proteomic analysis. Thus, we determined presence of absence of albuminuria as well as the mean glomerular volume of each transgenic animal and its corresponding control. Additionally, body weight, kidney weight and nose-rump-length were determined for each animal. Barati and colleagues (2007) chose a different approach for the creation of sample material. Mice were not selected by a defined disease stage, but according to their age. The presence of glomerular alterations as well as albuminuria was postulated, relying on experiences from earlier studies on mice of the same model.

5.3 Glomerulus isolation

Proteomic analysis was performed on isolated murine glomeruli instead of whole kidney samples due to several reasons. Early alterations in the course of progressive glomerulosclerosis become manifest in the glomeruli, but do not yet affect the rest of the kidney. Because glomeruli represent only about 2 – 4 % of the whole kidney volume in different species (Artacho-Perula et al., 1993; Nyengaard and Bendtsen, 1992; Wanke, 1996), a subproteome approach targeting isolated renal glomeruli was the method of choice. A crucial demand for the glomerulus isolation was to obtain sufficient glomeruli from one mouse to run a 2D-gel based proteomic analysis. For a classical 2D-gel at least 100 – 200 µg total protein are needed. For the 2D-DIGE approach as used in this study about 75 µg protein are sufficient per sample (Berendt et al., 2005; Frohlich et al., 2006).

Methods to isolate glomeruli from rats and rabbits using sieving techniques have already been described (Downer et al., 1988; Kreisberg et al., 1978). However, from mice it is difficult to isolate pure glomeruli by sieving, because the diameter of mouse glomeruli is relatively similar to their tubules (Takemoto et al., 2002). Fractional sieving or picking under a photomicroscope yield glomeruli, but far too less for a proteomic analysis. Isolation of mouse glomeruli after Fe_3O_4 perfusion has been reported, however the isolation efficiency was rather limited (Baelde et al., 1994).

To overcome these problems a recently published method for large scale glomerulus isolation was used in the present study (Takemoto et al., 2002). The method was modified and optimized in order to obtain samples of reproducible quality and quantity. During this process beads from different manufacturers were tested and the best results could be achieved using Dynabeads® M-450 Epoxy (Invitrogen,

Germany). With other beads the perfusion could not be performed without difficulty, resulting in losses of either quality / purity or quantity of the glomerulus isolates. At the end, with a yield of ~20,000 glomeruli, virtually all glomeruli present in two mouse kidneys could be isolated in about 100 minutes with only minimal contamination by non-glomerular cells (Bonvalet et al., 1977; Takemoto et al., 2002). Once lysed, 10,000 glomeruli yielded approximately 200 – 250 µg of total protein. Taken into account that two kidney slices and an aliquot for transcriptomic profiling were removed during the isolation procedure, about 250-300 µg total protein could be obtained from 11,000 – 13,000 glomeruli. This amount of protein proved to be sufficient to perform a differential proteomic analysis of glomeruli from each individual animal, avoiding a pooling of glomerular samples from different animals. The final protein amount was always dependent on size of the kidney slices, optimal perfusion as well as on losses during the washing steps. Sitek et al. (2006) could only obtain about 40 µg total protein from the glomeruli isolated out of one kidney with the same method. They also modified the original procedure of Takemoto et al. (2002) and perfused the kidneys directly with ice-cold PBS instead of 37°C warm PBS and only afterwards with Dynabeads. This might have led to a suboptimal perfusion and glomerulus isolation yield due to vasoconstriction of the preglomerular arterioles. Creating well defined sample material is crucial for a good proteomic analysis. Therefore, the quality and suitability for proteomic analysis was assessed in preliminary experiments during the optimization process. Additionally, glomeruli were isolated from a maximum of two mice per day in a narrow time-frame and under identical conditions.

5.4 Proteomic approach

Proteomic approaches targeting the differences in glomerular proteomes of healthy subjects and those with renal alterations have been very rare so far. Xu and colleagues (2005) revealed differences in the m/z patterns of sclerotic and non-sclerotic glomeruli in 5/6 nephrectomized rat in a direct mass spectrometric approach. Very recently, alterations in the cellular redox pathways and advanced glycation end product metabolism in glomeruli of *db/db* diabetic mice were revealed by a 2D-gel based differential proteomic analysis (Barati et al., 2007). Other studies focused on cultured glomerular mesangial cells or podocytes, but not on isolated

glomeruli (Barati et al., 2006; Kuncewicz et al., 2003; Ransom et al., 2005). To our knowledge, the present study is the first study comparing the differences in glomerular proteomes of two murine nephropathy models. For the 2D-gels a pH-gradient of 4-7 was chosen, because in this pH-gradient a sufficiently wide range of proteins can be separated. An increased resolution is provided as compared to a broader pH-gradient of 3-10, resulting in less comigration of proteins (Westbrook et al., 2001). Differences in the formats of the gels run with samples from GH transgenic mice and their controls and those run with samples from $GIPR^{dn}$ transgenic mice and their controls are due different systems in which the gels were run. After scanning the images were submitted to DeCyder software analysis. During this analysis spots in all gels were positionally matched to each other and the intensities of the fluorescent signals of transgenic and control images were compared. In this study only spots that were present in all gels, had an average abundance ratio of ± 1.5, and had a p-value of $p < 0.01$ were considered as differentially abundant. The $p < 0.01$ instead of $p < 0.05$ was set in order to keep up stringent conditions as they are usually used in this laboratory (Berendt et al., 2005; Frohlich et al., 2006). Stringent criteria are set to minimize the detection of false positive results, even though more false negative results have to be accepted at the same time (Tonge et al., 2001). The reproducibility of the study can be visualized best by the line charts and the 3D-volume plots of each of the biological replicates. In this study a good resolution of the spots as well as reproducible changes in the intensity of most spots among the different gels could be observed. In some spots, the absolute normalized abundance values of a biological replicate was different from that of the other replicates as could be traced in the line charts. However, the statistical p-value was finally the determining criterium and the respective spots were nonetheless included in the analysis. In software-based evaluation of 2D-gels, user defined parameters for selection filters have a major influence on the number of proteins indicated by the software to be differentially represented in different samples (Gade et al., 2003). Therefore, the comparison of the number of differentially abundant proteins in this study with that of other studies has to be done carefully. For example, Barati and colleagues (2007) found 40 spots to be increased in their abundance in glomeruli of diabetic mice, having set a p-value of < 0.05. In the glomeruli of $GIPR^{dn}$ transgenic mice 42 spots were considered as differentially abundant with a p-value of < 0.01. With a change in the p-value to < 0.05 about 90 would have been considered as differentially

abundant. The increased absolute number of differentially abundant proteins in GIPR^{dn} transgenic mice in stage 2 vs. their controls as compared to GH transgenic mice in stage 2 vs. their controls – can be explained by a better resolution power of the Typhoon Scanner used for the gels which were run with samples from GIPR^{dn} transgenic mice and controls, as compared to the Ettan™ DIGE Imager used for the gels which were run with samples from GH transgenic mice and controls. A considerable increase in the number of differentially abundant proteins can be observed in the gels of GH transgenic mice vs. their controls in stage 1 as compared to stage 2 (5 vs. 22). This suggests the beginning of substantial changes in the protein pattern with the onset of albuminuria in these mice, even though animals in stage 2 were only four to five days older than those in stage 1. Even more, it confirms the choice of the examined disease stages with the focus on the onset of albuminuria to be a reasonable decision for the detection of alterations at a very early time point.

5.5 Identification of proteins

For the identification of differentially abundant protein spots preparative gels were run for each group stained with colloidal Coomassie. The use of the analytical fluorescent gels is problematic, because once the gel has been removed from the fluorescent scanner, the spots are no longer visible and one would have no control which spot would be picked (Tonge et al., 2001). Additionally, spots that are visible in the Coomassie stained gels, can be precisely excised under visual control, providing a high chance of identification by MALDI-TOF/TOF analysis. In the group of GH transgenic mice vs. their controls one gel was run for both stages consisting of samples from both one transgenic and one control mouse. In the group of GIPR^{dn} transgenic mice vs. their controls abundance ratios from -2.90 to +5.88 could be observered. To avoid underrepresentation of proteins in gels with pooled transgenic and control samples, separate gels of samples only from transgenic mice as well as only samples from control animals were run to achieve an optimal protein yield of picked spots. In order to obtain mass spectrometry spectra of optimal quality purification of peptides after tryptic hydrolysis of a protein prior to MALDI-TOF/TOF analysis is an important step (Lottspeich, 2006). For this purpose peptides were desalted and concentrated with pipette tips containing a miniature chromatography

column, so-called ZipTips. In the group of GIPR^{dn} transgenic mice vs. their controls some spots were very weak in the gel and therefore they were analysed by nano LC-MS/MS rather than MALDI-TOF/TOF analysis. The use of nano LC-MS/MS results in higher concentrations of the peptides derived from a protein spot reaching the MS-detector due to very low flow rates of about 240 nl/min (Frohlich and Arnold, 2006). This leads to higher signal to noise ratios and therefore to an enhanced sensitivity of the overall system. The nano LC-MS/MS analysis in this study is more sensitive than the MALDI-TOF/TOF analysis, but it is also very time-consuming – about 30 minutes for the analysis of one spot as compared to an analysis time of only a few minutes using MALDI-TOF/TOF mass spectrometry. Thus, LC-MS/MS is not routinely used for spot identification. Not all differentially abundant spots could be picked from the preparative gels, because they were either not detectable in these gels, could not be clearly distinguished from neighbouring spots or could not be assigned to the spot from the analytical images. Spots can be undetectable in Coomassie stained gels due to the lower sensitivity of colloidal Coomassie compared to fluorescence and the differential staining of proteins with different staining methods (Frohlich et al., 2006; Tonge et al., 2001). Although 500 µg protein were applied (2D-DIGE: 50 µg per dye), this increased protein amount cannot completely compensate the low sensitivity of the Coomassie staining. Some of the picked spots could not be identified, probably due to very low protein concentration within the spot. Taken together, in the group of GH transgenic mice in stage 2 vs. their controls and GIPR^{dn} transgenic mice in stage 2 vs. their controls about half of the differentially abundant spots could be successfully identified which could be observed in other studies as well (Frohlich et al., 2006; Tonge et al., 2001). Among them are several ambiguous identifications in which spots contain two or more different proteins. For these spots it cannot definitely be determined which of the proteins in the spot caused the differential abundance (Lilley et al., 2002) and had therefore to be excluded from further studies. Spots with several proteins are usually a result from comigration of proteins with similar molecular mass and pI (Westbrook et al., 2001). To further separate the proteins by their pI, gels with a narrower pH-gradient would have to be run. Molecular masses and pI of almost all unambiguously identified proteins as seen in the gel matched with the theoretical data, indicating that no protein degradation occurred during sample preparation (Gorg et al., 2004). However, in some cases differences in molecular mass or pI could be observed. If the molecular mass of a protein observed

in the gel is lower than indicated in the database, this is possibly a result of protein processing in the cell (Pratt et al., 2002). Generally, identification of proteins is being achieved by comparison of mass spectrometry data to the data of existing databases. Those databases include protein sequences that have been verified for the corresponding protein, but they also list sequences derived from cDNA. Often the sequence translated from cDNA into the sequence of amino acids includes the whole protein or precursor protein, which can be further processed in the cell, e.g. by cleavage of a leader peptide. Differences in pI can easily occur whenever a protein is posttranslationally modified. For example, phosphorylations will shift the pI to a more acidic region (Immler et al., 1998).

Taken together, eight unique proteins could be identified in the group of GH transgenic mice in stage 2 vs. their controls and 13 unique proteins in the group of $GIPR^{dn}$ transgenic mice in stage 2 vs. their controls, respectively. Annexin A4, dihydropyrimidinase-related protein 2 (DRP-2), tropomyosin as well as myosin regulatory light chain 2 were differentially abundant in the glomeruli of transgenic mice in both analysed mouse models. Alterations in cellular redox pathways and advanced glycation end product metabolism were recently observed in the glomeruli of *db/db* diabetic mice (Barati et al., 2007). Among the identified altered proteins were a number of proteins related to oxidative stress, participating in the tricarboxylic acid cycle as well as cytoskeletal proteins. Vinculin and tropomyosin were the only differentially abundant proteins that could also be detected in the present study. But nevertheless, proteins of the same functional groups were identified in this study, including heat shock protein 60 (HSP 60), sarcosine dehydrogenase (SarDH) and succinate dehydrogenase (DHSA). SarDH and DHSA were recently found to be altered in renal cortex of diabetic *db/db* mice (Tilton et al., 2007) among a high percentage of other mitochondrial proteins as well as cytoskeletal proteins. These results are consistent with an earlier proteomic study of whole kidney lysates from another diabetic mouse model, in which identified differentiall abundant proteins belonged to similar functional groups (Thongboonkerd et al., 2004). Like in the present study, the smooth muscle contractile elements tropomyosin and myosin light chain were among the identified proteins.

Identified proteins – known and possible functions in glomerulosclerosis:

Galectin-1 was increased in glomeruli of GH transgenic mice as compared to their controls. Galectins are a family of carbohydrate-binding proteins with an affinity for β-galactosides and are involved in cell growth, apoptosis and cell migration features (Mathieu et al., 2005). Galectin-1 is differentially expressed by various normal and pathological tissues and has both intracellular and extracelluar functions (Camby et al., 2006). It has been found to be expressed in isolated human glomeruli as well as in cultured mesangial cells and podocytes in several proteomic studies (Jiang et al., 2005; Ransom et al., 2005; Yoshida et al., 2005). Galectin-1 is highly expressed in human glomeruli, but not in tubuli (Uhlen et al., 2005). Apart from the lectin activity galectin-1 is involved in protein-protein interactions, binds to a number of extracelluar matrix (ECM) components, and plays a role in ECM assembly and remodeling (Camby et al., 2006). Galectin-1 is mitogenic for various cell types including mammalian vascular cells (Moiseeva et al., 2000). Recently it has been shown to play a critical role in angiogenesis and to be directly involved in endothelial cell proliferation and migration (Thijssen et al., 2006). Galectin-1 expression was increased in growth factor activated endothelial cells (Thijssen et al., 2006). Proliferation of endothelial cells in association with glomerular hypertrophy of GH transgenic mice has been demonstrated earlier (Wanke, 1996). Therefore, galectin-1 could play an important role in the course of glomerular hypertrophy.

Serum albumin was significantly increased in glomeruli of GH transgenic mice as compared to their controls. One possible reason would be that plasma or blood remained in the glomerular capillaries after the perfusion. The alterations in the abundance of glomeruli from transgenic animals as compared to the control animals are very consistent in every biological replicate. It is unlikely, that with every perfusion the same amount of blood would remain in the glomeruli of GH transgenic mice as well as the consistently lower amount in the glomeruli of control mice, which would be necessary to meet the statistically significant changes in abundance. Aditionally, a differential abundance of albumin between glomeruli of transgenic mice and those of controls were observed neither in GH transgenic mice in stage 1 nor in $GIPR^{dn}$ transgenic mice in stage 2 vs. their controls. The mesangium of the glomerulus has direct contact to the glomerular blood flow, because the endothelial

fenestrations open directly into the mesangium (Latta, 1992). This allows blood plasma to flow into the mesangium and plasma proteins like albumin to bind to the mesangial matrix. Deposits of increased amounts of normal components are recognized in glomerulosclersosis (Latta, 1992). It has been shown, that serum concentrations of total proteins are elevated in GH transgenic mice at an comparable age despite progressive renal protein loss (Fisch, 2004). This result is in line with previous findings in several GH transgenic mouse strains and is regarded as a result of increased hepatic protein synthesis (Brem et al., 1989; Wanke, 1996). In addition, albumin could be detected in the cytoplasm of podocytes of GH transgenic mice (Wanke, 1996). With albumin being the most abundant plasma protein an accumulation of albumin in the glomeruli of GH transgenic mice seems to be explainable, but still the question remains, in which part exactly it is accumulating, mesangium or podocytes.

Fibrinogen gamma chain has shown to be increased in the glomeruli of $GIPR^{dn}$ transgenic animals as compared to their controls. It is part of the fibrinogen which represents a heterohexamer containing two sets of three non-identical chains (α, β, γ). Increased glomerular fibrinogen deposition has been described in the remnant kidney model (Floege et al., 1992). Additionally, it is well known that in early stages of diabetic nephropathy (in type 1 and type 2 diabetes mellitus) fibrinogen levels in plasma are elevated which could lead to a deposition of fibrinogen in the glomeruli. There is also a correlation between the plasma level and albumin excretion in the urine (Klein et al., 2003; Lengyel et al., 2004; Tessari et al., 2006). Fibrinogen binds intimately to fibronectin (Colvin et al., 1979) which has been shown to play a critical role in the development of glomerulosclerosis and to be increased in sclerotic glomeruli (Shui et al., 2006). In the glomeruli of $GIPR^{dn}$ transgenic mice an increased deposition of fibronectin could also be demonstrated (Herbach, 2002; Schairer, 2006). Therefore, an increased binding of fibrinogen to fibronectin is likely and in combination with the presumption that diabetic mice display high levels of fibrinogen in plasma like humans, an increase in fibrinogen in glomeruli of $GIPR^{dn}$ transgenic mice is explainable. A further aspect to be looked on is the fact, that vascular endothelial growth factor (VEGF) obviously binds to fibrinogen and thereby stimulates endothelial cell proliferation (Sahni and Francis, 2000). VEGF is implicated in the development of proteinuria during diabetic nephropathy (Xia et al., 2007).

Glomerular hypertrophy is partly due to proliferation of endothelial cells and enhanced angiogenesis takes place in diabetic nephropathy (Wanke, 1996; Zent and Pozzi, 2007). In conclusion changes in glomerular fibrinogen levels could contribute to the pathogenetic processes in glomerular hypertrophy and albuminuria.

The heat shock protein 60 (HSP60) which was increased in glomeruli of GIPR^{dn} tg mice plays a major role in the folding and assembly of mitochondrial proteins and is exclusively detectable in mitochondria in the kidney (Muller et al., 1996). Even though HSP60 couldn't be localized in glomeruli by an immunhistochemical study (Muller et al., 1996), it has been found in several proteomic analyses of isolated human glomeruli (Yoshida et al., 2005), cultured mesangial cells as well as podocytes (Jiang et al., 2005; Ransom et al., 2005). In kidneys of rats with streptozotocin (STZ) induced diabetes mellitus it has recently been shown that the expression of HSP60 mRNA as well as the protein content is increased, probably due to increased oxidative stress in the context of diabetic metabolism (Oksala et al., 2007). An additional function of HSP60 is its ability to activate endothelial cells by an increase of the proinflammatory cytokine interleukin-6 and the induction of nuclear factor-κB (NF-κB) (Kol et al., 1999). The activation of NF-κB has been suggested to be an important step during diabetic nephropathy (Iwamoto et al., 2005; Schmid et al., 2006). Therefore, an increase of HSP60 might play a role as pathogentic factor in the course of diabetic nephropathy.

Another two mitochondrial proteins were increased in their abundance in glomeruli of GIPR^{dn} transgenic mice, sarcosine dehydrogenase and the flavoprotein subunit of the succinate dehydrogenase. Sarcosine dehydrogenase, highly expressed in the kidney, is a mitochondrial flavoenzyme involved in the oxidative degradation of choline to glycine which takes place in mitochondria (Bergeron et al., 1998). As many other mitochondrial proteins it has been shown to differ in its abundance in renal cortex of diabetic subjects, suggesting an altered mitochondrial metabolism during diabetes (Tilton et al., 2007). The flavoprotein subunit of the succinate dehydrogenase (SDH) is one of four subunits of this enzyme. SDH is involved in the tricarboxylic acid cycle and represents the complex II in the respiratory chain in the inner mitochondrial membrane. Like sarcosine dehydrogenase it has been found to be altered in diabetic renal cortex (Tilton et al., 2007). In mitochondria of renal cortex

of rats with STZ induced diabetes SDH activity was dramatically elevated after one month of diabetes. This was suggested to be a compensatory effect, because hypertrophic processes are energy dependent (Katyare and Satav, 2005).

Bleomycin hydrolase, which was decreased in the glomeruli of GIPR^{dn} transgenic mice, was originally discovered as an enzyme that inactivates the anticancer drug bleomycin (Sebti et al., 1989). It is widely distributed in many tissues, with highest activities in kidney and liver (Filderman and Lazo, 1991; Kamata et al., 2007), but its physiological function is yet to be unknown. Recently, a study has revealed its function as an intracellular homocysteine-thiolactonase which protects cells against homocysteine toxicity (Zimny et al., 2006). Homocysteine is known to induce endothelial dysfunction and hyperhomocysteinemia has been associated with microalbuminuria in diabetic patients (Huijberts et al., 2005; Ozmen et al., 2002). A decrease in bleomycin hydrolase as seen in the present study could therefore enhance homocysteine toxicity and contribute to the development of microalbuminuria.

Eukaryotic translation initiation factor 3 subunit 1 (eiF-3 alpha) was increased in the glomeruli of GIPR^{dn} transgenic mice and it represents one of at least ten subunits of eiF-3. EiF-3 is a large multisubunit complex that plays a central role in the initiation of translation (Block et al., 1998). It hasn't been described in connection with glomerulosclerosis or diabetic nephropathy, but its increased abundance in GIPR^{dn} tg mice might be associated with the mammalian target of rapamycin (mTOR) pathway. Eif-3 seems to mediate mTOR's role in translation initiation (Lee et al., 2007). mTOR is normally inactive in the kidney, but its activation plays an essential role in hypertrophic responses to insults like diabetes and compensatory renal hypertrophy, because mTOR activity stimulates cell growth and proliferation (Weimbs, 2006). Furthermore, the mTOR pathway has been shown to be activated in diabetic glomeruli and mediates mesangial cell hypertrophy (Nagai et al., 2005). Therefore an upregulation of eiF-3 might play a role in activation of the mTOR pathway and in the hypertrophic processes in the glomeruli.

Ig kappa chain C region was found to be increased in the glomeruli of GIPR^{dn} transgenic mice as compared to their controls. In the present study there is a

discrepancy between the molecular mass observed in the gel (approx 23 kDa) and in the database (approx 12 kDa). An Ig light chain consists of a constant (C) and a variable region. The protein identified is the C region of the kappa chain, but the higher molecular mass could be explained by the presence of the variable region which is not identified in the database. In a recent study Ig kappa chain was markedly increased in the plasma of rats with STZ induced diabetes (Kim et al., 2006). In patients with diabetes mellitus increased urinary excretion of Ig kappa light chains has been reported (Groop et al., 1990). In longstanding diabetes its excretion was positively correlated with urinary albumin excretion. An accurate mechanism responsible for increased levels remains uncertain. Glycation of kappa light chains is a known event and the glycated kappa light chains tend to form high molecular polymers (Groop et al., 1990). These polymers can't be freely filtered through the glomerular filtration barrier and an increase in kappa light chains in glomeruli of diabetic mice might be due to increased deposition of these polymers within the glomerulus.

Complement C4 B was increased in glomeruli of $GIPR^{dn}$ transgenic mice. In this study there is a discrepancy between the mass observed in the gel (22 kDa) and the one in the database (193 kDa). The mass in the database refers to the whole C4 B precursor, but in the gel there is probably only a fragment of it which would explain the smaller mass. C4b is a major activation product in the classical pathway of the complement system. It is an essential subunit of the C3 convertase (C4b2a) and the C5 convertase (C3bC4b2a) enzymes. The complement system plays an important role in the pathogenesis of diabetic complications one of which is diabetic nephropathy (Ostergaard et al., 2005). An increased deposition of complement C3 in glomeruli has been shown in different animal models of diabetes (Fujita et al., 1999; Mauer et al., 1972; Mauer et al., 1974; Michels et al., 1984; Wehner et al., 1972). The mechanism for an activation of the complement system in diabetic patients are still not known. Activation through intracellular generation of reactive oxygen species are considered as well as the fact that injured glomeruli bind to Ig and activate the complement system which seems to exacerbate glomerulosclerosis (Fujita et al., 1999; Ostergaard et al., 2005). With C4b being part of the complement pathway a deposition in diabetic glomeruli could be considered even though this hasn't been directly demonstrated yet. Plasma levels of C4, however, seem to be significantly

lower in about 25 % of diabetic patients despite a high level of C3 fragments indicating activation of complement. In addition there is a high prevalence of microalbuminuria in patients with low C4 levels (Barnett et al., 1984; Chiarelli et al., 1988).

Cytoskeletal proteins are high abundant proteins within glomerular cells and the cytoskeleton plays a very important role in maintaining the cells shape and motility. Especially in podocytes and mesangial cells a tight regulation of the cytoskeleton is necessary to keep up their special functions in the glomerulus, i.e. glomerular filtration barrier and mechanical support against the hydraulic pressures in the capillaries (Kriz et al., 1990). In the present study several cytoskeletal proteins were found to be altered in transgenic animals as compared to their controls in both mouse models and all of them showed an increased abundance. Hypertrophy of cells always comes along with an increased protein synthesis and larger cells need a stronger cytoskeleton to maintain shape and function. Cytoskeletal rearrangement, especially in the actin cytoskeleton, has been well described in the context of glomerulosclerosis in podocytes as well as in mesangial cells (El Nahas, 1996; Pavenstadt et al., 2003; Shankland, 2006; Simonson, 2007). Two members of the contractile apparatus, tropomyosin and myosin regulatory light chain 2 (MLRC2), were increased in the glomeruli of both GH transgenic and GIPR^{dn} transgenic mice. Nonmuscle myosin II plays an essential role in actin cytoskeleton organization and cellular motility (Watanabe et al., 2007). Myosin heavy chains have been demonstrated to be increased in hypertrophic glomeruli (Hiroi et al., 1996). As MLRC2 is part of the whole myosin II, an increase is likely, too. The exact isoform of the tropomyosin found in the gels could not be determined by the database results, but due to the highest protein score and distinct MS/MS peptide it is likely to be tropomyosin-1 (TPM-1), although a mixture of several isoforms cannot be ruled out. TPM-1 is the major isoform in mesangial cells (Ishino et al., 1991). It hasn’t been directly described in the context of glomerulosclerosis, but increased flows and hypertrophy make increased demands on the contractile apparatus of the glomerular cells (Kriz et al., 1990).

Vinculin and filamin-A, two important proteins in the organization of the actin cytoskeleton, were increased only in the glomeruli of GH transgenic mice. In the gels of GIPR^{dn} transgenic mice vs. their controls – run on a different electrophoretic

equipment – proteins of such a high molecular weight were not well resolved and could therefore not be detected as altered. So it is still possible, that these proteins are also altered in GIPR^{dn} transgenic mice. Vinculin links the actin filaments to the integrins in the basement membrane. An increased recruitment of vinculin has been associated with cellular responses to mechanichal stress applied to ligand-bound integrins by enlarging their focal adhesions (Ziegler et al., 2006). This has also be shown in TGF-β stimulated mesangial cells (Hubchak et al., 2003). Filamin-A plays an important role in crosslinking actin filaments as well as in signalling towards changes in cytoskeletal rearrangements (Popowicz et al., 2006). Changes in the actin cytoskeleton are likely to involve this protein. DRP-2 also represents an actin binding protein in addition to its functions mentioned below.
Several spots in the group of GIPR^{dn} transgenic mice vs. their controls have been identified as actin, but like tropomyosin the exact isoform couldn't be determined by the database search. The highest protein score and the matching of at least one distinct peptide suggest the presence of cytoplasmic actin, but other isoforms could be present as well. Molecular mass and pI in the gel are mostly consistent with database results, but spot 40 has a very low molecular weight and in this case it is likely that only a fragment of actin is present in the actual spot. Smooth muscle-alpha actin is known to be increased in activated mesangial cells and also in hypertrophic glomeruli (Floege et al., 1992). Although most of the altered cytoskeletal proteins have already been described in the glomerulosclerotic process, it is still unclear, whether they only represent the occurring structural changes or might also play a role in the pathogenesis of glomerulosclerosis.

Annexin A4 was found to be decreased in glomeruli of both GH and GIPR^{dn} transgenic mice. It has high expression levels in the kidney and is predominantly found in epithelial cells (Dreier et al., 1998; Markoff and Gerke, 2005). Annexin A4 has been detected in tubuli and Bowman's capsule as well as in cultured podocytes and mesangial cells (Dreier et al., 1998; Jiang et al., 2005; Ransom et al., 2005). This calcium binding protein hasn't been described in the context of glomerulosclerosis yet, but it seems to be involved in several functions in the kidney including kidney development, membrane organization and the regulation of calcium-activated epithelial chloride channels (Markoff and Gerke, 2005). Studies on Annexin A4a deficient mice revealed striking morphological alterations in the kidney and

suggested an important role for this protein in kidney development (Li et al., 2003). This is supported by a study on *Xenopus laevis,* in which downregulation of Annexin A4 led to a disturbed development of pronephric tubules (Seville et al., 2002). As mentioned above it has been shown that annexin A4 plays an inhibitory role in the regulation of calcium-activated epithelial chloride (Cl^-) conductance (Kaetzel et al., 1994). Inhibition of annexin A4 leads to an increase in Cl^- conductance. Interestingly, studies on podocytes in the intact glomerulus of the rat revealed that angiotensin II (Ang II) depolarized podocytes by opening a Cl^- conductance and that this process may be regulated by intracellular calcium activity (Gloy et al., 1998). It is known that Ang II increases the cytosolic calcium activity in cells (Gloy et al., 1998) and contributes to the pathogenesis of glomerulosclerosis (Fogo, 1994; Kriz et al., 1994). Annexin A4 might be involved in the process of the Ang II related depolarization of podocytes. Its decreased abundance could diminish the inhibitory effect and increase the Ang II effect of influencing the contractile state of podocyte foot processes. Recently, Annexin A4 has been shown to form a complex with rabphilin and synaptotagmin in neurons, suggesting a possible role in synaptic exocytosis (Willshaw et al., 2004). Because podocytes seem to be related to neurons (Kobayashi et al., 2004; Rastaldi et al., 2003), there might be another role for annexin A4 in these cells. Taken together, annexin A4 seems to be an interesting candidate protein and further studies will reveal possible functions in the glomerulus.

The other protein which was decreased in glomeruli of GH transgenic as well as of $GIPR^{dn}$ transgenic mice is the dihydropyrimidinase related protein-2 (DRP-2) also known as collapsing response mediator protein 2 (CRMP-2). Except for the liver DRP-2 is widely expressed in different tissues, with highest levels in the brain (Hamajima et al., 1996). Most of the knowledge on the biological significance of DRP-2 has been in the context of its function in neurons. However, a recent study could demonstrate that DRP-2 is involved in signalling pathways that regulate the proliferation of non-neuronal cells with phosphorylation of DRP-2 playing an important role (Tahimic et al., 2006). DRP-2 hasn't been described in the context of glomerular alterations, but it has been detected in cultured podocytes and glomeruli by proteomic analysis (Ransom et al., 2005; Yoshida et al., 2005). Because podocytes share many cell biological characteristics with neurons (Kobayashi et al., 2004; Rastaldi et al., 2003), it is interesting to look on the neuronal functions of DRP-

2. DRP-2 has emerged as a crucial regulator of microtubule dynamics during neurite/axonal growth (Fukata et al., 2002). Non-phosphorylated DRP-2 binds with high affinity to tubulin heterodimers and enhances microtubule formation (Arimura et al., 2005). Phosphorylation by Rho-kinase has been shown to prevent the association of DRP-2 with tubulin dimers thereby having a negative effect on DRP-2 function (Arimura et al., 2005; Mimura et al., 2006). In podocytes, microtubules are essential for an intact structure of major podocyte processes, connecting the cell body with the GBM-anchored actin network in foot processes and disruption of microtubules results in severe damage of the major processes (Pavenstadt et al., 2003). For Rho-kinase has been shown to be involved in the development of glomerulosclerosis (Hayashi et al., 2006) and plays a pivotal role in the formation of podocyte processes (Kobayashi et al., 2004), decreased levels of DRP-2 or phosphorylation could be involved in podocyte injury. In the present study three spots in the glomeruli of GH transgenic mice were identified as DRP-2 which only differed in their pI, indicating different phosphorylation states of the protein. In conclusion, DRP-2 seems to be a very interesting candidate protein and further studies will be necessary to clarify the exact localization and function of DRP-2 within the glomerulus.

In summary, the differential proteomic analysis of well defined glomerulus samples of GH transgenic mice and their controls as well as of diabetic $GIPR^{dn}$ transgenic mice and their controls was successfully performed. Out of eight identified differentially abundant proteins in the group of GH transgenic mice in stage 2 vs. their controls and out of 13 identified proteins in the group of $GIPR^{dn}$ transgenic mice in stage 2 vs. their controls, respectively, an intersection of four proteins could be build. Two of these proteins, annexin A4 and DRP-2, represent promising candidate proteins on which further hypothesis driven studies should be performed.

6. Perspective

Differential proteomic analysis of glomeruli from two murine models of nephropathy revealed a number of differentially abundant proteins in the stage of glomerular hypertrophy together with a beginning albuminuria in each of the analysed models. Annexin A4 and DRP-2, two of the proteins that were differentially abundant in the glomeruli of GH transgenic mice in stage 2 vs. their controls and $GIPR^{dn}$ transgenic mice in stage 2 vs. their controls, are of interest for further hypothesis driven investigations. The exact localization of these proteins within the glomerulus as well as a confirmation of the altered abundances applying immunohistochemistry will be essential to go into detail about possible roles and functions of the proteins in the course of glomerular hypertrophy and albuminuria. Genetically modified mice would be of immense use for further functional studies.

7. Summary

The present study focuses on progressive glomerulosclerosis which is known as a complication of a variety of systemic diseases and plays a crucial role in the progression of chronic renal failure. Therefore, the study of the pathogenesis of progressive glomerulosclerosis is a key issue in nephrologic research. Precursor lesions of glomerulosclerosis include the development of glomerular hypertrophy followed by albuminuria. The present study addressed the question, whether these early glomerular alterations lead to differences in the abundance levels of distinct proteins in the glomeruli. Therefore, the glomerular proteomes of two different mouse models of nephropathy were analysed at defined stages of renal alterations. Because glomeruli represent only about 2 – 4 % of the whole kidney volume, a subproteome approach targeting isolated renal glomeruli was the method of choice. The first mouse model, growth hormone (GH) transgenic mice, are a well characterized model for progressive glomerulosclerosis. The second mouse model, diabetic transgenic mice expressing a dominant negative glucose-dependent insulinotropic polypeptide receptor ($GIPR^{dn}$), represent a model for diabetes-associated glomerular lesions. Both transgenic mouse models develop glomerular hypertrophy and albuminuria. Pairs of male transgenic mice and their corresponding non-transgenic littermate control animals were investigated in the stage of glomerular hypertrophy together with a beginning albuminuria (stage 2). In GH transgenic and corresponding control mice the additional stage of glomerular hypertrophy without albuminuria was investigated (stage 1). To judge the degree of glomerular hypertrophy in an objective manner, the mean glomerular volume of the transgenic animals as compared to the respective controls was determined by quantitative stereological analysis. The onset of albuminuria in transgenic animals in stage 2 was determined by SDS-PAGE based analyses of urine samples taken on consecutive time points and was confirmed by Western blot and ELISA analyses. Glomerulus isolation was performed in a magnetic field after perfusion of the kidneys with spherical superparamagnetic beads, enabling a very high yield of approximately 10,000 glomerlui per mouse kidney within 100 minutes. For differential quantitative proteomic analysis of glomerular proteomes from $GIPR^{dn}$ transgenic as well as GH transgenic mice versus their corresponding wild-type controls, the two dimensional difference gel electrophoresis (2D-DIGE) technique was applied in a pH gradient of 4-7. Differentially abundant spots were identified by matrix assisted laser desorption ionization – time of flight / time of flight

(MALDI-TOF/TOF) mass spectrometry analysis. Five differentially abundant protein spots were detected in GH transgenic mice in stage 1 as compared to their controls, but none of these spots could be unambiguously identified. Analysis of glomeruli from GH transgenic mice in stage 2 vs. those of the corresponding controls revealed 22 differentially abundant protein spots. Eight proteins could be unambiguously identified and three spots contained two or more proteins. Analyzing the glomeruli of $GIPR^{dn}$ transgenic mice in stage 2 vs. those of the corresponding controls, a number of 42 differentially abundant protein spots could be detected, and out of them 13 proteins could be unambiguously identified. Another seven spots were identified with mixed identities, containing two or more proteins. Most of the identified proteins have protein binding function or belong to the cytoskeleton. Molecular functions of other proteins include calcium ion binding, hydrolase activity or transporter activity. By comparison of the eight identified proteins in the group of GH transgenic mice and the 13 identified proteins in the group of $GIPR^{dn}$ transgenic mice an intersection of four identical proteins could be build (Tropomyosin, Myosin regulatory light chain 2, Annexin A4 as well as dihydropyrimidinase-related protein 2). Tropomyosin and Myosin regulatory light chain 2 represent structural constituents of the cytoskeleton which is known to undergo alterations in the course of glomerular growth processes. Annexin A4 and dihydropyrimidinase-related protein 2 (DRP-2) have not yet been described in the context of the development of glomerular lesions. But both of them have been shown to be present in neuronal cells. Because podocytes are known to share many similarities to neurons, the question arises, which kind of functions these proteins have in glomerular podocytes and in glomerular growth processes.

The results of the present study provide an excellent basis for further hypothesis-driven approaches aiming at a better understanding of the molecular mechanisms involved in glomerular growth processes and the pathogenesis of glomerulosclerosis.

8. Zusammenfassung

Im Mittelpunkt der vorliegenden Arbeit steht die progressive Glomerulosklerose, die als Komplikation diverser systemischer Grundkrankheiten bekannt ist sowie eine entscheidende Rolle bei der Progression der chronischen renalen Insuffizienz spielt. Die Pathogenese der progressiven Glomerulosklerose stellt daher einen nephrologischen Forschungsschwerpunkt dar. Die Vorläuferläsionen der Glomerulosklerose beinhalten die Entwicklung einer glomerulären Hypertrophie gefolgt vom Auftreten einer Albuminurie. In der vorliegenden Studie wurde die Fragestellung bearbeitet, ob sich Frühstadien der Glomerulosklerose-Entwicklung auf Proteinebene widerspiegeln. Aus diesem Grund wurde das glomeruläre Proteom zweier muriner Nephropathiemodelle in definierten Stadien renaler Veränderungen analysiert. Es wurde ein Subproteomansatz gewählt, der ausschließlich isolierte Glomerula beinhaltet. Bei den beiden murinen Nephropathiemodellen handelt es sich zum einen um Wachstumshormon (GH) – transgene Mäuse, die ein gut charakterisiertes Modell für die progressive Glomerulosklerose darstellen und zum anderen um diabetische transgene Mäuse, die einen dominant negativen glucose-dependent insulinotropic polypeptide Rezeptor ($GIPR^{dn}$) exprimieren und ein Modell für Diabetes-assoziierte Nierenschäden repräsentieren. Beide transgene Mausmodelle entwickeln eine glomeruläre Hypertrophie und eine Albuminurie. Paare von männlichen transgenen Mäusen und deren korrespondierenden Wildtyp Kontrolltieren wurden im Stadium der glomerulären Hypertrophie zusammen mit einer beginnenden Albuminurie (Stadium 2) untersucht. GH transgene Mäuse und ihre Kontrollen wurden zudem noch im vorausgehenden Stadium der glomerulären Hypertrophie ohne Albuminurie (Stadium 1) analysiert. Zur Beurteilung der glomerulären Hypertrophie erfolgte die Bestimmung des mittleren Glomerulumvolumens mittels quantitativ stereologischer Methoden. Das Einsetzen der Albuminurie in transgenen Tieren im Stadium 2 wurde anhand einer SDS-PAGE basierten Urinproteinanalyse bestimmt. Die dafür nötigen Urinproben wurden an definierten aufeinanderfolgenden Zeitpunkten gewonnen. Das Vorliegen einer Albuminurie wurde mittels Western Blot und ELISA Analysen bestätigt. Die Glomerula wurden nach Perfusion der Nieren mit sphärischen superparamagnetischen Beads in einem Magnetfeld isoliert. Dieses ermöglichte eine sehr hohe Ausbeute von ca. 10.000 Glomerula pro Mausniere in etwa 100 Minuten. Die differentiell quantitative Analyse des glomerulären Proteoms von GH transgenen und $GIPR^{dn}$ transgenen Mäusen im Vergleich zu ihren jeweiligen Kontrolltieren

erfolgte mittels der zweidimensionalen Differenz-Gelelektrophorese in einem pH-Gradienten von 4 – 7. Differentiell abundante Proteinspots wurden mit Matrix assistierter Laser Desorptions Ionisations Tandem-Massenspektrometrie (MALDI-TOF/TOF) identifiziert. Bei GH transgenen Mäusen im Stadium 1 konnten im Vergleich zu den Kontrolltieren fünf differentiell abundante Proteinspots nachgewiesen werden, allerdings ließ sich keiner dieser Spots eindeutig identifizieren. Die Analyse von Glomerula GH transgener Mäuse im Stadium 2 ergab im Vergleich zu den Kontrollen 22 differentiell abundante Proteinspots. Aus diesen Spots konnten acht Proteine zweifelsfrei identifiziert werden, in drei Spots waren zwei oder mehr Proteine enthalten. Bei $GIPR^{dn}$ transgenen Mäusen ergab die Analyse des glomerulären Proteoms im Vergleich zu den entsprechenden Kontrollen 42 differentiell abundante Spots, aus diesen 13 Proteine eindeutig identifiziert werden konnten. In sieben der 42 Spots waren wiederum Mischungen aus zwei oder mehr Proteinen zu finden. Die meisten der identifizierten Proteine haben proteinbindende Funktion oder repräsentieren Komponenten des Zytoskeletts. Molekulare Funktionen anderer identifizierter Proteine beinhalten Kalziumionen- bindende Funktion, Hydrolaseaktivität oder Transporteraktivität. Durch Vergleich der acht identifizierten Proteine in der Gruppe der GH transgenen Mäuse mit den 13 identifizierten Proteinen in der Gruppe der $GIPR^{dn}$ transgenen Mäuse, konnte eine Schnittmenge von vier identischen Proteinen (Tropomyosin, Myosin regulatory light chain 2, Annexin A4 sowie Dihydropyrimidinase-related protein 2) gebildet werden. Tropomyosin und Myosin regulatory light chain 2 repräsentieren zytoskeletale Proteine. Annexin A4 und Dihydropyrimidinase-related protein 2 (DRP-2) sind bislang noch nicht im Zusammenhang mit der Entwicklung glomerulärer Läsionen beschrieben worden. Allerdings ist das Vorkommen dieser beiden Proteine in neuronalen Zellen bekannt. Da zwischen Podozyten und Neuronen große Übereinstimmungen bestehen, stellt sich die Frage nach den Funktionen von Annexin A4 und DRP-2 in glomerulären Podozyten sowie im Rahmen glomerulärer Wachstumsprozesse. Die Ergebnisse der vorliegenden Arbeit liefern die Basis für weiterführende, hypothesengetriebene Forschungsansätze zur Klärung der an glomerulären Wachstumsprozessen und der Entwicklung glomerulosklerotischer Alterationen beteiligten molekularen Mechanismen.

9. References

Adachi, J., Kumar, C., Zhang, Y., Olsen, J. V., and Mann, M. (2006). The human urinary proteome contains more than 1500 proteins, including a large proportion of membrane proteins. Genome Biol *7*, R80.

Ahmed, N., and Rice, G. E. (2005). Strategies for revealing lower abundance proteins in two-dimensional protein maps. J Chromatogr B Analyt Technol Biomed Life Sci *815*, 39-50.

Alban, A., David, S. O., Bjorkesten, L., Andersson, C., Sloge, E., Lewis, S., and Currie, I. (2003). A novel experimental design for comparative two-dimensional gel analysis: two-dimensional difference gel electrophoresis incorporating a pooled internal standard. Proteomics *3*, 36-44.

Anders, H., and Schlondorff, D. (2000). Murine models of renal disease: possibilities and problems in studies using mutant mice. Exp Nephrol *8*, 181-193.

Anderson, S., Meyer, T. W., Rennke, H. G., and Brenner, B. M. (1985). Control of glomerular hypertension limits glomerular injury in rats with reduced renal mass. J Clin Invest *76*, 612-619.

Arimura, N., Menager, C., Kawano, Y., Yoshimura, T., Kawabata, S., Hattori, A., Fukata, Y., Amano, M., Goshima, Y., Inagaki, M.*, et al.* (2005). Phosphorylation by Rho kinase regulates CRMP-2 activity in growth cones. Mol Cell Biol *25*, 9973-9984.

Artacho-Perula, E., Roldan-Villalobos, R., Salcedo-Leal, I., and Vaamonde-Lemos, R. (1993). Stereological estimates of volume-weighted mean glomerular volume in streptozotocin-diabetic rats. Lab Invest *68*, 56-61.

Arthur, J. M., Thongboonkerd, V., Scherzer, J. A., Cai, J., Pierce, W. M., and Klein, J. B. (2002). Differential expression of proteins in renal cortex and medulla: a proteomic approach. Kidney Int *62*, 1314-1321.

Baelde, J. J., Bergijk, E. C., Hoedemaeker, P. J., de Heer, E., and Bruijn, J. A. (1994). Optimal method for RNA extraction from mouse glomeruli. Nephrol Dial Transplant *9*, 304-308.

Barati, M. T., Merchant, M. L., Kain, A. B., Jevans, A. W., McLeish, K. R., and Klein, J. B. (2007). Proteomic analysis defines altered cellular redox pathways and advanced glycation end-product metabolism in glomeruli of db/db diabetic mice. Am J Physiol Renal Physiol *293*, F1157-1165.

Barati, M. T., Rane, M. J., Klein, J. B., and McLeish, K. R. (2006). A proteomic screen identified stress-induced chaperone proteins as targets of Akt phosphorylation in mesangial cells. J Proteome Res *5*, 1636-1646.

Barnett, A. H., Mijovic, C., Fletcher, J., Chesner, I., Kulkuska-Langlands, B. M., Holder, R., and Bradwell, A. R. (1984). Low plasma C4 concentrations: association with microangiopathy in insulin dependent diabetes. Br Med J (Clin Res Ed) *289*, 943-945.

Berendt, F. J., Frohlich, T., Schmidt, S. E., Reichenbach, H. D., Wolf, E., and Arnold, G. J. (2005). Holistic differential analysis of embryo-induced alterations in the proteome of bovine endometrium in the preattachment period. Proteomics *5*, 2551-2560.

Bergeron, F., Otto, A., Blache, P., Day, R., Denoroy, L., Brandsch, R., and Bataille, D. (1998). Molecular cloning and tissue distribution of rat sarcosine dehydrogenase. Eur J Biochem *257*, 556-561.

Bergstein, J. M. (1999). A practical approach to proteinuria. Pediatr Nephrol *13*, 697-700.

Block, K. L., Vornlocher, H. P., and Hershey, J. W. (1998). Characterization of cDNAs encoding the p44 and p35 subunits of human translation initiation factor eIF3. J Biol Chem *273*, 31901-31908.

Blutke, A., Block, C., Kemter, E., Wolf, E., Herbach, N., and Wanke, R. (2005). Large scale isolation of glomeruli from murine kidneys: Comparison of different methods and solutions for methodological problems, In Proceedings of the 23rd Meeting of the European Society of Veterinary Pathology (Naples, Italy).

Bonvalet, J. P., Champion, M., Courtalon, A., Farman, N., Vandewalle, A., and Wanstok, F. (1977). Number of glomeruli in normal and hypertrophied kidneys of mice and guinea-pigs. J Physiol *269*, 627-641.

Bradford, M. M. (1976). A rapid and sensitive method for the quantitation of microgram quantities of protein utilizing the principle of protein-dye binding. Anal Biochem *72*, 248-254.

Brem, G., and Wanke, R. (1988). Phenotypic and pathomorphological characteristics in a half-sib-family of transgenic mice carrying foreign MT-hGH genes, In New developments in biosciences: their implications for laboratory animal science, A. C. Beynen, and H. A. Solleveld, eds. (Dordrecht: Martin Nijhoff Publishers), pp. 93-98.

Brem, G., Wanke, R., Wolf, E., Buchmuller, T., Muller, M., Brenig, B., and Hermanns, W. (1989). Multiple consequences of human growth hormone expression in transgenic mice. Mol Biol Med *6*, 531-547.

Brenner, B. M., Meyer, T. W., and Hostetter, T. H. (1982). Dietary protein intake and the progressive nature of kidney disease: the role of hemodynamically mediated glomerular injury in the pathogenesis of progressive glomerular sclerosis in aging, renal ablation, and intrinsic renal disease. N Engl J Med *307*, 652-659.

Bueler, M. R., Wiederkehr, F., and Vonderschmitt, D. J. (1995). Electrophoretic, chromatographic and immunological studies of human urinary proteins. Electrophoresis *16*, 124-134.

Camby, I., Le Mercier, M., Lefranc, F., and Kiss, R. (2006). Galectin-1: a small protein with major functions. Glycobiology *16*, 137R-157R.

Cheung, P. Y., Lai, W. P., Lau, H. Y., Lo, S. C., and Wong, M. S. (2002). Acute and chronic effect of dietary phosphorus restriction on protein expression in young rat renal proximal tubules. Proteomics *2*, 1211-1219.

Chiarelli, F., Verrotti, A., La Penna, G., and Morgese, G. (1988). Low serum C4 concentrations in type-1 diabetes mellitus. Eur J Pediatr *147*, 197-198.

Churg, J., and Sobin, L. H. (1982). Renal disease: Classification and atlas of glomerular diseases (Tokyo, New York: Igaku-Shoin).

Colvin, R. B., Gardner, P. I., Roblin, R. O., Verderber, E. L., Lanigan, J. M., and Mosesson, M. W. (1979). Cell surface fibrinogen-fibrin receptors on cultured human

fibroblasts. Association with fibronectin (cold insoluble globulin, LETS protein) and loss in SV40 transformed cells. Lab Invest *41*, 464-473.

Cortes, P., Dumler, F., Goldman, J., and Levin, N. W. (1987). Relationship between renal function and metabolic alterations in early streptozocin-induced diabetes in rats. Diabetes *36*, 80-87.

Curthoys, N. P., Taylor, L., Hoffert, J. D., and Knepper, M. A. (2007). Proteomic analysis of the adaptive response of rat renal proximal tubules to metabolic acidosis. Am J Physiol Renal Physiol *292*, F140-147.

D'Ambrosio, C., Arena, S., Talamo, F., Ledda, L., Renzone, G., Ferrara, L., and Scaloni, A. (2005). Comparative proteomic analysis of mammalian animal tissues and body fluids: bovine proteome database. J Chromatogr B Analyt Technol Biomed Life Sci *815*, 157-168.

Daniels, B. S., and Hostetter, T. H. (1990). Adverse effects of growth in the glomerular microcirculation. Am J Physiol *258*, F1409-1416.

De Vecchi, A. F., Dratwa, M., and Wiedemann, M. E. (1999). Healthcare systems and end-stage renal disease (ESRD) therapies--an international review: costs and reimbursement/funding of ESRD therapies. Nephrol Dial Transplant *14 Suppl 6*, 31-41.

Doi, T., Striker, L. J., Gibson, C. C., Agodoa, L. Y., Brinster, R. L., and Striker, G. E. (1990). Glomerular lesions in mice transgenic for growth hormone and insulinlike growth factor-I. I. Relationship between increased glomerular size and mesangial sclerosis. Am J Pathol *137*, 541-552.

Doi, T., Striker, L. J., Quaife, C., Conti, F. G., Palmiter, R., Behringer, R., Brinster, R., and Striker, G. E. (1988). Progressive glomerulosclerosis develops in transgenic mice chronically expressing growth hormone and growth hormone releasing factor but not in those expressing insulinlike growth factor-1. Am J Pathol *131*, 398-403.

Downer, G., Phan, S. H., and Wiggins, R. C. (1988). Analysis of renal fibrosis in a rabbit model of crescentic nephritis. J Clin Invest *82*, 998-1006.

Dreier, R., Schmid, K. W., Gerke, V., and Riehemann, K. (1998). Differential expression of annexins I, II and IV in human tissues: an immunohistochemical study. Histochem Cell Biol *110*, 137-148.

el Nahas, A. M. (1989). Glomerulosclerosis: insights into pathogenesis and treatment. Nephrol Dial Transplant *4*, 843-853.

El Nahas, A. M. (1996). Glomerulosclerosis: intrinsic and extrinsic pathways. Nephrol Dial Transplant *11*, 773-777.

El Nahas, A. M., and Bello, A. K. (2005). Chronic kidney disease: the global challenge. Lancet *365*, 331-340.

ERA-EDTA-Registry (2007). ERA-EDTA Registry 2005 Annual Report Academic Medical Center, Department of Medical Informatics, Amsterdam, The Netherlands.

Filderman, A. E., and Lazo, J. S. (1991). Murine strain differences in pulmonary bleomycin metabolism. Biochem Pharmacol *42*, 195-198.

Fisch, T. (2004) Effects of insulin-like growth factor-binding protein-2 (IGFBP2) overexpression on adrenal and renal growth processes and functions: findings in transgenic mouse models., Dissertation to achieve the doctor title of veterinary medicine Ludwig-Maximilians University Munich.

Floege, J., Burns, M. W., Alpers, C. E., Yoshimura, A., Pritzl, P., Gordon, K., Seifert, R. A., Bowen-Pope, D. F., Couser, W. G., and Johnson, R. J. (1992). Glomerular cell proliferation and PDGF expression precede glomerulosclerosis in the remnant kidney model. Kidney Int *41*, 297-309.

Fogo, A. (1994). Internephron heterogeneity of growth factors and sclerosis. Kidney Int Suppl *45*, S24-26.

Fogo, A., and Ichikawa, I. (1989). Evidence for the central role of glomerular growth promoters in the development of sclerosis. Semin Nephrol *9*, 329-342.

Fogo, A., and Ichikawa, I. (1991). Evidence for a pathogenic linkage between glomerular hypertrophy and sclerosis. Am J Kidney Dis *17*, 666-669.

Fogo, A. B. (1999). Mesangial matrix modulation and glomerulosclerosis. Exp Nephrol *7*, 147-159.

Fogo, A. B. (2000). Glomerular hypertension, abnormal glomerular growth, and progression of renal diseases. Kidney Int Suppl *75*, S15-21.

Fogo, A. B. (2003). Animal models of FSGS: lessons for pathogenesis and treatment. Semin Nephrol *23*, 161-171.

Fogo, A. B. (2006). Progression versus regression of chronic kidney disease. Nephrol Dial Transplant *21*, 281-284.

Frei, U., and Schober-Halstenberg, H.-J. (2006). Nierenersatztherapie in Deutschland. QuaSi-Niere Jahresbericht 2005/2006.

Fries, J. W., Sandstrom, D. J., Meyer, T. W., and Rennke, H. G. (1989). Glomerular hypertrophy and epithelial cell injury modulate progressive glomerulosclerosis in the rat. Lab Invest *60*, 205-218.

Frohlich, T., and Arnold, G. J. (2006). Proteome research based on modern liquid chromatography--tandem mass spectrometry: separation, identification and quantification. J Neural Transm *113*, 973-994.

Frohlich, T., Helmstetter, D., Zobawa, M., Crecelius, A. C., Arzberger, T., Kretzschmar, H. A., and Arnold, G. J. (2006). Analysis of the HUPO Brain Proteome reference samples using 2-D DIGE and 2-D LC-MS/MS. Proteomics *6*, 4950-4966.

Fujita, T., Ohi, H., Komatsu, K., Endo, M., Ohsawa, I., and Kanmatsuse, K. (1999). Complement activation accelerates glomerular injury in diabetic rats. Nephron *81*, 208-214.

Fukata, Y., Itoh, T. J., Kimura, T., Menager, C., Nishimura, T., Shiromizu, T., Watanabe, H., Inagaki, N., Iwamatsu, A., Hotani, H., and Kaibuchi, K. (2002). CRMP-2 binds to tubulin heterodimers to promote microtubule assembly. Nat Cell Biol *4*, 583-591.

Gade, D., Thiermann, J., Markowsky, D., and Rabus, R. (2003). Evaluation of two-dimensional difference gel electrophoresis for protein profiling. Soluble proteins of the marine bacterium Pirellula sp. strain 1. J Mol Microbiol Biotechnol *5*, 240-251.

Gilbertson, D. T., Liu, J., Xue, J. L., Louis, T. A., Solid, C. A., Ebben, J. P., and Collins, A. J. (2005). Projecting the number of patients with end-stage renal disease in the United States to the year 2015. J Am Soc Nephrol *16*, 3736-3741.

Gloy, J., Henger, A., Fischer, K. G., Nitschke, R., Bleich, M., Mundel, P., Schollmeyer, P., Greger, R., and Pavenstadt, H. (1998). Angiotensin II modulates cellular functions of podocytes. Kidney Int Suppl *67*, S168-170.

Goldszer, R. C., Sweet, J., and Cotran, R. S. (1984). Focal segmental glomerulosclerosis. Annu Rev Med *35*, 429-449.

Gonzalez-Buitrago, J. M., Ferreira, L., and Lorenzo, I. (2007). Urinary proteomics. Clin Chim Acta *375*, 49-56.

Gorg, A., Weiss, W., and Dunn, M. J. (2004). Current two-dimensional electrophoresis technology for proteomics. Proteomics *4*, 3665-3685.

Grassmann, A., Gioberge, S., Moeller, S., and Brown, G. (2006). End-stage renal disease: global demographics in 2005 and observed trends. Artif Organs *30*, 895-897.

Greengauz-Roberts, O., Stoppler, H., Nomura, S., Yamaguchi, H., Goldenring, J. R., Podolsky, R. H., Lee, J. R., and Dynan, W. S. (2005). Saturation labeling with cysteine-reactive cyanine fluorescent dyes provides increased sensitivity for protein expression profiling of laser-microdissected clinical specimens. Proteomics *5*, 1746-1757.

Groop, L., Makipernaa, A., Stenman, S., DeFronzo, R. A., and Teppo, A. M. (1990). Urinary excretion of kappa light chains in patients with diabetes mellitus. Kidney Int *37*, 1120-1125.

Gygi, S. P., Corthals, G. L., Zhang, Y., Rochon, Y., and Aebersold, R. (2000). Evaluation of two-dimensional gel electrophoresis-based proteome analysis technology. Proc Natl Acad Sci U S A *97*, 9390-9395.

Hamajima, N., Matsuda, K., Sakata, S., Tamaki, N., Sasaki, M., and Nonaka, M. (1996). A novel gene family defined by human dihydropyrimidinase and three related proteins with differential tissue distribution. Gene *180*, 157-163.

Hayashi, K., Wakino, S., Kanda, T., Homma, K., Sugano, N., and Saruta, T. (2006). Molecular mechanisms and therapeutic strategies of chronic renal injury: role of rho-kinase in the development of renal injury. J Pharmacol Sci *100*, 29-33.

Hayes, R. N., and Gross, M. L. (1990). Collision-induced dissociation. Methods Enzymol *193*, 237-263.

Heine, G., Raida, M., and Forssmann, W. G. (1997). Mapping of peptides and protein fragments in human urine using liquid chromatography-mass spectrometry. J Chromatogr A *776*, 117-124.

Henzel, W. J., Billeci, T. M., Stults, J. T., Wong, S. C., Grimley, C., and Watanabe, C. (1993). Identifying proteins from two-dimensional gels by molecular mass searching of peptide fragments in protein sequence databases. Proc Natl Acad Sci U S A *90*, 5011-5015.

Henzel, W. J., Watanabe, C., and Stults, J. T. (2003). Protein identification: the origins of peptide mass fingerprinting. J Am Soc Mass Spectrom *14*, 931-942.

Heptinstall, R. H. (1992). End-stage renal disease, In Pathology of the kidney, R. H. Heptinstall, ed., pp. 713-778.

Herbach, N. (2002) Clinical and pathological characterization of a novel animal model of diabetes mellitus expressing a dominant negative glucose-dependent insulinotropic polypeptide receptor ($GIPR^{dn}$), Dissertation to achieve the doctor title of veterinary medicine Ludwig-Maximilians-University, Munich.

Herbach, N., Goeke, B., Schneider, M., Hermanns, W., Wolf, E., and Wanke, R. (2005). Overexpression of a dominant negative GIP receptor in transgenic mice results in disturbed postnatal pancreatic islet and beta-cell development. Regul Pept *125*, 103-117.

Herbach, N., Göke, B., Hermanns, W., Wolf, E., and Wanke, R. (2003). Diabetes-associated kidney lesions in $GIPR^{dn}$ transgenic mice, a novel animal model of diabetes mellitus. Diabetes *52, Suppl. 1*, A186.

Hermanns, W., Liebig, K., and Schulz, L. C. (1981). Postembedding immunohistochemical demonstration of antigen in experimental polyarthritis using plastic embedded whole joints. Histochemistry *73*, 439-446.

Hiroi, J., Kimura, K., Aikawa, M., Tojo, A., Suzuki, Y., Nagamatsu, T., Omata, M., Yazaki, Y., and Nagai, R. (1996). Expression of a nonmuscle myosin heavy chain in glomerular cells differentiates various types of glomerular disease in rats. Kidney Int *49*, 1231-1241.

Hirose, K., Osterby, R., Nozawa, M., and Gundersen, H. J. (1982). Development of glomerular lesions in experimental long-term diabetes in the rat. Kidney Int *21*, 689-695.

Hoeflich, A., Nedbal, S., Blum, W. F., Erhard, M., Lahm, H., Brem, G., Kolb, H. J., Wanke, R., and Wolf, E. (2001). Growth inhibition in giant growth hormone transgenic mice by overexpression of insulin-like growth factor-binding protein-2. Endocrinology *142*, 1889-1898.

Hoffert, J. D., van Balkom, B. W., Chou, C. L., and Knepper, M. A. (2004). Application of difference gel electrophoresis to the identification of inner medullary collecting duct proteins. Am J Physiol Renal Physiol *286*, F170-179.

Hoorn, E. J., Hoffert, J. D., and Knepper, M. A. (2005). Combined proteomics and pathways analysis of collecting duct reveals a protein regulatory network activated in vasopressin escape. J Am Soc Nephrol *16*, 2852-2863.

Horlyck, A., Gundersen, H. J., and Osterby, R. (1986). The cortical distribution pattern of diabetic glomerulopathy. Diabetologia *29*, 146-150.

Hubchak, S. C., Runyan, C. E., Kreisberg, J. I., and Schnaper, H. W. (2003). Cytoskeletal rearrangement and signal transduction in TGF-beta1-stimulated mesangial cell collagen accumulation. J Am Soc Nephrol *14*, 1969-1980.

Huijberts, M. S., Becker, A., and Stehouwer, C. D. (2005). Homocysteine and vascular disease in diabetes: a double hit? Clin Chem Lab Med *43*, 993-1000.

Ichikawa, I., Ikoma, M., and Fogo, A. (1991). Glomerular growth promoters, the common key mediator for progressive glomerular sclerosis in chronic renal diseases. Adv Nephrol Necker Hosp *20*, 127-148.

Ichikawa, I., Ma, J., Motojima, M., and Matsusaka, T. (2005). Podocyte damage damages podocytes: autonomous vicious cycle that drives local spread of glomerular sclerosis. Curr Opin Nephrol Hypertens *14*, 205-210.

Immler, D., Gremm, D., Kirsch, D., Spengler, B., Presek, P., and Meyer, H. E. (1998). Identification of phosphorylated proteins from thrombin-activated human platelets isolated by two-dimensional gel electrophoresis by electrospray ionization-tandem mass spectrometry (ESI-MS/MS) and liquid chromatography-electrospray ionization-mass spectrometry (LC-ESI-MS). Electrophoresis *19*, 1015-1023.

Ishino, T., Kobayashi, R., Wakui, H., Fukushima, Y., Nakamoto, Y., and Miura, A. B. (1991). Biochemical characterization of contractile proteins of rat cultured mesangial cells. Kidney Int *39*, 1118-1124.

Iwamoto, M., Mizuiri, S., Arita, M., and Hemmi, H. (2005). Nuclear factor-kappaB activation in diabetic rat kidney: evidence for involvement of P-selectin in diabetic nephropathy. Tohoku J Exp Med *206*, 163-171.

Jain, S., Rajput, A., Kumar, Y., Uppuluri, N., Arvind, A. S., and Tatu, U. (2005). Proteomic analysis of urinary protein markers for accurate prediction of diabetic kidney disorder. J Assoc Physicians India *53*, 513-520.

Janech, M. G., Raymond, J. R., and Arthur, J. M. (2007). Proteomics in renal research. Am J Physiol Renal Physiol *292*, F501-512.

Jiang, X. S., Tang, L. Y., Cao, X. J., Zhou, H., Xia, Q. C., Wu, J. R., and Zeng, R. (2005). Two-dimensional gel electrophoresis maps of the proteome and phosphoproteome of primitively cultured rat mesangial cells. Electrophoresis *26*, 4540-4562.

Kaetzel, M. A., Chan, H. C., Dubinsky, W. P., Dedman, J. R., and Nelson, D. J. (1994). A role for annexin IV in epithelial cell function. Inhibition of calcium-activated chloride conductance. J Biol Chem *269*, 5297-5302.

Kamata, Y., Itoh, Y., Kajiya, A., Karasawa, S., Sakatani, C., Takekoshi, S., Osamura, R. Y., and Takeda, A. (2007). Quantification of neutral cysteine protease bleomycin hydrolase and its localization in rat tissues. J Biochem (Tokyo) *141*, 69-76.

Katyare, S. S., and Satav, J. G. (2005). Effect of streptozotocin-induced diabetes on oxidative energy metabolism in rat kidney mitochondria. A comparative study of early and late effects. Diabetes Obes Metab *7*, 555-562.

Kim, S. W., Hwang, H. J., Kim, H. M., Lee, M. C., Shik Lee, M., Choi, J. W., and Yun, J. W. (2006). Effect of fungal polysaccharides on the modulation of plasma proteins in streptozotocin-induced diabetic rats. Proteomics *6*, 5291-5302.

Klahr, S. (1999). Mechanisms of progression of chronic renal damage. J Nephrol *12 Suppl 2*, S53-62.

Klahr, S., Schreiner, G., and Ichikawa, I. (1988). The progression of renal disease. N Engl J Med *318*, 1657-1666.

Klein, R. L., Hunter, S. J., Jenkins, A. J., Zheng, D., Semler, A. J., Clore, J., and Garvey, W. T. (2003). Fibrinogen is a marker for nephropathy and peripheral vascular disease in type 1 diabetes: studies of plasma fibrinogen and fibrinogen gene polymorphism in the DCCT/EDIC cohort. Diabetes Care *26*, 1439-1448.

Klose, J. (1975). Protein mapping by combined isoelectric focusing and electrophoresis of mouse tissues. A novel approach to testing for induced point mutations in mammals. Humangenetik *26*, 231-243.

Kobayashi, N., Gao, S. Y., Chen, J., Saito, K., Miyawaki, K., Li, C. Y., Pan, L., Saito, S., Terashita, T., and Matsuda, S. (2004). Process formation of the renal glomerular podocyte: is there common molecular machinery for processes of podocytes and neurons? Anat Sci Int *79*, 1-10.

Kol, A., Bourcier, T., Lichtman, A. H., and Libby, P. (1999). Chlamydial and human heat shock protein 60s activate human vascular endothelium, smooth muscle cells, and macrophages. J Clin Invest *103*, 571-577.

Kreisberg, J. I., Hoover, R. L., and Karnovsky, M. J. (1978). Isolation and characterization of rat glomerular epithelial cells in vitro. Kidney Int *14*, 21-30.

Kriz, W. (2002). Podocyte is the major culprit accounting for the progression of chronic renal disease. Microsc Res Tech *57*, 189-195.

Kriz, W., Elger, M., Lemley, K., and Sakai, T. (1990). Structure of the glomerular mesangium: a biomechanical interpretation. Kidney Int Suppl *30*, S2-9.

Kriz, W., Elger, M., Nagata, M., Kretzler, M., Uiker, S., Koeppen-Hageman, I., Tenschert, S., and Lemley, K. V. (1994). The role of podocytes in the development of glomerular sclerosis. Kidney Int Suppl *45*, S64-72.

Kriz, W., and LeHir, M. (2005). Pathways to nephron loss starting from glomerular diseases-insights from animal models. Kidney Int *67*, 404-419.

Kuncewicz, T., Sheta, E. A., Goldknopf, I. L., and Kone, B. C. (2003). Proteomic analysis of S-nitrosylated proteins in mesangial cells. Mol Cell Proteomics *2*, 156-163.

Lafferty, H. M., and Brenner, B. M. (1990). Are glomerular hypertension and "hypertrophy" independent risk factors for progression of renal disease? Semin Nephrol *10*, 294-304.

Latta, H. (1992). An approach to the structure and function of the glomerular mesangium. J Am Soc Nephrol *2*, S65-73.

Lee, C. H., Inoki, K., and Guan, K. L. (2007). mTOR pathway as a target in tissue hypertrophy. Annu Rev Pharmacol Toxicol *47*, 443-467.

Lefkowitz, R. J., and Caron, M. G. (1988). Adrenergic receptors. Adv Second Messenger Phosphoprotein Res *21*, 1-10.

Lehmann, R., and Schleicher, E. D. (2000). Molecular mechanism of diabetic nephropathy. Clin Chim Acta *297*, 135-144.

Lengyel, Z., Voros, P., Toth, L. K., Nemeth, C., Kammerer, L., Mihaly, M., Tornoci, L., and Rosivall, L. (2004). Urinary albumin excretion is correlated to fibrinogen levels and protein S activity in patients with type 1 diabetes mellitus without overt diabetic nephropathy. Wien Klin Wochenschr *116*, 240-245.

Li, B., Dedman, J. R., and Kaetzel, M. A. (2003). Intron disruption of the annexin IV gene reveals novel transcripts. J Biol Chem *278*, 43276-43283.

Lilley, K. S., and Friedman, D. B. (2004). All about DIGE: quantification technology for differential-display 2D-gel proteomics. Expert Rev Proteomics *1*, 401-409.

Lilley, K. S., Razzaq, A., and Dupree, P. (2002). Two-dimensional gel electrophoresis: recent advances in sample preparation, detection and quantitation. Curr Opin Chem Biol *6*, 46-50.

Lottspeich, F. (2006). Massenspektrometrie, In Bioanalytik, F. Lottspeich, and J. W. Engels, eds. (Heidelberg: Spektrum Akademischer Verlag), pp. 329-372.

Magni, F., Sarto, C., Valsecchi, C., Casellato, S., Bogetto, S. F., Bosari, S., Di Fonzo, A., Perego, R. A., Corizzato, M., Doro, G.*, et al.* (2005). Expanding the proteome two-dimensional gel electrophoresis reference map of human renal cortex by peptide mass fingerprinting. Proteomics *5*, 816-825.

Markoff, A., and Gerke, V. (2005). Expression and functions of annexins in the kidney. Am J Physiol Renal Physiol *289*, F949-956.

Marshall, T., and Williams, K. (1996). Two-dimensional electrophoresis of human urinary proteins following concentration by dye precipitation. Electrophoresis *17*, 1265-1272.

Mathieu, A., Saal, I., Vuckovic, A., Ransy, V., Vereerstraten, P., Kaltner, H., Gabius, H. J., Kiss, R., Decaestecker, C., Salmon, I., and Remmelink, M. (2005). Nuclear galectin-3 expression is an independent predictive factor of recurrence for adenocarcinoma and squamous cell carcinoma of the lung. Mod Pathol *18*, 1264-1271.

Mauer, S. M., Michael, A. F., Fish, A. J., and Brown, D. M. (1972). Spontaneous immunoglobulin and complement deposition in glomeruli of diabetic rats. Lab Invest *27*, 488-494.

Mauer, S. M., Sutherland, D. E., Steffes, M. W., Leonard, R. J., Najarian, J. S., Michael, A. F., and Brown, D. M. (1974). Pancreatic islet transplantation. Effects on the glomerular lesions of experimental diabetes in the rat. Diabetes *23*, 748-753.

McGrane, M. M., de Vente, J., Yun, J., Bloom, J., Park, E., Wynshaw-Boris, A., Wagner, T., Rottman, F. M., and Hanson, R. W. (1988). Tissue-specific expression and dietary regulation of a chimeric phosphoenolpyruvate carboxykinase/bovine growth hormone gene in transgenic mice. J Biol Chem *263*, 11443-11451.

McLuckey, S. A. (1992). Principles of collisional activation in analytical mass spectrometry. J Am Soc Mass Spectrom *3*, 599-614.

Michels, L. D., O'Donnell, M. P., and Keane, W. F. (1984). Glomerular hemodynamic and structural correlations in long-term experimental diabetic rats. J Lab Clin Med *103*, 840-847.

Mimura, F., Yamagishi, S., Arimura, N., Fujitani, M., Kubo, T., Kaibuchi, K., and Yamashita, T. (2006). Myelin-associated glycoprotein inhibits microtubule assembly by a Rho-kinase-dependent mechanism. J Biol Chem *281*, 15970-15979.

Mischak, H., Kaiser, T., Walden, M., Hillmann, M., Wittke, S., Herrmann, A., Knueppel, S., Haller, H., and Fliser, D. (2004). Proteomic analysis for the assessment of diabetic renal damage in humans. Clin Sci (Lond) *107*, 485-495.

Mitka, M. (2005). Kidney failure rates end 20-year climb. Jama *294*, 2563.

Moiseeva, E. P., Javed, Q., Spring, E. L., and de Bono, D. P. (2000). Galectin 1 is involved in vascular smooth muscle cell proliferation. Cardiovasc Res *45*, 493-502.

Mora, J. F., Van Berkel, G. J., Enke, C. G., Cole, R. B., Martinez-Sanchez, M., and Fenn, J. B. (2000). Electrochemical processes in electrospray ionization mass spectrometry. J Mass Spectrom *35*, 939-952.

Muller, E., Neuhofer, W., Ohno, A., Rucker, S., Thurau, K., and Beck, F. X. (1996). Heat shock proteins HSP25, HSP60, HSP72, HSP73 in isoosmotic cortex and hyperosmotic medulla of rat kidney. Pflugers Arch *431*, 608-617.

Nagai, K., Matsubara, T., Mima, A., Sumi, E., Kanamori, H., Iehara, N., Fukatsu, A., Yanagita, M., Nakano, T., Ishimoto, Y.*, et al.* (2005). Gas6 induces Akt/mTOR-mediated mesangial hypertrophy in diabetic nephropathy. Kidney Int *68*, 552-561.

Newman, D. J., Thakkar, H., and Gallagher, H. (2000). Progressive renal disease: does the quality of the proteinuria matter or only the quantity? Clin Chim Acta *297*, 43-54.

Nishihara, J. C., and Champion, K. M. (2002). Quantitative evaluation of proteins in one- and two-dimensional polyacrylamide gels using a fluorescent stain. Electrophoresis *23*, 2203-2215.

Nyengaard, J. R., and Bendtsen, T. F. (1992). Glomerular number and size in relation to age, kidney weight, and body surface in normal man. Anat Rec *232*, 194-201.

O'Farrell, P. H. (1975). High resolution two-dimensional electrophoresis of proteins. J Biol Chem *250*, 4007-4021.

Odoni, G., and Ritz, E. (1999). Diabetic nephropathy--what have we learned in the last three decades? J Nephrol *12 Suppl 2*, S120-124.

Oh, J., Pyo, J. H., Jo, E. H., Hwang, S. I., Kang, S. C., Jung, J. H., Park, E. K., Kim, S. Y., Choi, J. Y., and Lim, J. (2004). Establishment of a near-standard two-dimensional human urine proteomic map. Proteomics *4*, 3485-3497.

Oksala, N. K., Lappalainen, J., Laaksonen, D. E., Khanna, S., Kaarniranta, K., Sen, C. K., and Atalay, M. (2007). Alpha-lipoic Acid modulates heat shock factor-1 expression in streptozotocin-induced diabetic rat kidney. Antioxid Redox Signal *9*, 497-506.

Olson, J. L., and Heptinstall, R. H. (1988). Nonimmunologic mechanisms of glomerular injury. Lab Invest *59*, 564-578.

Osterby, R., and Gundersen, H. J. (1980). Fast accumulation of basement membrane material and the rate of morphological changes in acute experimental diabetic glomerular hypertrophy. Diabetologia *18*, 493-500.

Ostergaard, J., Hansen, T. K., Thiel, S., and Flyvbjerg, A. (2005). Complement activation and diabetic vascular complications. Clin Chim Acta *361*, 10-19.

Ozmen, B., Ozmen, D., Turgan, N., Habif, S., Mutaf, I., and Bayindir, O. (2002). Association between homocysteinemia and renal function in patients with type 2 diabetes mellitus. Ann Clin Lab Sci *32*, 279-286.

Palmiter, R. D., Brinster, R. L., Hammer, R. E., Trumbauer, M. E., Rosenfeld, M. G., Birnberg, N. C., and Evans, R. M. (1982). Dramatic growth of mice that develop from eggs microinjected with metallothionein-growth hormone fusion genes. Nature *300*, 611-615.

Pavenstadt, H., Kriz, W., and Kretzler, M. (2003). Cell biology of the glomerular podocyte. Physiol Rev *83*, 253-307.

Pedersen, S. K., Harry, J. L., Sebastian, L., Baker, J., Traini, M. D., McCarthy, J. T., Manoharan, A., Wilkins, M. R., Gooley, A. A., Righetti, P. G.*, et al.* (2003). Unseen proteome: mining below the tip of the iceberg to find low abundance and membrane proteins. J Proteome Res *2*, 303-311.

Peng, J., and Gygi, S. P. (2001). Proteomics: the move to mixtures. J Mass Spectrom *36*, 1083-1091.

Pennington, S. R., Wilkins, M. R., Hochstrasser, D. F., and Dunn, M. J. (1997). Proteome analysis: from protein characterization to biological function Trends Cell Biol *7*, 168-173.

Perico, N., Codreanu, I., Schieppati, A., and Remuzzi, G. (2005). Pathophysiology of disease progression in proteinuric nephropathies. Kidney Int Suppl, S79-82.

Popowicz, G. M., Schleicher, M., Noegel, A. A., and Holak, T. A. (2006). Filamins: promiscuous organizers of the cytoskeleton. Trends Biochem Sci *31*, 411-419.

Pratt, J. M., Petty, J., Riba-Garcia, I., Robertson, D. H., Gaskell, S. J., Oliver, S. G., and Beynon, R. J. (2002). Dynamics of protein turnover, a missing dimension in proteomics. Mol Cell Proteomics *1*, 579-591.

Ransom, R. F., Vega-Warner, V., Smoyer, W. E., and Klein, J. (2005). Differential proteomic analysis of proteins induced by glucocorticoids in cultured murine podocytes. Kidney Int *67*, 1275-1285.

Rastaldi, M. P., Armelloni, S., Berra, S., Li, M., Pesaresi, M., Poczewski, H., Langer, B., Kerjaschki, D., Henger, A., Blattner, S. M.*, et al.* (2003). Glomerular podocytes possess the synaptic vesicle molecule Rab3A and its specific effector rabphilin-3a. Am J Pathol *163*, 889-899.

Remuzzi, G. (1995). Abnormal protein traffic through the glomerular barrier induces proximal tubular cell dysfunction and causes renal injury. Curr Opin Nephrol Hypertens *4*, 339-342.

Remuzzi, G., Benigni, A., and Remuzzi, A. (2006). Mechanisms of progression and regression of renal lesions of chronic nephropathies and diabetes. J Clin Invest *116*, 288-296.

Rennke, H. G., and Klein, P. S. (1989). Pathogenesis and significance of nonprimary focal and segmental glomerulosclerosis. Am J Kidney Dis *13*, 443-456.

Romen, W. (1976). [On the pathogenesis of the glomerulosclerosis ultrastructural and autoradiographic investigations on the rat kidney (author's transl)]. Veroff Pathol, 1-101.

Ruggenenti, P., and Remuzzi, G. (2006). Time to abandon microalbuminuria? Kidney Int *70*, 1214-1222.

Sahni, A., and Francis, C. W. (2000). Vascular endothelial growth factor binds to fibrinogen and fibrin and stimulates endothelial cell proliferation. Blood *96*, 3772-3778.

Sarto, C., Marocchi, A., Sanchez, J. C., Giannone, D., Frutiger, S., Golaz, O., Wilkins, M. R., Doro, G., Cappellano, F., Hughes, G.*, et al.* (1997). Renal cell carcinoma and normal kidney protein expression. Electrophoresis *18*, 599-604.

Schairer, I. (2006) Diabetes-assoziierte Nierenveränderungen bei GIPR^{dn}-transgenen Mäusen verschiedener Lebensaltersstufen, Dissertation zur Erlangung der tiermedizinischen Doktorwürde, Ludwig-Maximilians Univerity, Munich.

Schmid, H., Boucherot, A., Yasuda, Y., Henger, A., Brunner, B., Eichinger, F., Nitsche, A., Kiss, E., Bleich, M., Grone, H. J.*, et al.* (2006). Modular activation of

nuclear factor-kappaB transcriptional programs in human diabetic nephropathy. Diabetes *55*, 2993-3003.

Schreiner, G. F. (1990). Pathways leading from glomerular injury to glomerulosclerosis. Contrib Nephrol *86*, 1-14; discussion 15-18.

Schwartz, M. M., and Lewis, E. J. (1985). Focal segmental glomerular sclerosis: the cellular lesion. Kidney Int *28*, 968-974.

Sebti, S. M., Mignano, J. E., Jani, J. P., Srimatkandada, S., and Lazo, J. S. (1989). Bleomycin hydrolase: molecular cloning, sequencing, and biochemical studies reveal membership in the cysteine proteinase family. Biochemistry *28*, 6544-6548.

Seville, R. A., Nijjar, S., Barnett, M. W., Masse, K., and Jones, E. A. (2002). Annexin IV (Xanx-4) has a functional role in the formation of pronephric tubules. Development *129*, 1693-1704.

Shankland, S. J. (2006). The podocyte's response to injury: role in proteinuria and glomerulosclerosis. Kidney Int *69*, 2131-2147.

Sharma, K., Lee, S., Han, S., Lee, S., Francos, B., McCue, P., Wassell, R., Shaw, M. A., and RamachandraRao, S. P. (2005). Two-dimensional fluorescence difference gel electrophoresis analysis of the urine proteome in human diabetic nephropathy. Proteomics *5*, 2648-2655.

Shaw, J., Rowlinson, R., Nickson, J., Stone, T., Sweet, A., Williams, K., and Tonge, R. (2003). Evaluation of saturation labelling two-dimensional difference gel electrophoresis fluorescent dyes. Proteomics *3*, 1181-1195.

Shirato, I., Sakai, T., Kimura, K., Tomino, Y., and Kriz, W. (1996). Cytoskeletal changes in podocytes associated with foot process effacement in Masugi nephritis. Am J Pathol *148*, 1283-1296.

Shui, H. A., Ka, S. M., Lin, J. C., Lee, J. H., Jin, J. S., Lin, Y. F., Sheu, L. F., and Chen, A. (2006). Fibronectin in blood invokes the development of focal segmental glomerulosclerosis in mouse model. Nephrol Dial Transplant *21*, 1794-1802.

Shumway, J. T., and Gambert, S. R. (2002). Diabetic nephropathy-pathophysiology and management. Int Urol Nephrol *34*, 257-264.

Simonson, M. S. (2007). Phenotypic transitions and fibrosis in diabetic nephropathy. Kidney Int *71*, 846-854.

Sitek, B., Potthoff, S., Schulenborg, T., Stegbauer, J., Vinke, T., Rump, L. C., Meyer, H. E., Vonend, O., and Stuhler, K. (2006). Novel approaches to analyse glomerular proteins from smallest scale murine and human samples using DIGE saturation labelling. Proteomics *6*, 4337-4345.

Spahr, C. S., Davis, M. T., McGinley, M. D., Robinson, J. H., Bures, E. J., Beierle, J., Mort, J., Courchesne, P. L., Chen, K., Wahl, R. C.*, et al.* (2001). Towards defining the urinary proteome using liquid chromatography-tandem mass spectrometry. I. Profiling an unfractionated tryptic digest. Proteomics *1*, 93-107.

Stierle, H. E., Oser, B., and Boesken, W. H. (1990). Improved classification of proteinuria by semiautomated ultrathin SDS polyacrylamide gel electrophoresis. Clin Nephrol *33*, 168-173.

Striker, G. E., He, C. J., Liu, Z. H., Yang, D. C., Zalups, R. K., Esposito, C., and Striker, L. J. (1995). Pathogenesis of nonimmune glomerulosclerosis: studies in animals and potential applications to humans. Lab Invest *73*, 596-605.

Striker, L. J. (1993). Modern renal biopsy interpretation: can we predict glomerulosclerosis? Semin Nephrol *13*, 508-515.

Tahimic, C. G., Tomimatsu, N., Nishigaki, R., Fukuhara, A., Toda, T., Kaibuchi, K., Shiota, G., Oshimura, M., and Kurimasa, A. (2006). Evidence for a role of Collapsin response mediator protein-2 in signaling pathways that regulate the proliferation of non-neuronal cells. Biochem Biophys Res Commun *340*, 1244-1250.

Takemoto, M., Asker, N., Gerhardt, H., Lundkvist, A., Johansson, B. R., Saito, Y., and Betsholtz, C. (2002). A new method for large scale isolation of kidney glomeruli from mice. Am J Pathol *161*, 799-805.

Tanaka, K., Waki, H., Ido, Y., Akita, S., Yoshida, Y., Yoshida, T., and Matsuo, T. (1988). Protein and polymer analyses up to m/z 100 000 by laser ionization time-of-flight mass spectrometry. Rapid communications in Mass Spectrometry *2*, 151-153.

Tessari, P., Kiwanuka, E., Barazzoni, R., Vettore, M., and Zanetti, M. (2006). Diabetic nephropathy is associated with increased albumin and fibrinogen production in patients with type 2 diabetes. Diabetologia *49*, 1955-1961.

Thijssen, V. L., Postel, R., Brandwijk, R. J., Dings, R. P., Nesmelova, I., Satijn, S., Verhofstad, N., Nakabeppu, Y., Baum, L. G., Bakkers, J.*, et al.* (2006). Galectin-1 is essential in tumor angiogenesis and is a target for antiangiogenesis therapy. Proc Natl Acad Sci U S A *103*, 15975-15980.

Thongboonkerd, V. (2004). Proteomics in nephrology: current status and future directions. Am J Nephrol *24*, 360-378.

Thongboonkerd, V., Barati, M. T., McLeish, K. R., Benarafa, C., Remold-O'Donnell, E., Zheng, S., Rovin, B. H., Pierce, W. M., Epstein, P. N., and Klein, J. B. (2004). Alterations in the renal elastin-elastase system in type 1 diabetic nephropathy identified by proteomic analysis. J Am Soc Nephrol *15*, 650-662.

Thongboonkerd, V., Chutipongtanate, S., Kanlaya, R., Songtawee, N., Sinchaikul, S., Parichatikanond, P., Chen, S. T., and Malasit, P. (2006). Proteomic identification of alterations in metabolic enzymes and signaling proteins in hypokalemic nephropathy. Proteomics *6*, 2273-2285.

Thongboonkerd, V., Gozal, E., Sachleben, L. R., Jr., Arthur, J. M., Pierce, W. M., Cai, J., Chao, J., Bader, M., Pesquero, J. B., Gozal, D., and Klein, J. B. (2002a). Proteomic analysis reveals alterations in the renal kallikrein pathway during hypoxia-induced hypertension. J Biol Chem *277*, 34708-34716.

Thongboonkerd, V., and Malasit, P. (2005). Renal and urinary proteomics: current applications and challenges. Proteomics *5*, 1033-1042.

Thongboonkerd, V., McLeish, K. R., Arthur, J. M., and Klein, J. B. (2002b). Proteomic analysis of normal human urinary proteins isolated by acetone precipitation or ultracentrifugation. Kidney Int *62*, 1461-1469.

Thongboonkerd, V., Zheng, S., McLeish, K. R., Epstein, P. N., and Klein, J. B. (2005). Proteomic Identification and Immunolocalization of Increased Renal Calbindin-D28k Expression in OVE26 Diabetic Mice. Rev Diabet Stud *2*, 19-26.

Tilton, R. G., Haidacher, S. J., Lejeune, W. S., Zhang, X., Zhao, Y., Kurosky, A., Brasier, A. R., and Denner, L. (2007). Diabetes-induced changes in the renal cortical proteome assessed with two-dimensional gel electrophoresis and mass spectrometry. Proteomics *7*, 1729-1742.

Tonge, R., Shaw, J., Middleton, B., Rowlinson, R., Rayner, S., Young, J., Pognan, F., Hawkins, E., Currie, I., and Davison, M. (2001). Validation and development of fluorescence two-dimensional differential gel electrophoresis proteomics technology. Proteomics *1*, 377-396.

Uhlen, M., Bjorling, E., Agaton, C., Szigyarto, C. A., Amini, B., Andersen, E., Andersson, A. C., Angelidou, P., Asplund, A., Asplund, C.*, et al.* (2005). A human protein atlas for normal and cancer tissues based on antibody proteomics. Mol Cell Proteomics *4*, 1920-1932.

Unlu, M., Morgan, M. E., and Minden, J. S. (1997). Difference gel electrophoresis: a single gel method for detecting changes in protein extracts. Electrophoresis *18*, 2071-2077.

Valkova, N., Yunis, R., Mak, S. K., Kang, K., and Kultz, D. (2005). Nek8 mutation causes overexpression of galectin-1, sorcin, and vimentin and accumulation of the major urinary protein in renal cysts of jck mice. Mol Cell Proteomics *4*, 1009-1018.

van Balkom, B. W., Hoffert, J. D., Chou, C. L., and Knepper, M. A. (2004). Proteomic analysis of long-term vasopressin action in the inner medullary collecting duct of the Brattleboro rat. Am J Physiol Renal Physiol *286*, F216-224.

Volz, A. (1997) Klonierung und funktionelle Charakterisierung des humanen GIP-Rezeptors, Dissertation zur Erlangung des Doktorgrades der Naturwissenschaften, University of Marburg.

Waldherr, R., and Derks, H. (1989). [Clinical pathology of the glomerulus--from phenomenon to entity. Focal sclerosis]. Verh Dtsch Ges Pathol *73*, 71-82.

Wang, S., LaPage, J., and Hirschberg, R. (2000). Proteinuria and progression of chronic renal disease. Kidney Blood Press Res *23*, 167-169.

Wanke, R. (1996) Zur Morpho- und Pathogenese der progressiven Glomerulosklerose, Habilitationsschrift, Ludwig-Maximilians-Universität München.

Wanke, R., Hermanns, W., Folger, S., Wolf, E., and Brem, G. (1991). Accelerated growth and visceral lesions in transgenic mice expressing foreign genes of the growth hormone family: an overview. Pediatr Nephrol *5*, 513-521.

Wanke, R., Kahnt, E., Weis, S., Wolf, E., Brem, G., and Hermanns, W. (1993). Pathological and quantitative morphological changes in the kidney of mice transgenic for growth hormone. Exp Clin Endocrinol *101*, 115.

Wanke, R., Wolf, E., Brem, G., and Hermanns, W. (1996). Physiology and pathology of growth-studies in GH transgenic mice. J Anim Breed Genet *113*, 445-456.

Wanke, R., Wolf, E., Brem, G., and Hermanns, W. (2001). [Role of podocyte damage in the pathogenesis of glomerulosclerosis and tubulointerstitial lesions: findings in the growth hormone transgenic mouse model of progressive nephropathy]. Verh Dtsch Ges Pathol *85*, 250-256.

Wanke, R., Wolf, E., Hermanns, W., Folger, S., Buchmuller, T., and Brem, G. (1992). The GH-transgenic mouse as an experimental model for growth research: clinical and pathological studies. Horm Res *37 Suppl 3*, 74-87.

Watanabe, T., Hosoya, H., and Yonemura, S. (2007). Regulation of myosin II dynamics by phosphorylation and dephosphorylation of its light chain in epithelial cells. Mol Biol Cell *18*, 605-616.

Wehner, H., Hohn, D., Faix-Schade, U., Huber, H., and Walzer, P. (1972). Glomerular changes in mice with spontaneous hereditary diabetes. Lab Invest *27*, 331-340.

Weibel, E. R., and Gomez, D. M. (1962). A principle for counting tissue structures on random sections. J Appl Physiol *17*, 343-348.

Weimbs, T. (2006). Regulation of mTOR by polycystin-1: is polycystic kidney disease a case of futile repair? Cell Cycle *5*, 2425-2429.

Westbrook, J. A., Yan, J. X., Wait, R., Welson, S. Y., and Dunn, M. J. (2001). Zooming-in on the proteome: very narrow-range immobilised pH gradients reveal more protein species and isoforms. Electrophoresis *22*, 2865-2871.

Wiggins, J. E., Goyal, M., Sanden, S. K., Wharram, B. L., Shedden, K. A., Misek, D. E., Kuick, R. D., and Wiggins, R. C. (2005). Podocyte hypertrophy, "adaptation," and "decompensation" associated with glomerular enlargement and glomerulosclerosis in the aging rat: prevention by calorie restriction. J Am Soc Nephrol *16*, 2953-2966.

Willshaw, A., Grant, K., Yan, J., Rockliffe, N., Ambavarapu, S., Burdyga, G., Varro, A., Fukuoka, S., and Gawler, D. (2004). Identification of a novel protein complex containing annexin A4, rabphilin and synaptotagmin. FEBS Lett *559*, 13-21.

Wittke, S., Fliser, D., Haubitz, M., Bartel, S., Krebs, R., Hausadel, F., Hillmann, M., Golovko, I., Koester, P., Haller, H.*, et al.* (2003). Determination of peptides and proteins in human urine with capillary electrophoresis-mass spectrometry, a suitable tool for the establishment of new diagnostic markers. J Chromatogr A *1013*, 173-181.

Witzmann, F. A., Fultz, C. D., Grant, R. A., Wright, L. S., Kornguth, S. E., and Siegel, F. L. (1998). Differential expression of cytosolic proteins in the rat kidney cortex and medulla: preliminary proteomics. Electrophoresis *19*, 2491-2497.

Wolf, E., Kahnt, E., Ehrlein, J., Hermanns, W., Brem, G., and Wanke, R. (1993). Effects of long-term elevated serum levels of growth hormone on life expectancy of mice: lessons from transgenic animal models. Mech Ageing Dev *68*, 71-87.

Wolf, E., and Wanke, R. (1997). Growth hormone overproduction in transgenic mice: Phenotypic alterations and deduced animal models, In Welfare aspects of transgenic animals, L. F. M. van Zutphen, and M. van der Meer, eds. (Berlin: Springer Verlag).

Wolf, G. (2000). Cell cycle regulation in diabetic nephropathy. Kidney Int Suppl *77*, S59-66.

Xia, L., Wang, H., Munk, S., Frecker, H., Goldberg, H. J., Fantus, I. G., and Whiteside, C. I. (2007). Reactive Oxygen Species, PKC-{beta}1, and PKC-{zeta} Mediate High Glucose-induced Vascular Endothelial Growth Factor Expression in Mesangial Cells. Am J Physiol Endocrinol Metab.

Xu, B. J., Shyr, Y., Liang, X., Ma, L. J., Donnert, E. M., Roberts, J. D., Zhang, X., Kon, V., Brown, N. J., Caprioli, R. M., and Fogo, A. B. (2005). Proteomic patterns and prediction of glomerulosclerosis and its mechanisms. J Am Soc Nephrol *16*, 2967-2975.

Yasuda, Y., Horie, A., Odani, H., Iwase, H., and Hiki, Y. (2004). Application of mass spectrometry to IgA nephropathy: structural and biological analyses of underglycosylated IgA1 molecules. Contrib Nephrol *141*, 170-188.

Yoshida, Y., Fogo, A., Shiraga, H., Glick, A. D., and Ichikawa, I. (1988). Serial micropuncture analysis of single nephron function in subtotal renal ablation. Kidney Int *33*, 855-867.

Yoshida, Y., Kawamura, T., Ikoma, M., Fogo, A., and Ichikawa, I. (1989). Effects of antihypertensive drugs on glomerular morphology. Kidney Int *36*, 626-635.

Yoshida, Y., Miyazaki, K., Kamiie, J., Sato, M., Okuizumi, S., Kenmochi, A., Kamijo, K., Nabetani, T., Tsugita, A., Xu, B.*, et al.* (2005). Two-dimensional electrophoretic profiling of normal human kidney glomerulus proteome and construction of an extensible markup language (XML)-based database. Proteomics *5*, 1083-1096.

Zent, R., and Pozzi, A. (2007). Angiogenesis in diabetic nephropathy. Semin Nephrol *27*, 161-171.

Ziegler, W. H., Liddington, R. C., and Critchley, D. R. (2006). The structure and regulation of vinculin. Trends Cell Biol *16*, 453-460.

Zimny, J., Sikora, M., Guranowski, A., and Jakubowski, H. (2006). Protective mechanisms against homocysteine toxicity: the role of bleomycin hydrolase. J Biol Chem *281*, 22485-22492.

Zoja, C., Abbate, M., and Remuzzi, G. (2006). Progression of chronic kidney disease: insights from animal models. Curr Opin Nephrol Hypertens *15*, 250-257.

10. Attachment

10.1 Silver stain for SDS-PAGE mini gels

1. Fixation solution	60 minutes
99.6 % Ethanol	500 ml
Glacial acetic acid (Applichem, Germany)	120 ml
37 % Formaldehyde (Applichem, Germany)	0.5 ml
ad 1000 ml distilled water	
2. Washing in 50 % ethanol	3 times 20 minutes
Pre-treatment	1 minute
Sodium thiosulfate (Applichem, Germany)	0.05 g
in 50 ml distilled water	
3. Washing in distilled water	3 times 20 seconds
Impregnation	20 minutes
Silver nitrate (Applichem, Germany)	0.05 g
37 % Formaldehyde	37 µl
ad 50 ml distilled water	
4. Washing in distilled water	2 times 20 seconds
Develop	until bands become visible
Sodium carbonate (Merck, Germany)	3 g
Sodium thiosulfate	0.2 mg
37 % Formaldehyde	50 µl
ad 100 ml distilled water	
5. Washing in distilled water	20 seconds
Stop solution	
0.1 M EDTA (Sigma, Germany)	

10.2 Staining procedures for plastic embedded sections

10.2.1 Hemalaun & Eosin (H&E)

1.	Mayer's hemalaun (Applichem, Germany)	30 minutes
2.	Rinse in tap water	10 minutes
3.	1 % HCl-Alcohol	1 second
4.	Rinse in tap water	10 minutes
5.	Dry	
6.	Eosine Y (Merck, Germany)	5 minutes
7.	Distilled water	3 times 3 seconds
8.	Dry	
9.	Mount with glass cover slips using Histofluid® (Superior, Germany)	

10.2.2 Periodic acid-Schiff stain (PAS)

1.	1 % periodic acid (Applichem, Germany)	15 minutes
2.	Distilled water	3 times 3 seconds
3.	Schiff's reagent (Merck, Germany)	30-60 minutes
4.	Rinse in tap water	30 minutes
5.	Dry	
6.	Mayer's hemalaun (Applichem, Germany)	35 minutes
7.	Rinse in tap water	10 minutes
8.	1 % HCl alcohol	1 second
9.	Rinse in tap water	10 minutes
10.	Dry	
11.	Mount under glass cover slips using Histofluid® (Superior, Germany)	

10.3 PMF spectra of unambiguously identified differentially abundant spots

10.3.1 GH transgenic mice in stage 2 vs. their controls

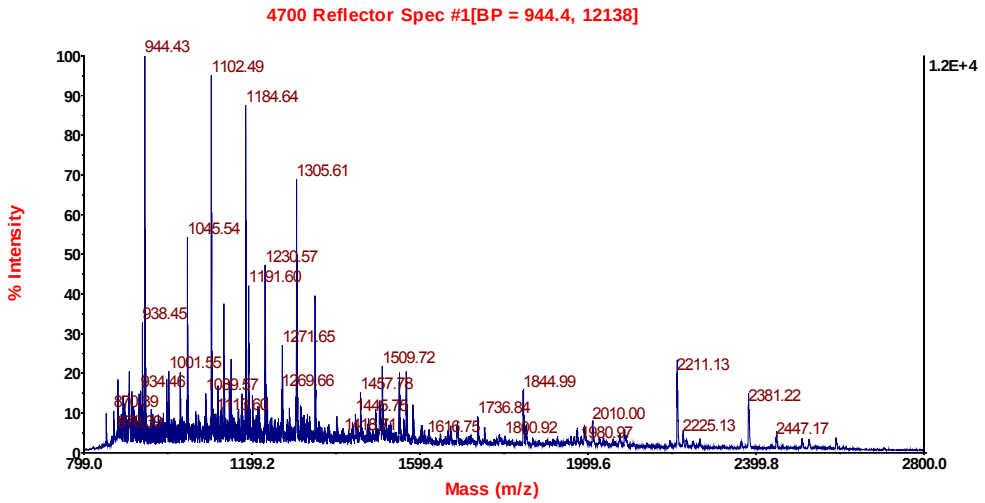

Spot 1, GH transgenic mice vs. their controls

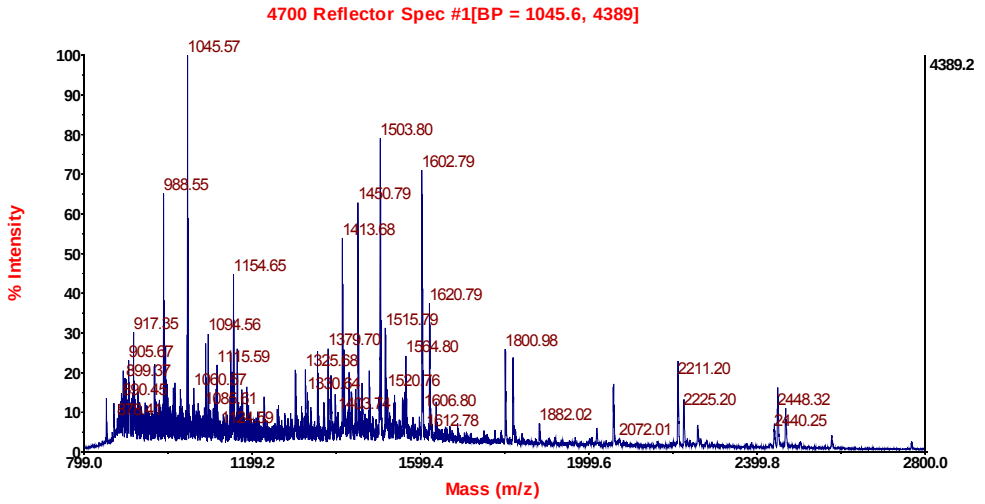

Spot 2, GH transgenic mice vs. their controls

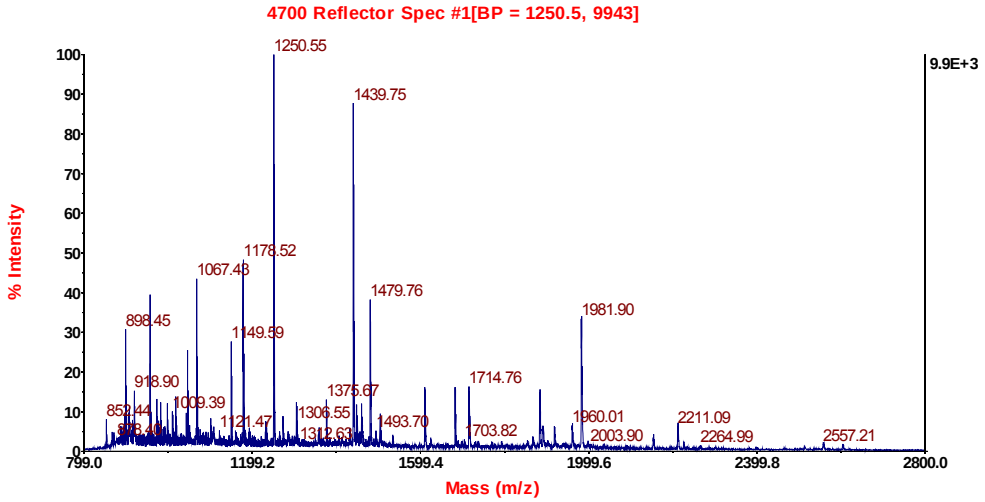

Spot 6, GH transgenic mice vs. their controls

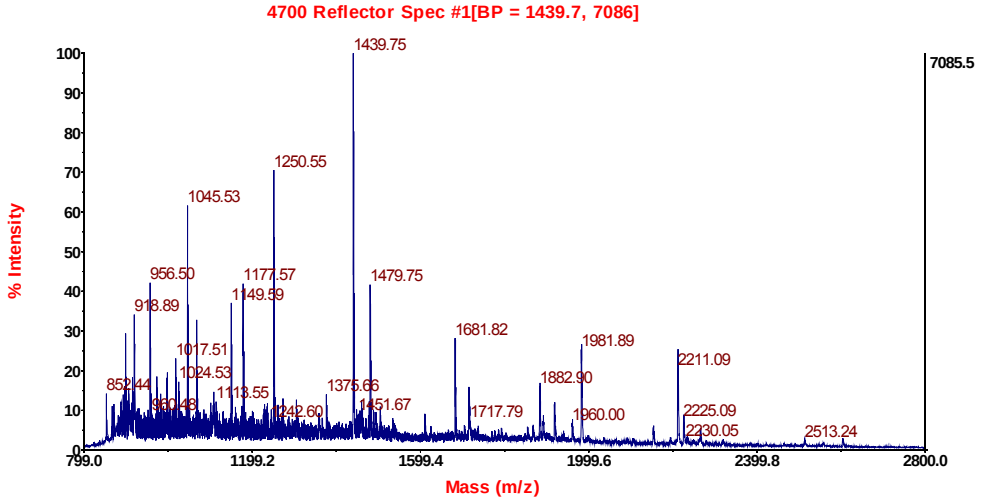

Spot 7, GH transgenic mice vs. their controls

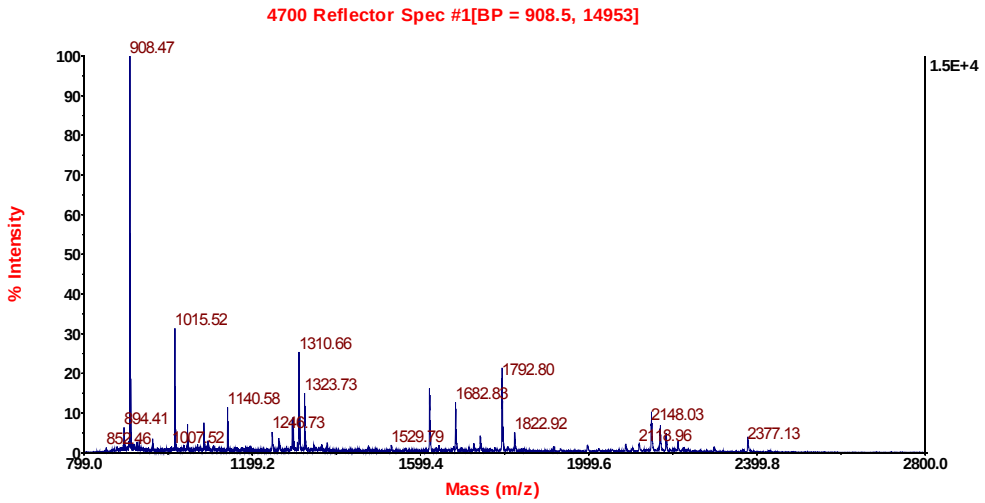

Spot 8, GH transgenic mice vs. their controls

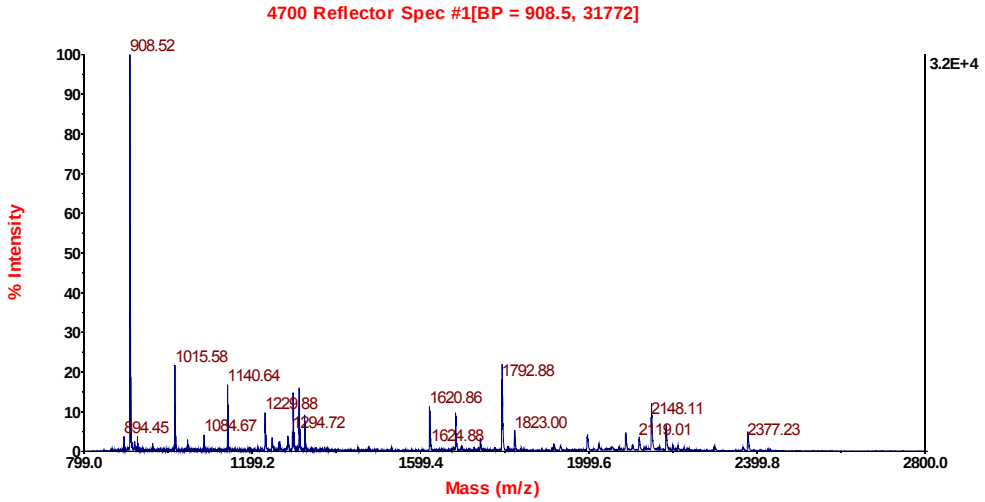

Spot 11, GH transgenic mice vs. their controls

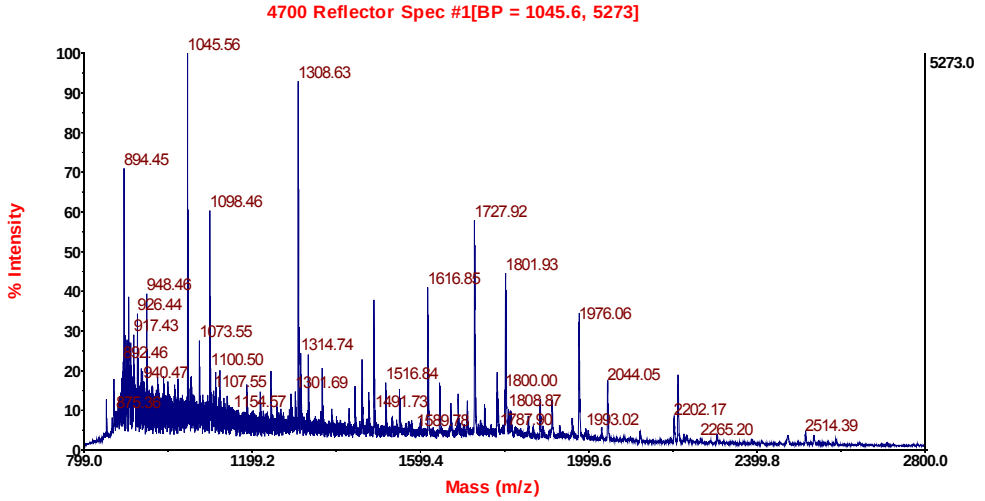

Spot 15, GH transgenic mice vs. their controls

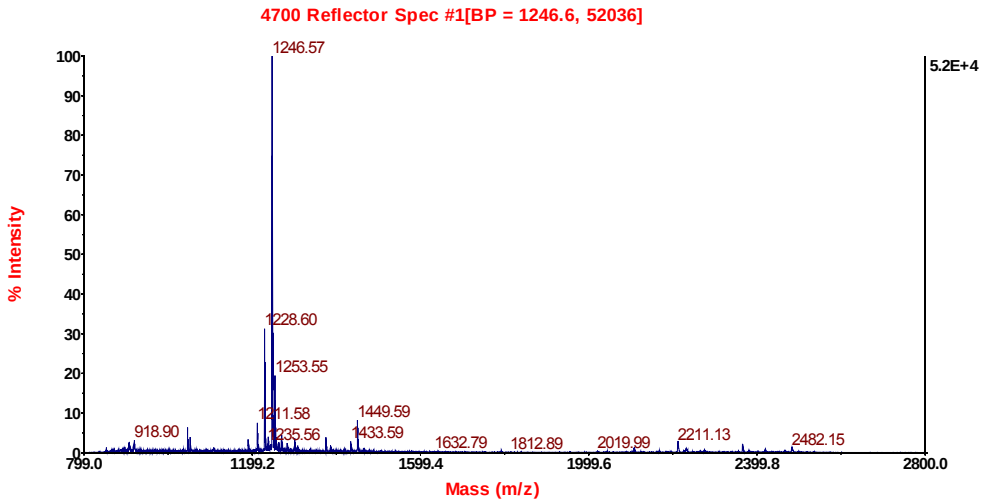

Spot 19, GH transgenic mice vs. their controls

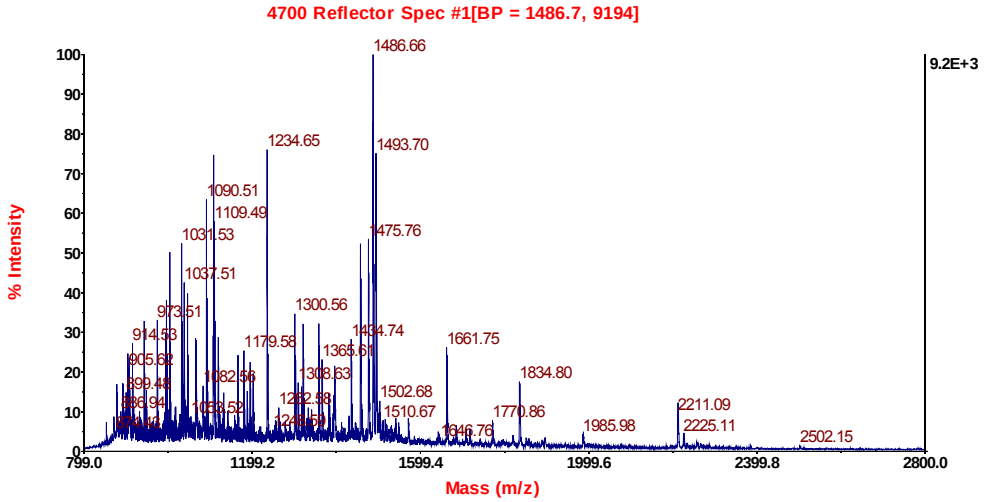

Spot 20, GH transgenic mice vs. their controls

10.3.2 GIPR^{dn} transgenic mice in stage 2 vs. their controls

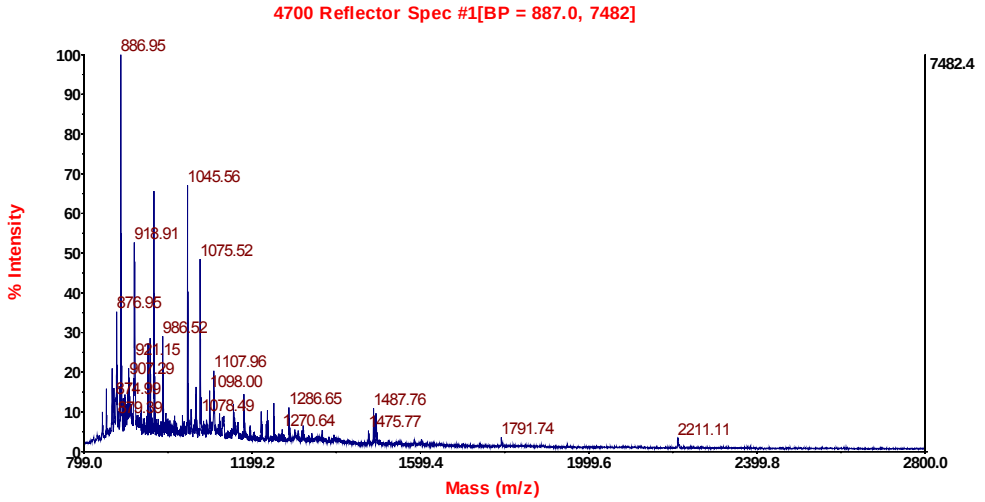

Spot 1, GIPR^{dn} transgenic mice vs. their controls

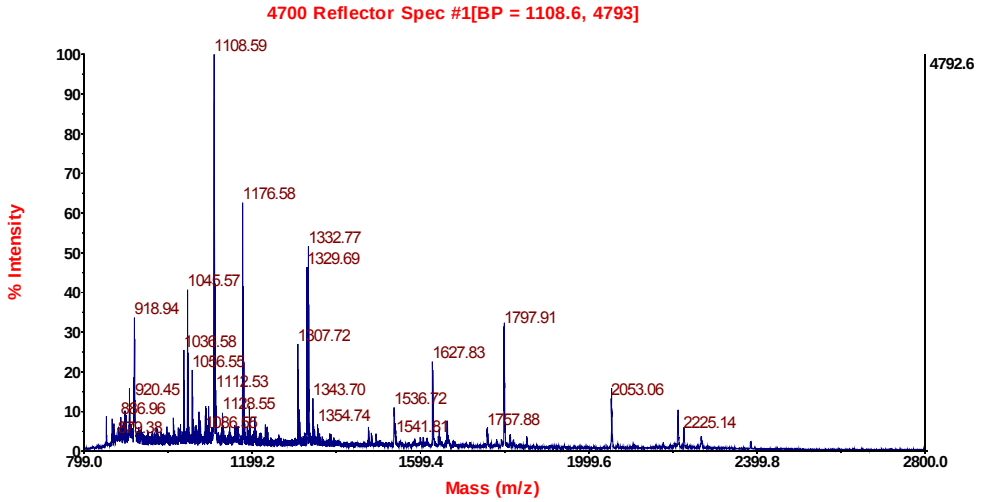

Spot 3, GIPR^{dn} transgenic mice vs. their controls

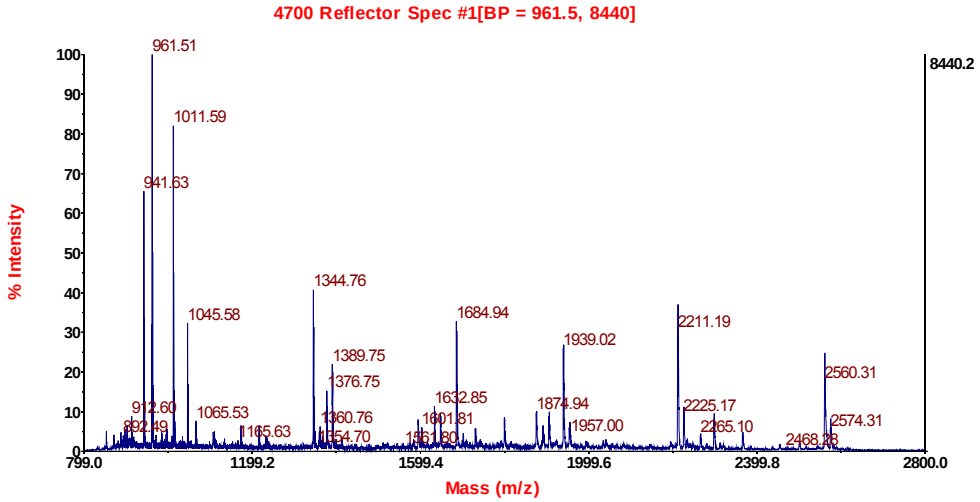

Spot 7, GIPR^{dn} transgenic mice vs. their controls

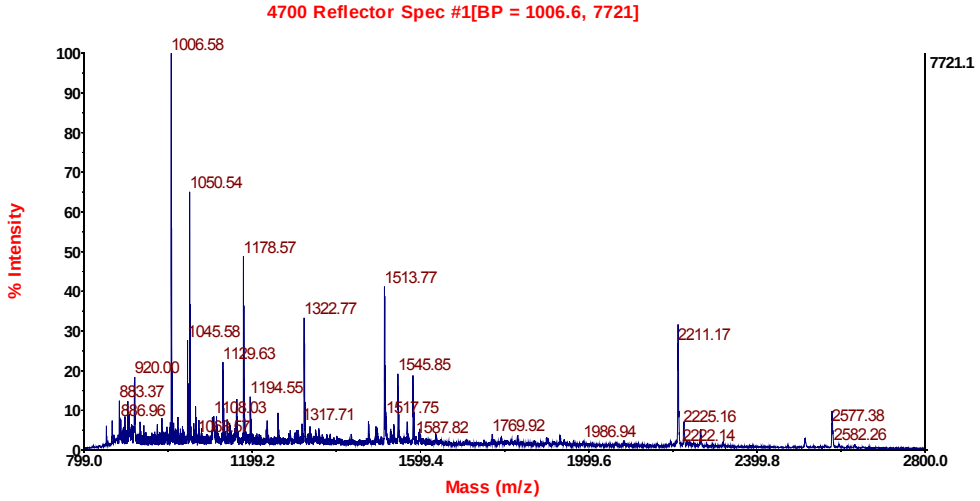

Spot 10, GIPR^{dn} transgenic mice vs. their controls

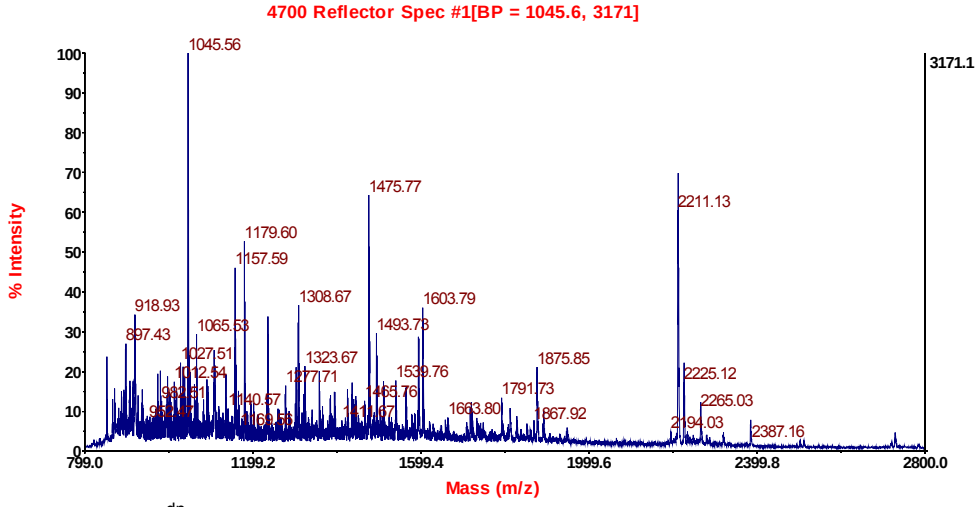

Spot 13, GIPR^{dn} transgenic mice vs. their controls

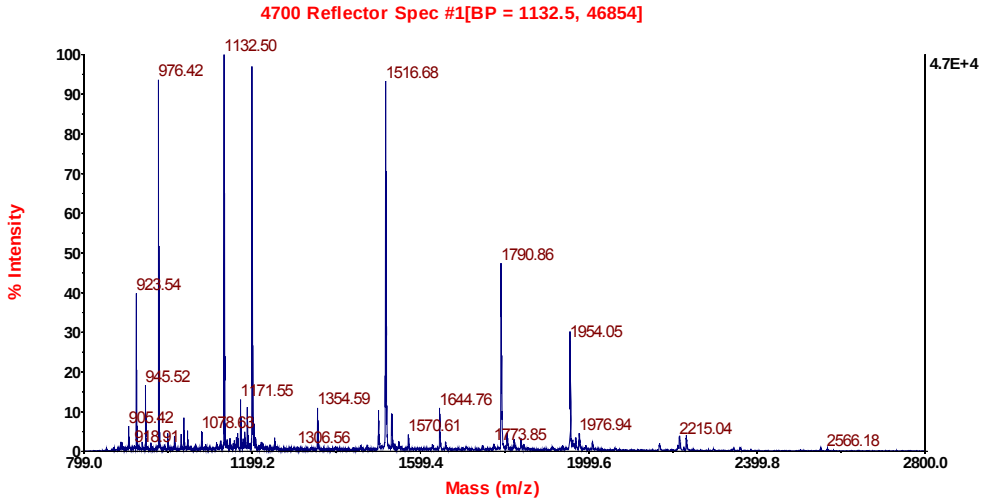

Spot 16, GIPR^{dn} transgenic mice vs. their controls

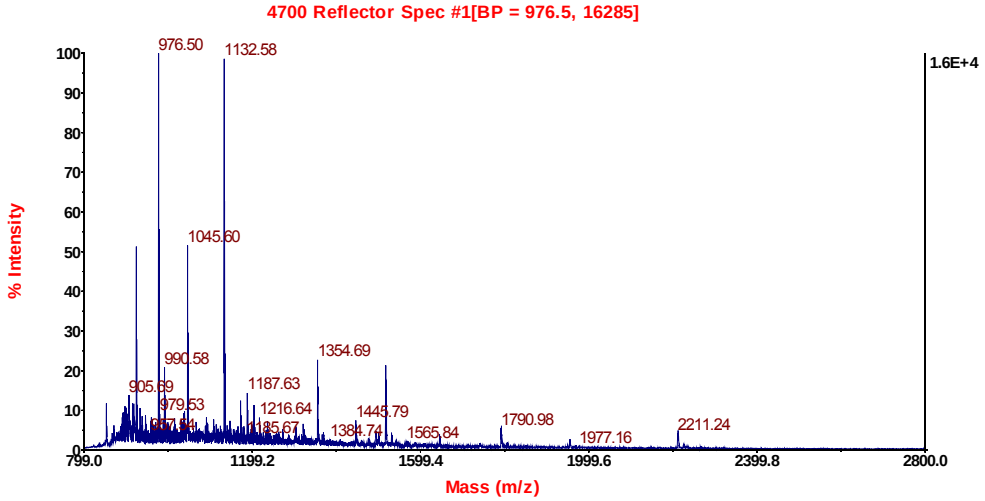

Spot 17, GIPR^{dn} transgenic mice vs. their controls

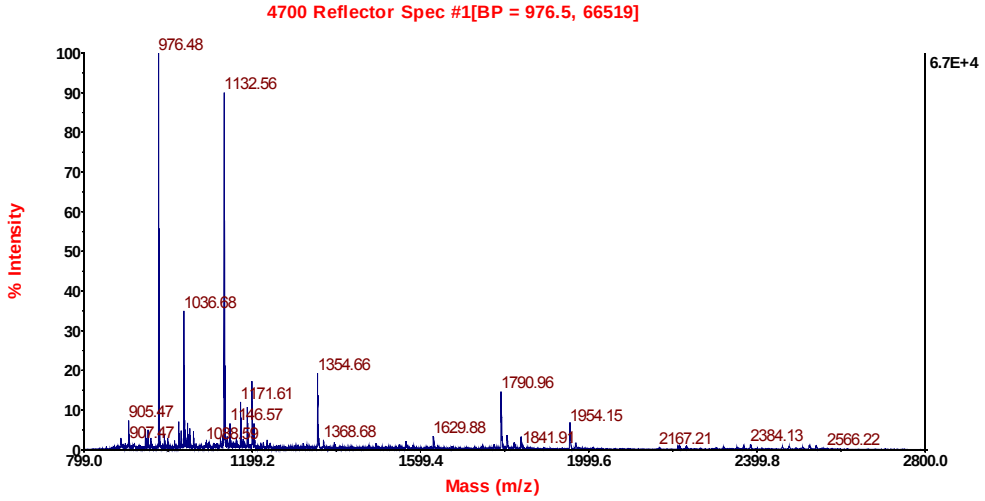

Spot 18, GIPR^{dn} transgenic mice vs. their controls

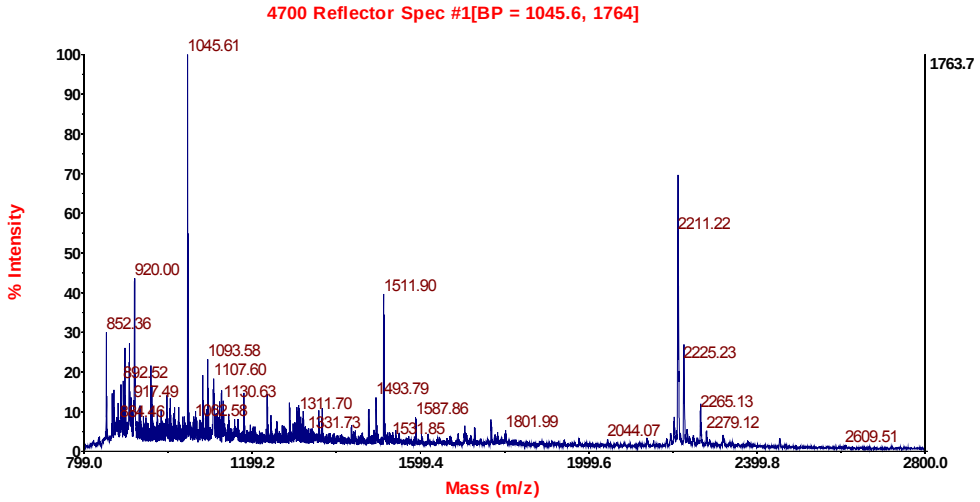

Spot 22, GIPR^{dn} transgenic mice vs. their controls

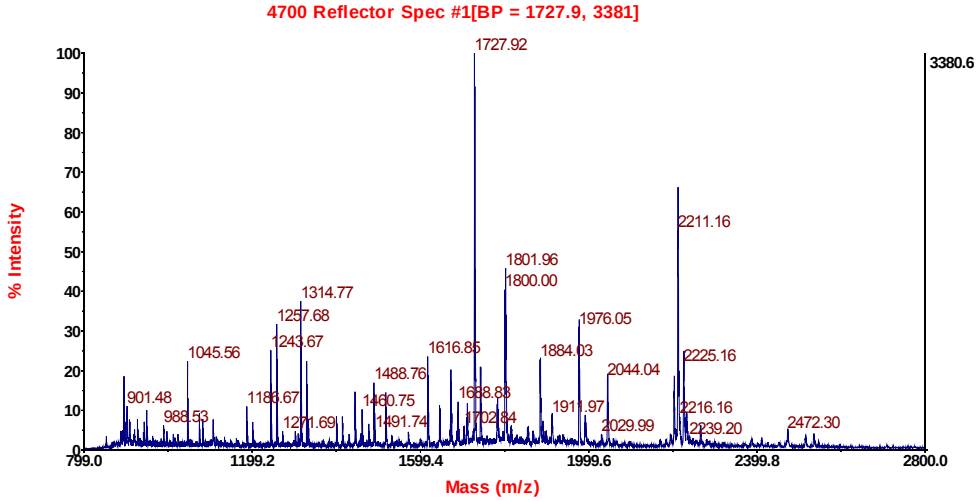

Spot 24, GIPR^{dn} transgenic mice vs. their controls

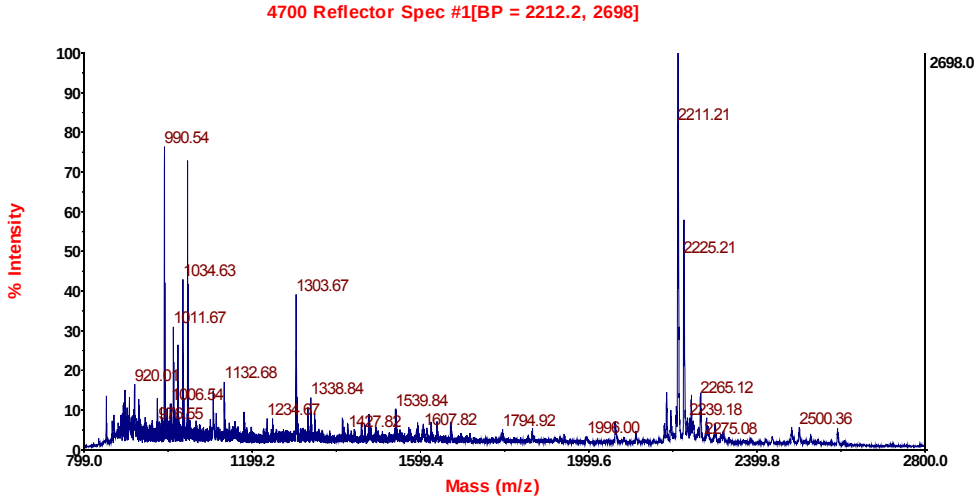

Spot 28, GIPR^{dn} transgenic mice vs. their controls

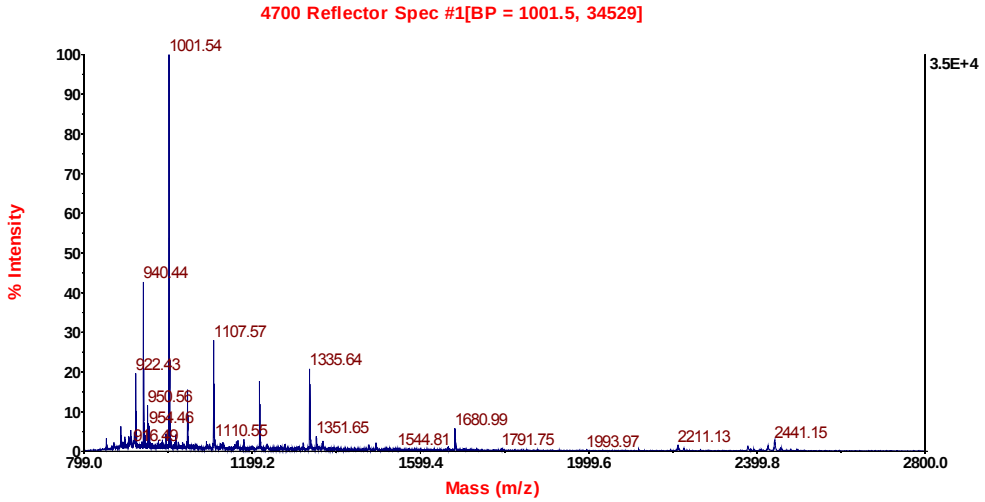

Spot 35, GIPR^{dn} transgenic mice vs. their controls

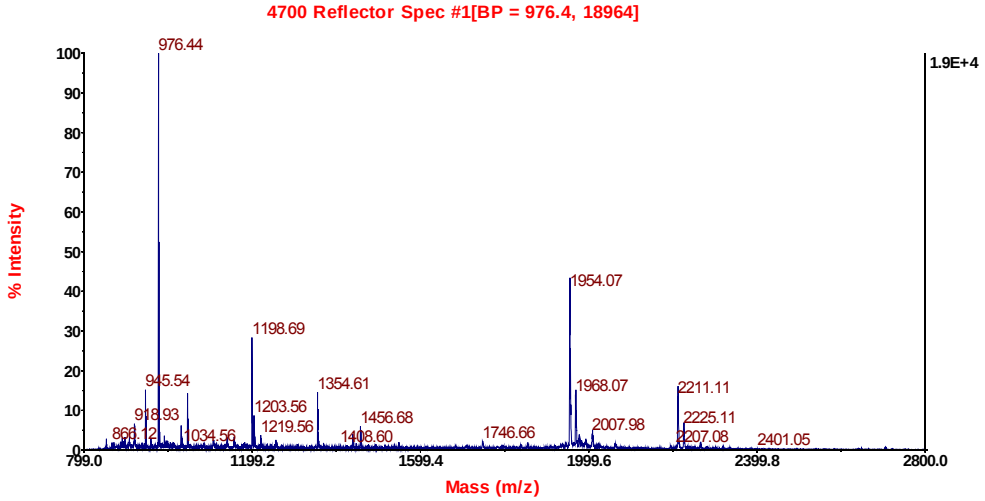

Spot 40, GIPR^{dn} transgenic mice vs. their controls

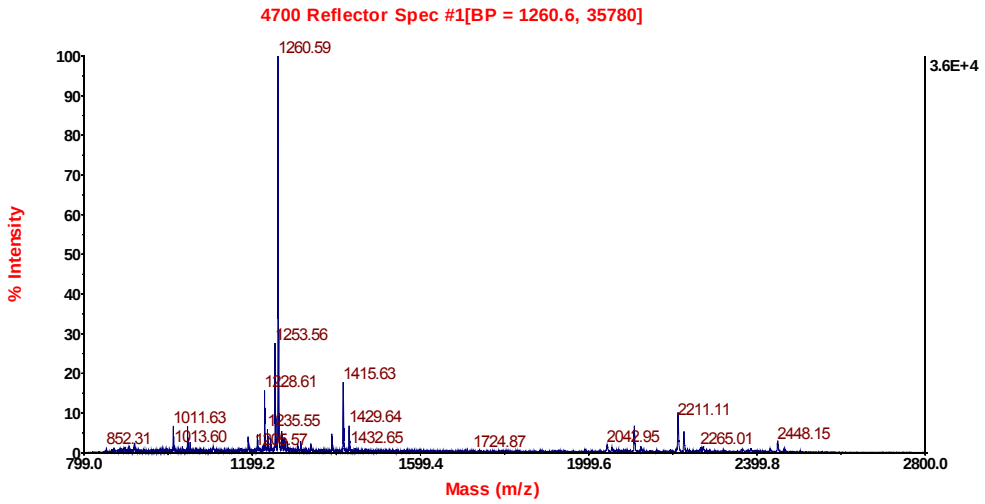

Spot 42, GIPR^{dn} transgenic mice vs. their controls

Acknowledgement

I would like to thank Prof. Dr. R. Wanke for giving me the opportunity to do this dissertation, for the time he spent discussing the different features of this doctorate, especially the experimental design of the study and the critical reading of the manuscript. Im very grateful for his great support.

I wish to thank Dr. G. J. Arnold for his supervision in the proteomics part of this study and giving me the opportunity to work in his laboratory. The many discussions with him and his advice were a great support for me.

Especially I would like to thank Andreas Blutke for a very productive teamwork and endless discussions.

Further, I show my gratitude to Dr. N. Herbach for her advice and the time she spent discussing different aspects of the study.

My thanks go to Dr. E. Kemter for fruitful discussions and advice, especially during the establishment and optimization of the glomerulus isolation, as well as for the critical reading of the manuscript.

I wish to thanks the team of the AG Arnold for their support in proteomic issues. Especially, I would like to thand Dr. F. Berendt for introducing me into the proteomic techniques and performing preliminary experiments during the establishment of the glomerulus isolation. For assistance with mass spectrometry issues and for the conduction of the LC-ESI-MS/MS identifications I want to thank Dr. Th. Fröhlich.

Thank you to the team of the Toplab GmbH, Martinsried, for running a part of the 2D-gels.

I wish to thank the laboratory for clinical chemistry of the clinic for small animal internal medicine of the Ludwig-Maximilians-University, Munich for analysing urine samples.

Dr. K. Weber gave us the opportunity to do the software assisted readout and analysis of the ELISA experiments in the Institute of Physiology. Thank you very much for the help.

I wish to thank all employees at the Institute of Veterinary Pathology for their help, especially Adrian Ciolovan, Sabine Zwirz, Heike Sperling and Angela Siebert.

And not to forget I would like to thank all members of the graduate college “Functional genomics in veterinary medicine” for a great time and the opportunity to get insights in topics outside the own topic.

At last, I am very grateful to my family and friends for human support in difficult times.